

© ESO

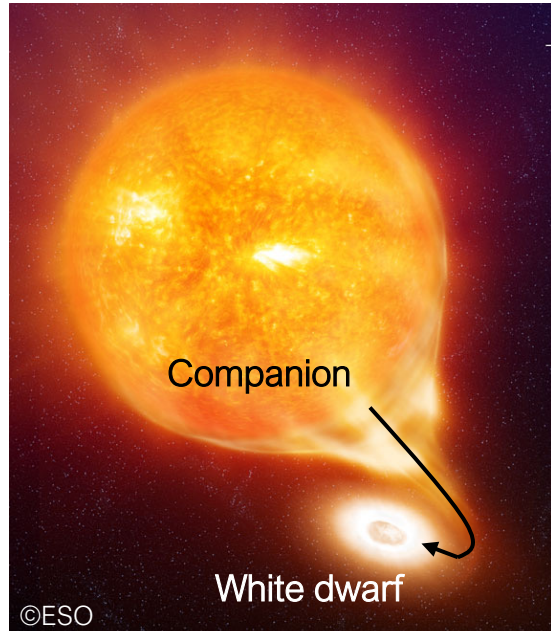
Understanding ^{22}Na cosmic abundance



C. Fougères¹, F. de Oliveira Santos¹ et al.
¹GANIL CEA/DRF-CNRS/IN2P3, Caen (France)

Astrophysical motivations

Stellar objects of interest

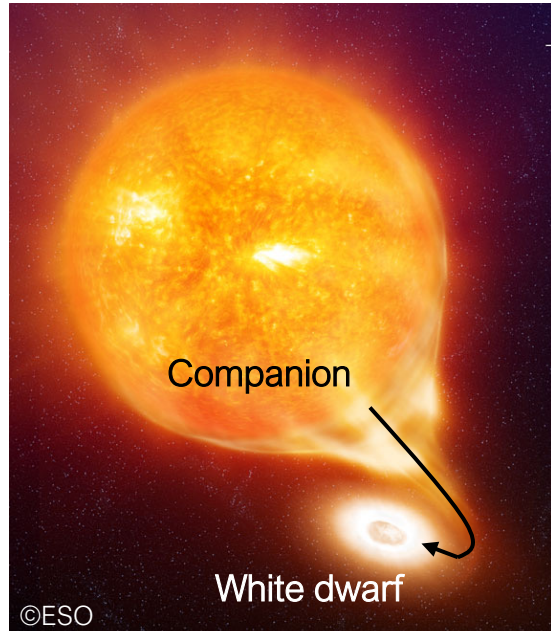


Binary system {red giant + white dwarf}
Matter accretion → explosive hydrogen burning at surface

Impacts

- Abundances of nuclei
- Isotopic composition of meteoritic presolar grains *Black (1972)*
- Test of Nova models
- Number of supernovae SNIa (dark energy)

Stellar objects of interest



Binary system {red giant + white dwarf}
Matter accretion → explosive hydrogen burning at surface

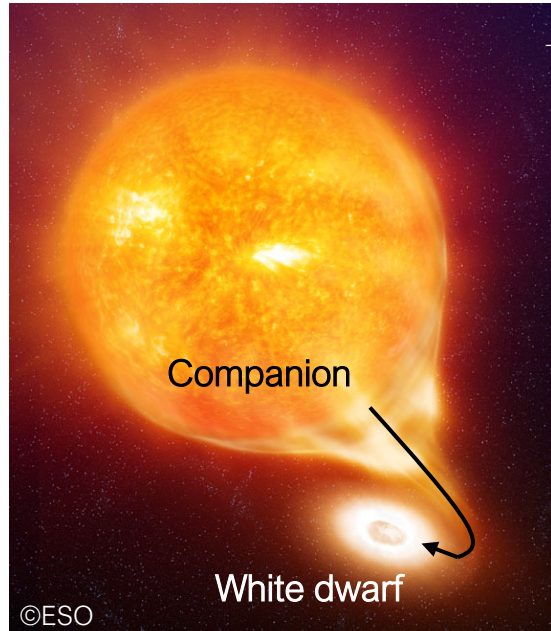
Impacts

- Abundances of nuclei
- Isotopic composition of meteoritic presolar grains *Black (1972)*
- Test of Nova models
- Number of supernovae SNIa (dark energy)

Uncertainties

*Accretion dynamics,
initial WD temp.*

Stellar objects of interest



Binary system {red giant + white dwarf}
Matter accretion → explosive hydrogen burning at surface

Impacts

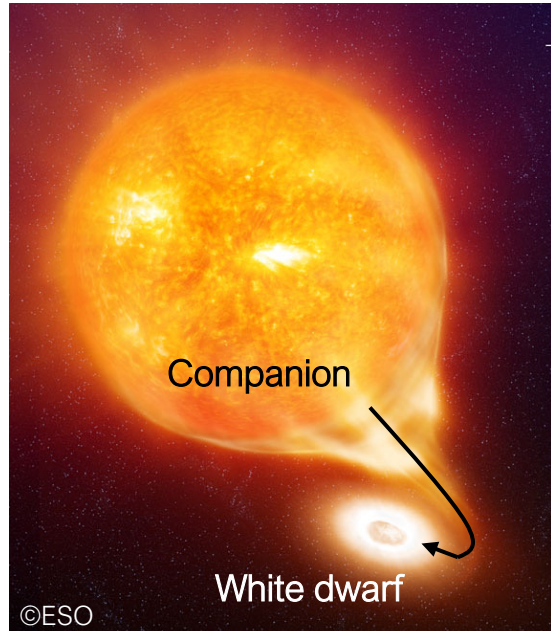
- Abundances of nuclei
- Isotopic composition of meteoritic presolar grains *Black (1972)*
- Test of Nova models
- Number of supernovae SNIa (dark energy)

Need of astronomical observables

Uncertainties

*Accretion dynamics,
initial WD temp.*

Stellar objects of interest



Binary system {red giant + white dwarf}
Matter accretion → explosive hydrogen burning at surface

Impacts

- Abundances of nuclei
- Isotopic composition of meteoritic presolar grains *Black (1972)*
- Test of Nova models
- Number of supernovae SNIa (dark energy)

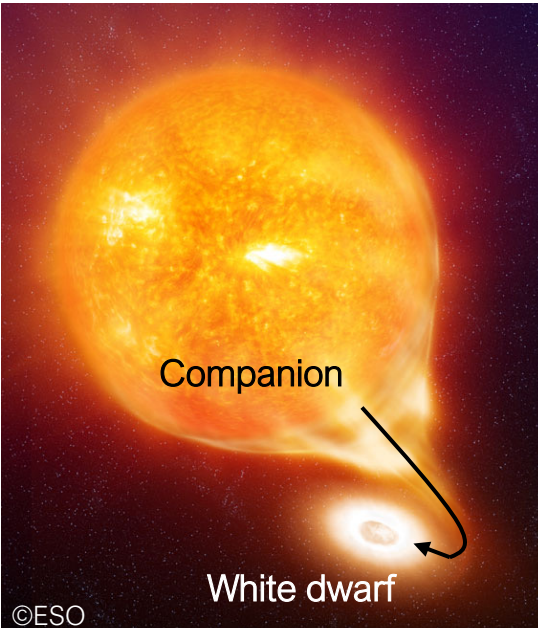
Need of astronomical observables

Uncertainties

*Accretion dynamics,
initial WD temp.*

©ESO
O⁺Ne novae

Stellar objects of interest



Binary system {red giant + white dwarf}
Matter accretion → explosive hydrogen burning at surface

Impacts

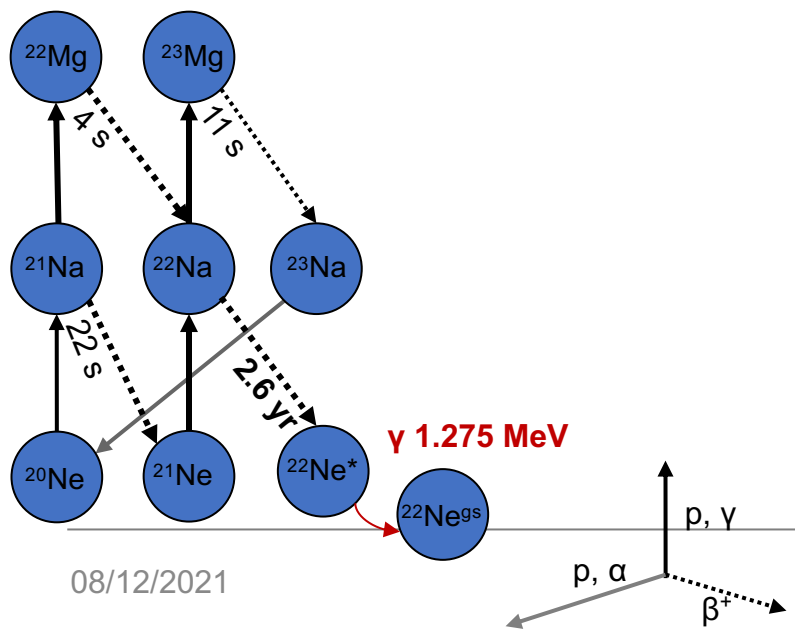
- Abundances of nuclei
- Isotopic composition of meteoritic presolar grains *Black (1972)*
- Test of Nova models
- Number of supernovae SNIa (dark energy)

Need of astronomical observables

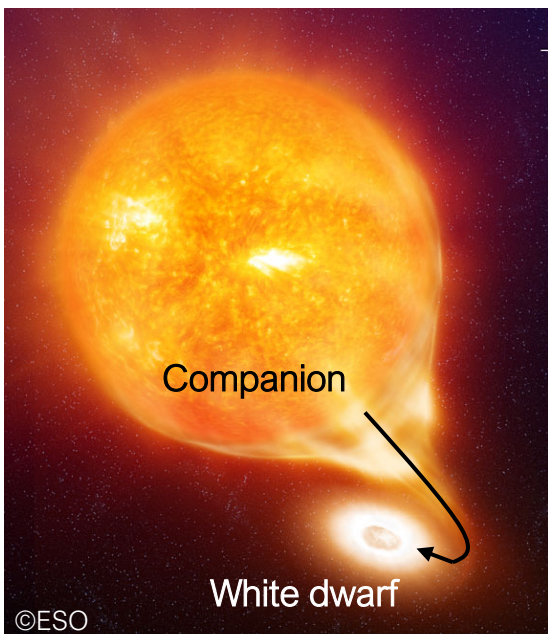
Uncertainties

*Accretion dynamics,
initial WD temp.*

O Ne novae



Stellar objects of interest



Binary system {red giant + white dwarf}
Matter accretion → explosive hydrogen burning at surface

Impacts

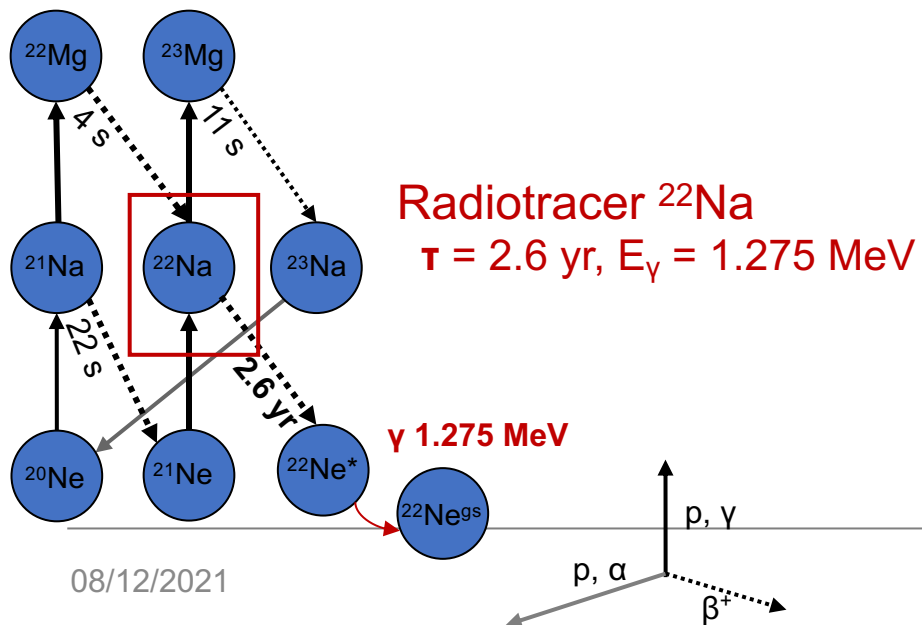
- Abundances of nuclei
- Isotopic composition of meteoritic presolar grains *Black (1972)*
- Test of Nova models
- Number of supernovae SNIa (dark energy)

Need of astronomical observables

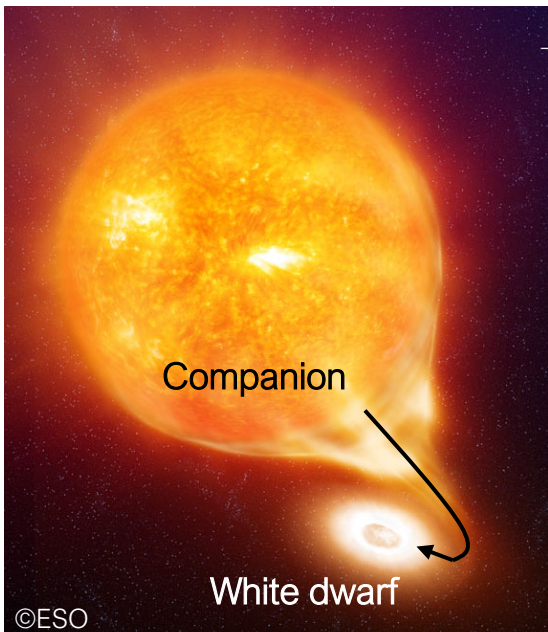
Uncertainties

*Accretion dynamics,
initial WD temp.*

O/Ne novae



Stellar objects of interest



Binary system {red giant + white dwarf}
Matter accretion → explosive hydrogen burning at surface

Impacts

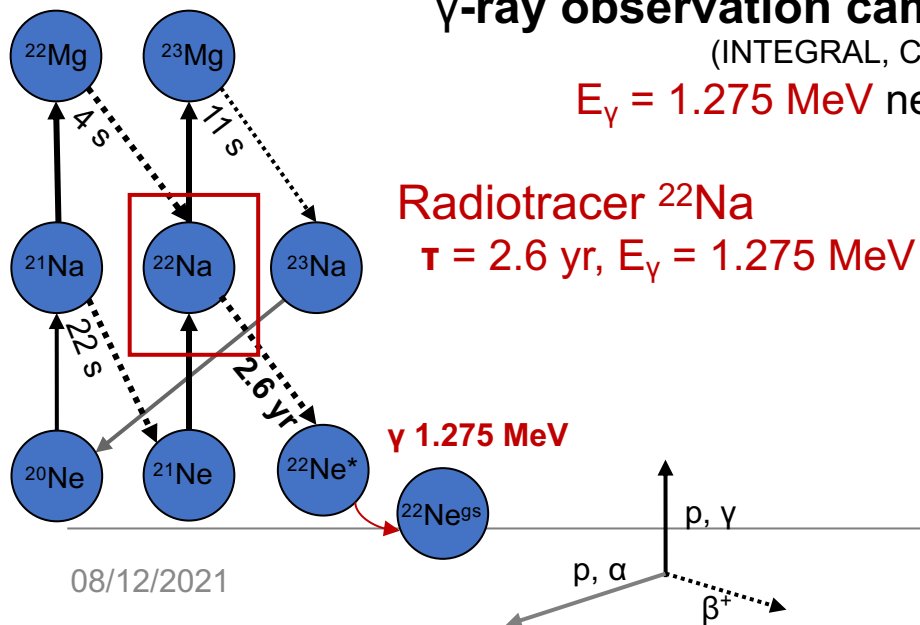
- Abundances of nuclei
- Isotopic composition of meteoritic presolar grains *Black (1972)*
- Test of Nova models
- Number of supernovae SNIa (dark energy)

Need of astronomical observables

Uncertainties

*Accretion dynamics,
initial WD temp.*

O Ne novae



γ-ray observation campaigns

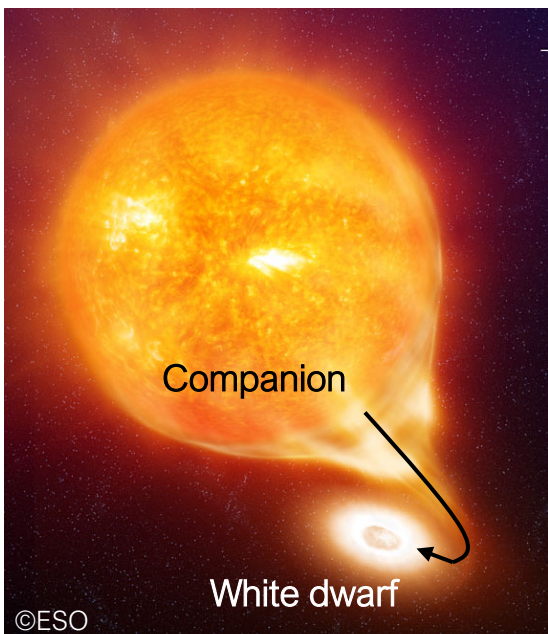
(INTEGRAL, COMPTEL...)

$E_\gamma = 1.275 \text{ MeV}$ never seen

Radiotracer ^{22}Na

$\tau = 2.6 \text{ yr}$, $E_\gamma = 1.275 \text{ MeV}$

Stellar objects of interest



Binary system {red giant + white dwarf}
Matter accretion → explosive hydrogen burning at surface

Impacts

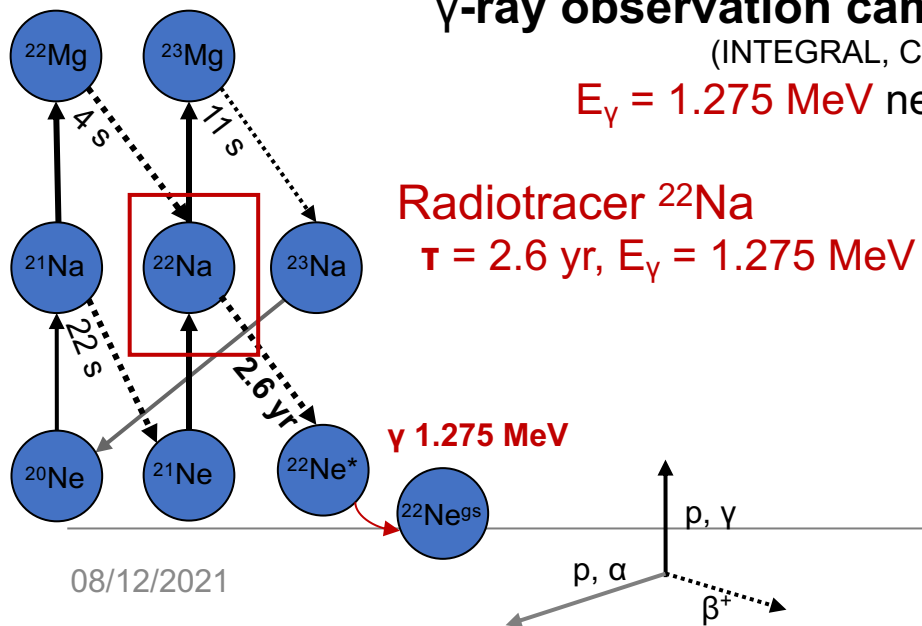
- Abundances of nuclei
- Isotopic composition of meteoritic presolar grains *Black (1972)*
- Test of Nova models
- Number of supernovae SNIa (dark energy)

Need of astronomical observables

Uncertainties

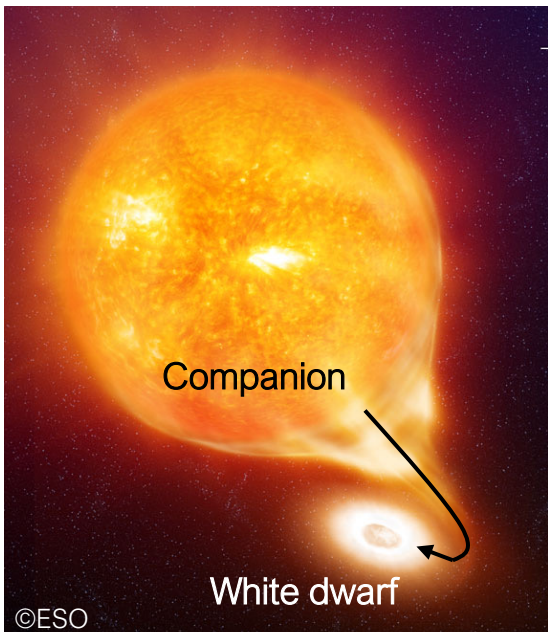
*Accretion dynamics,
initial WD temp.*

ONe novae



Sensitivity improved by x30
De Angelis, Tatischeff et al. (2017)

Stellar objects of interest



Binary system {red giant + white dwarf}
Matter accretion → explosive hydrogen burning at surface

Impacts

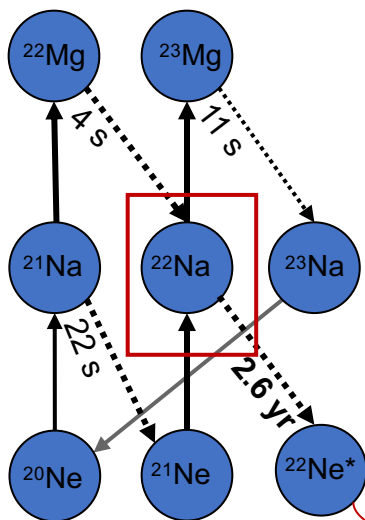
- Abundances of nuclei
- Isotopic composition of meteoritic presolar grains *Black (1972)*
- Test of Nova models
- Number of supernovae SNIa (dark energy)

Need of astronomical observables

Uncertainties

*Accretion dynamics,
initial WD temp.*

ONE novae



γ-ray observation campaigns

(INTEGRAL, COMPTEL...)

$E_\gamma = 1.275 \text{ MeV}$ never seen

Radiotracer ^{22}Na

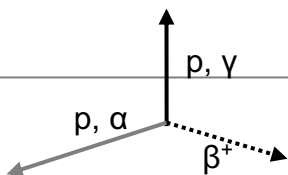
$\tau = 2.6 \text{ yr}$, $E_\gamma = 1.275 \text{ MeV}$



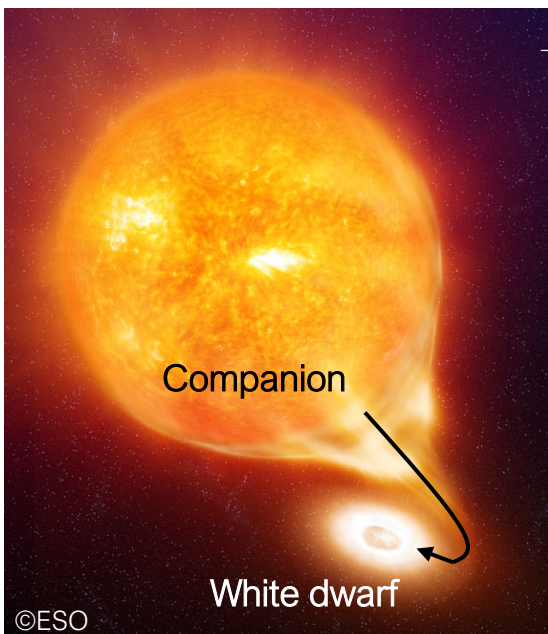
Sensitivity improved by x30

De Angelis, Tatischeff et al. (2017)

*^{22}Na abundance in
novae
Detection limit*



Stellar objects of interest



Binary system {red giant + white dwarf}
Matter accretion → explosive hydrogen burning at surface

Impacts

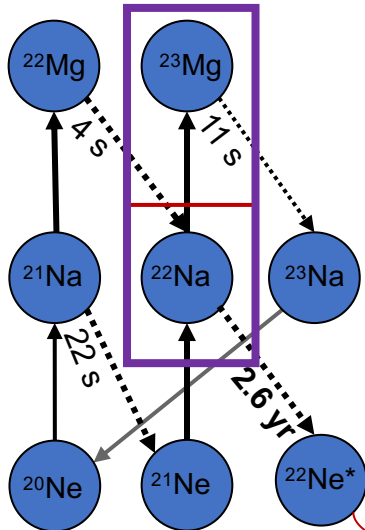
- Abundances of nuclei
- Isotopic composition of meteoritic presolar grains *Black (1972)*
- Test of Nova models
- Number of supernovae SNIa (dark energy)

Need of astronomical observables

Uncertainties

*Accretion dynamics,
initial WD temp.*

ONE novae



γ-ray observation campaigns

(INTEGRAL, COMPTEL...)

$E_\gamma = 1.275 \text{ MeV}$ never seen

Radiotracer ^{22}Na

$\tau = 2.6 \text{ yr}$, $E_\gamma = 1.275 \text{ MeV}$

$\gamma 1.275 \text{ MeV}$



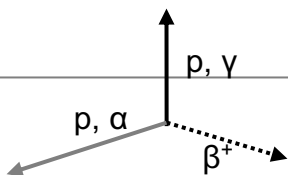
Sensitivity improved by x30

De Angelis, Tatischeff et al. (2017)

^{22}Na abundance in novae

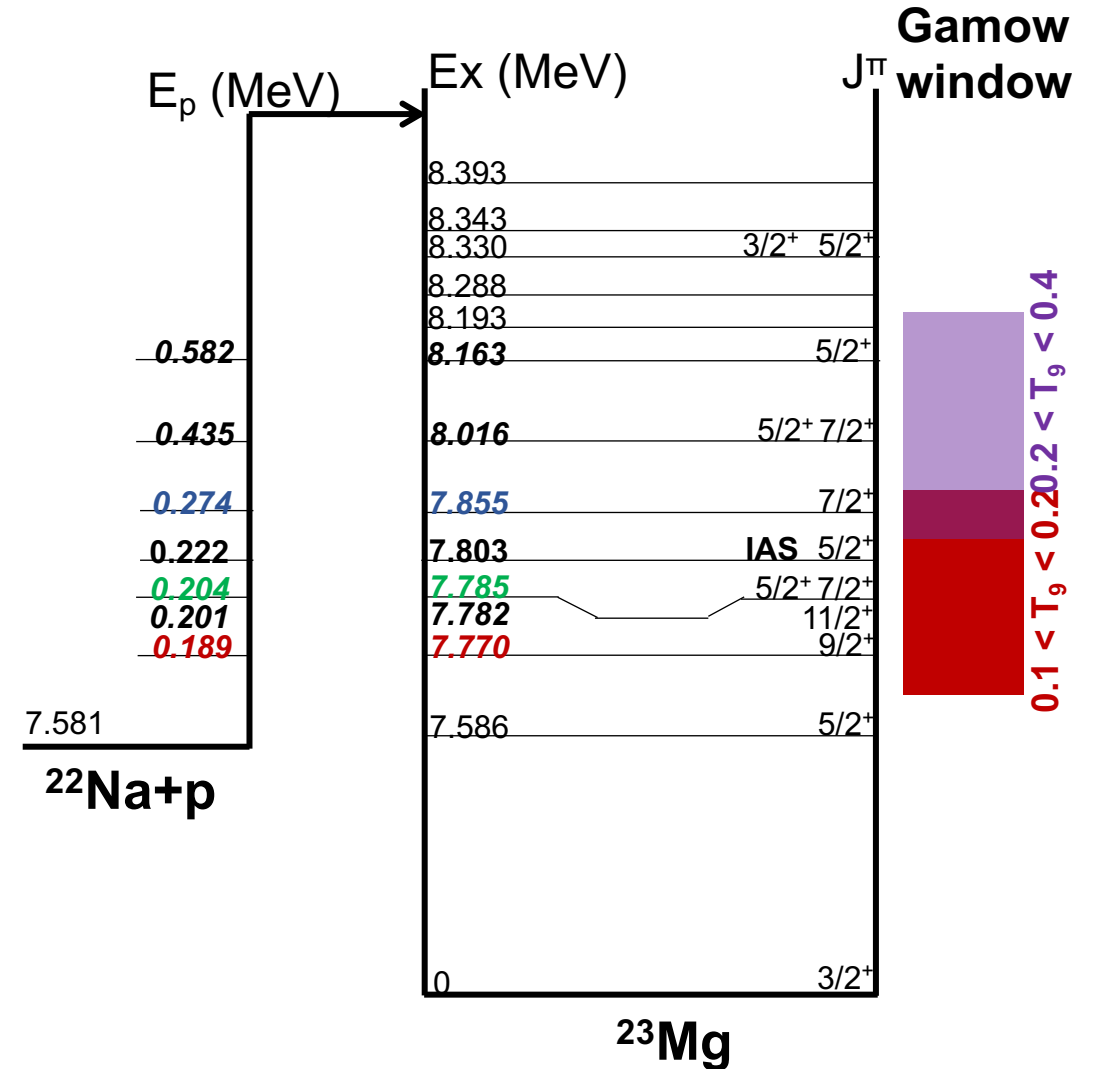
Detection limit

$^{22}\text{Na}(p, \gamma)^{23}\text{Mg}^$ rate*



Destruction $^{22}\text{Na}(p, \gamma)^{23}\text{Mg}$

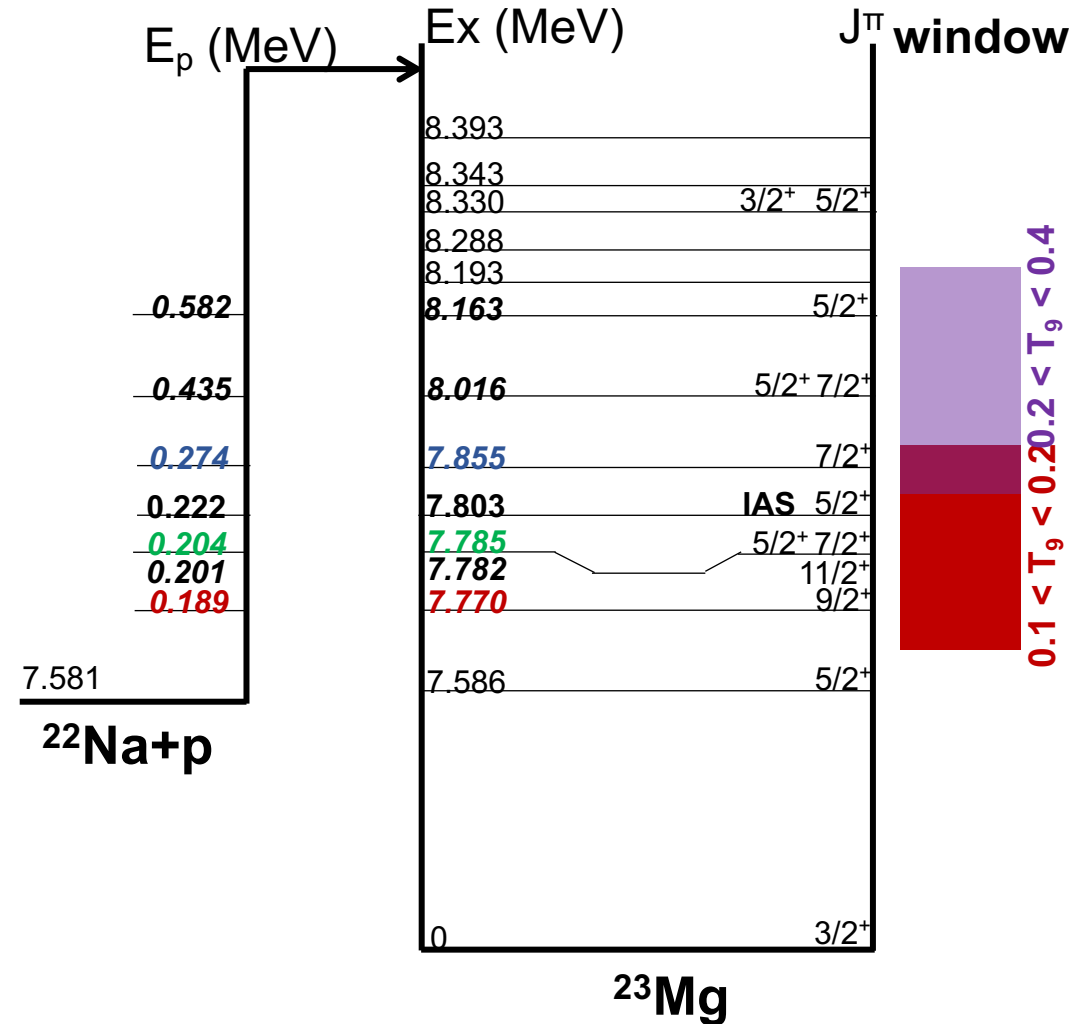
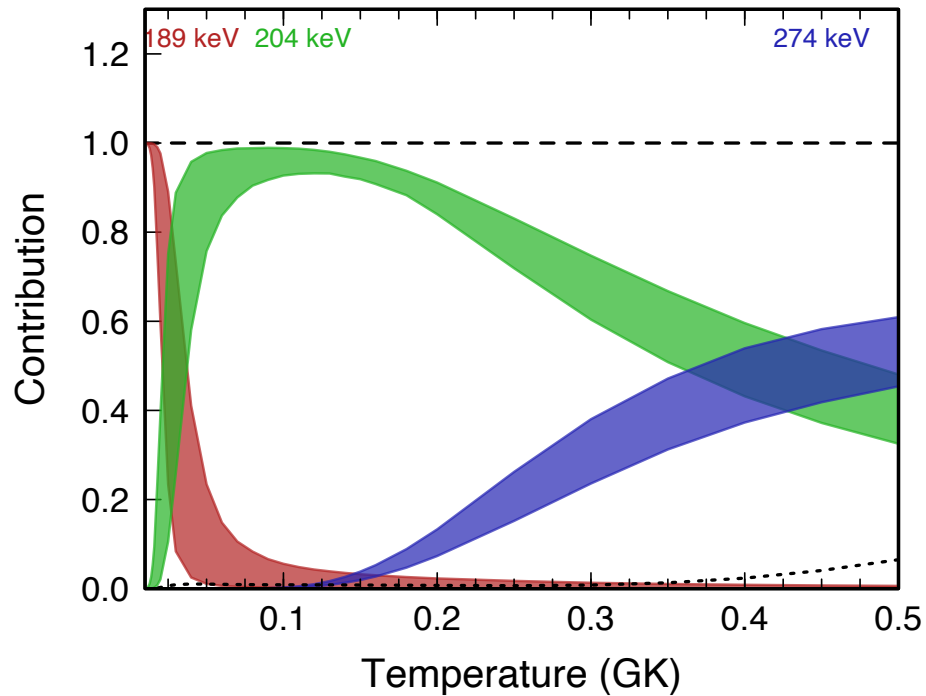
$$\langle \sigma v \rangle_{\text{tot}} = \sum_{\text{R}} \left(\frac{2\pi}{\mu(^{22}\text{Na}, p) k_{\text{B}} T} \right)^{\frac{3}{2}} \times \hbar^2 \times \omega \gamma \times \exp\left(-\frac{E_{\text{R}}}{k_{\text{B}} T}\right)$$



Destruction $^{22}\text{Na}(p, \gamma)^{23}\text{Mg}$

$$\langle \sigma v \rangle_{\text{tot}} = \sum_R \left(\frac{2\pi}{\mu(^{22}\text{Na}, p) k_B T} \right)^{\frac{3}{2}} \times \hbar^2 \times \omega \gamma \times \exp\left(-\frac{E_R}{k_B T}\right)$$

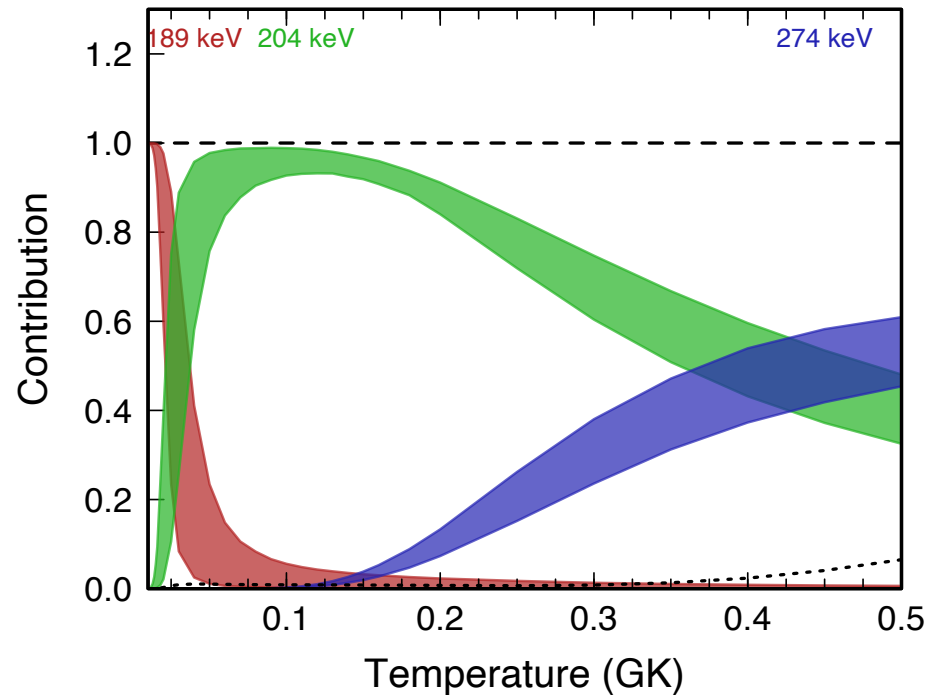
Direct $\omega\gamma$ measurements, TRIUMF $^{22}\text{Na}(p, \gamma)^{23}\text{Mg}$ Sallaska et al. (2011)



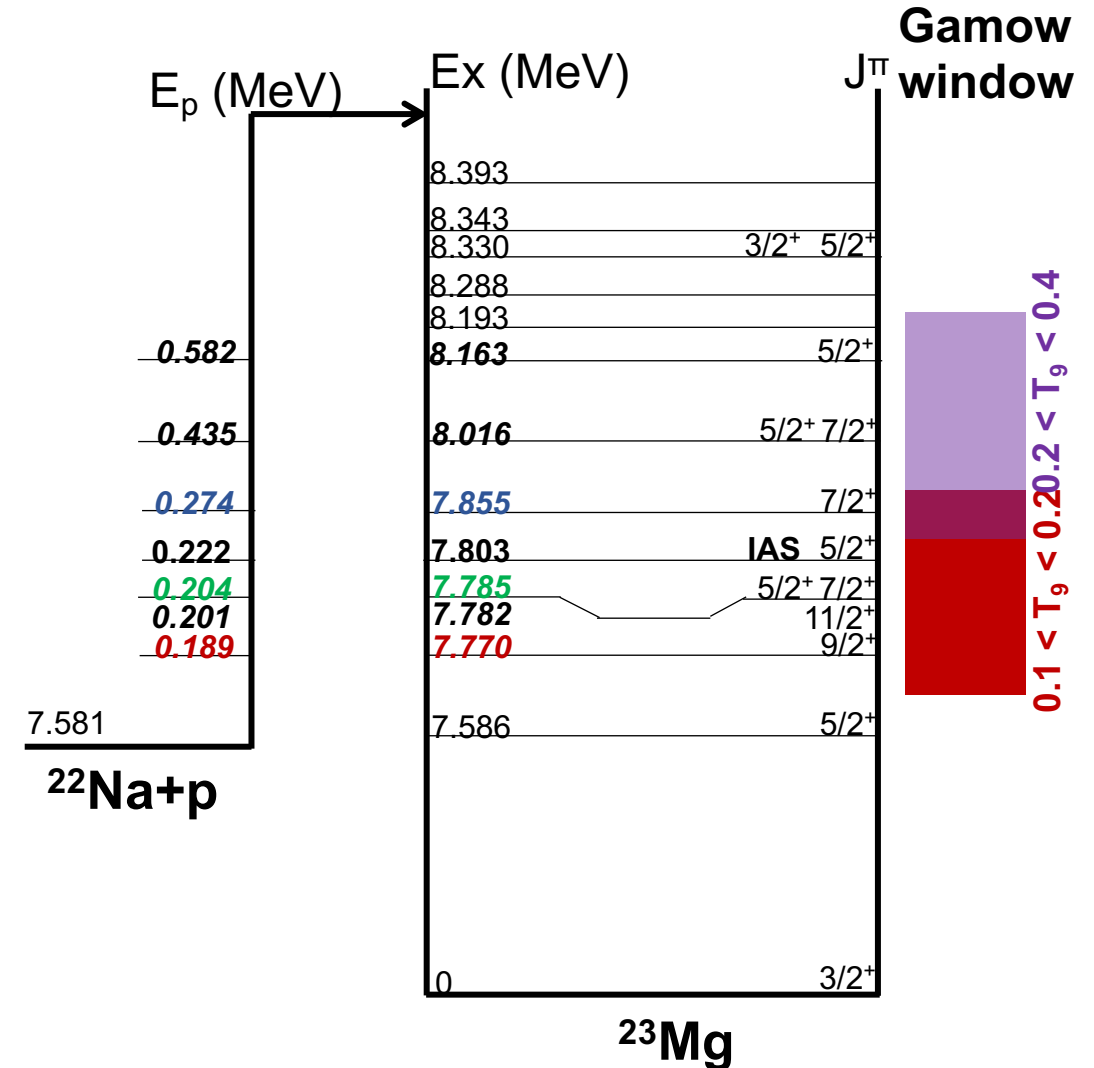
Destruction $^{22}\text{Na}(p, \gamma)^{23}\text{Mg}$

$$\langle \sigma v \rangle_{\text{tot}} = \sum_R \left(\frac{2\pi}{\mu(^{22}\text{Na}, p) k_B T} \right)^{\frac{3}{2}} \times \hbar^2 \times \omega \gamma \times \exp\left(-\frac{E_R}{k_B T}\right)$$

Direct $\omega\gamma$ measurements, TRIUMF $^{22}\text{Na}(p, \gamma)^{23}\text{Mg}$ Sallaska et al. (2011)



Dominant resonance
Ex=7.785 MeV, $E_R=0.204$ MeV in $^{23}\text{Mg}^*$

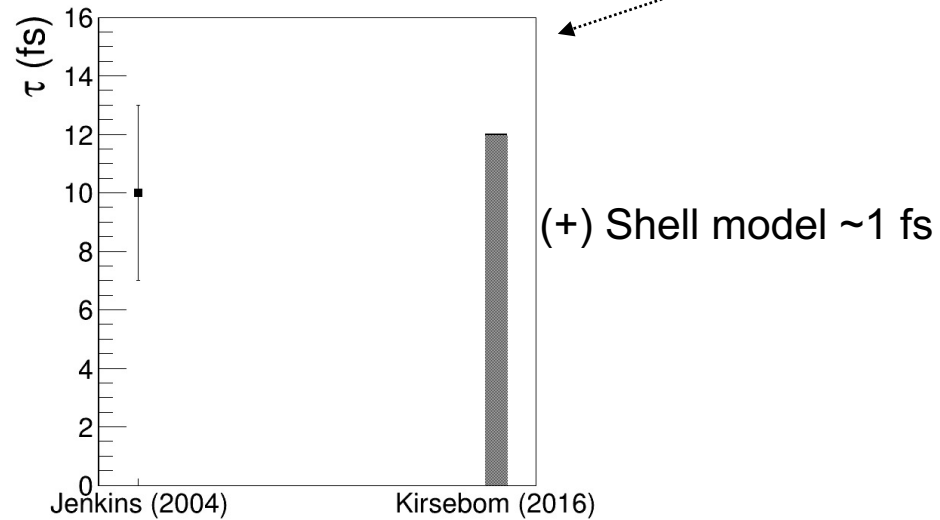


Indirect access to ω_γ at $E_R = 0.204$ MeV

$$\omega_\gamma = \frac{2J_{23\text{Mg}} + 1}{(2J_{22\text{Na}} + 1)(2J_p + 1)} \times \frac{\hbar}{\tau} \times \text{BR}_p(1 - \text{BR}_p)$$

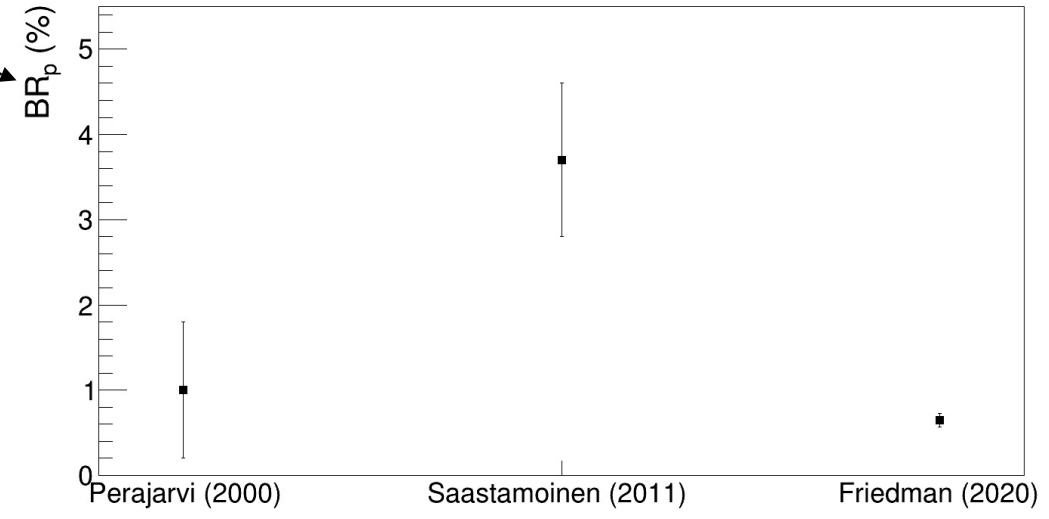
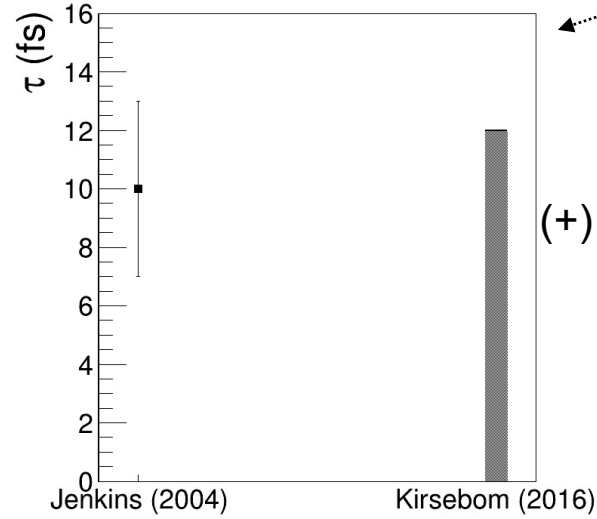
Indirect access to $\omega\gamma$ at $E_R = 0.204$ MeV

$$\omega\gamma = \frac{2J_{23\text{Mg}} + 1}{(2J_{22\text{Na}} + 1)(2J_p + 1)} \times \frac{\hbar}{\tau} \times \text{BR}_p(1 - \text{BR}_p)$$



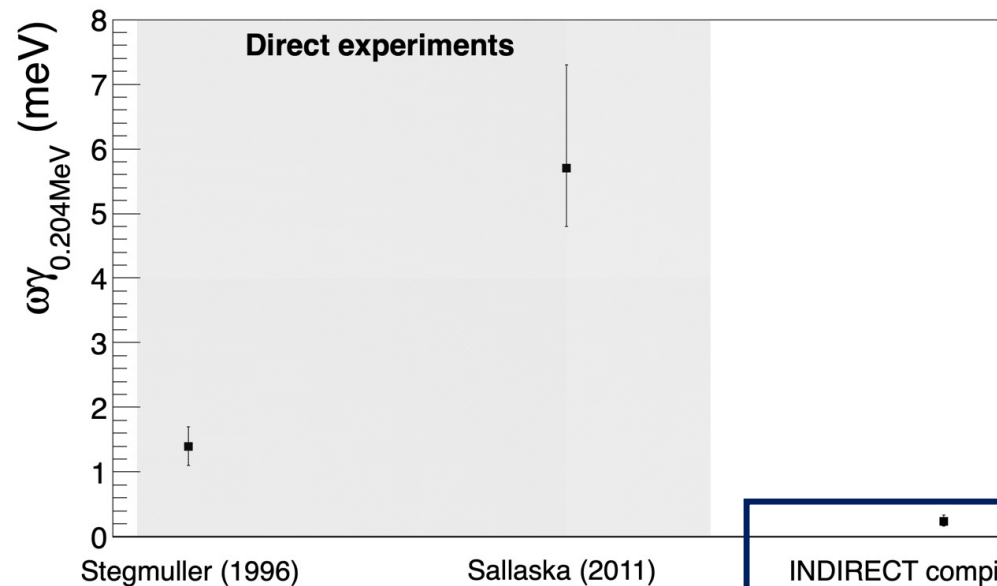
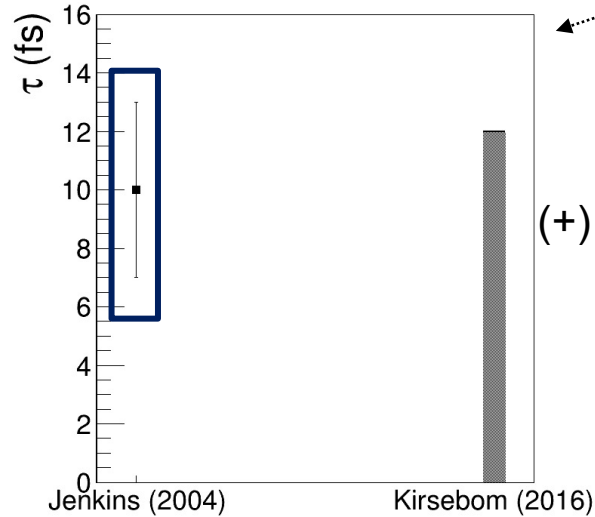
Indirect access to $\omega\gamma$ at $E_R = 0.204$ MeV

$$\omega\gamma = \frac{2J_{23\text{Mg}} + 1}{(2J_{22\text{Na}} + 1)(2J_p + 1)} \times \frac{\hbar}{\tau} \times \text{BR}_p(1 - \text{BR}_p)$$



Indirect access to $\omega\gamma$ at $E_R = 0.204$ MeV

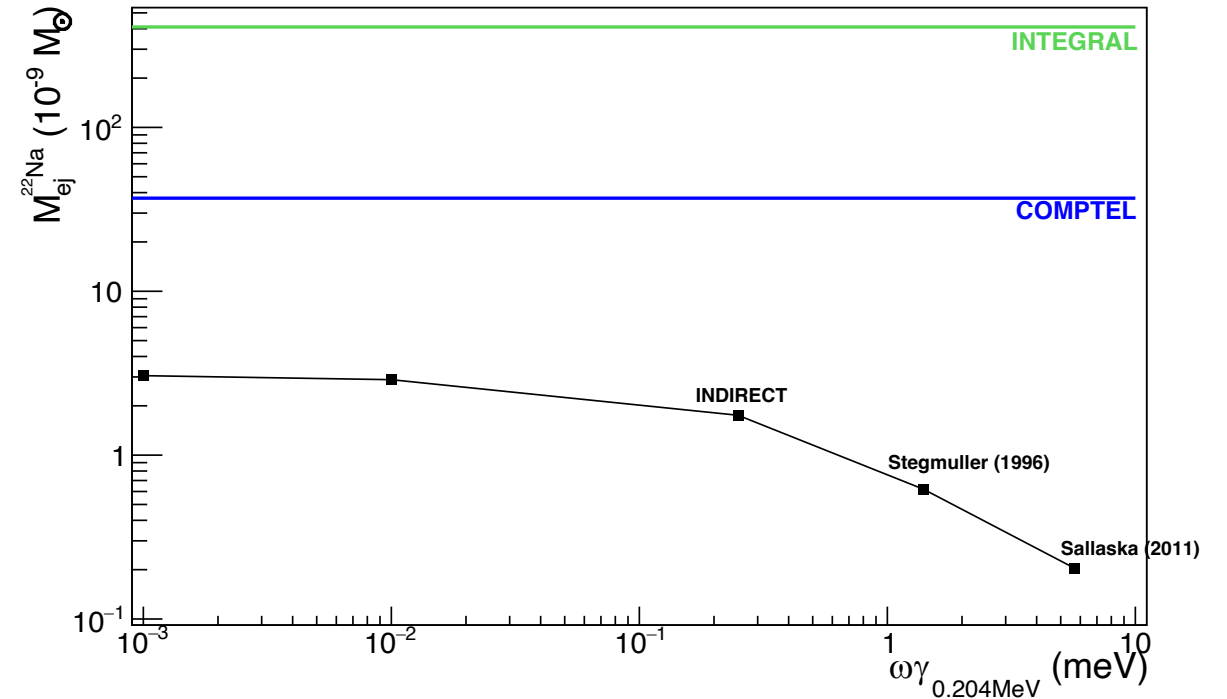
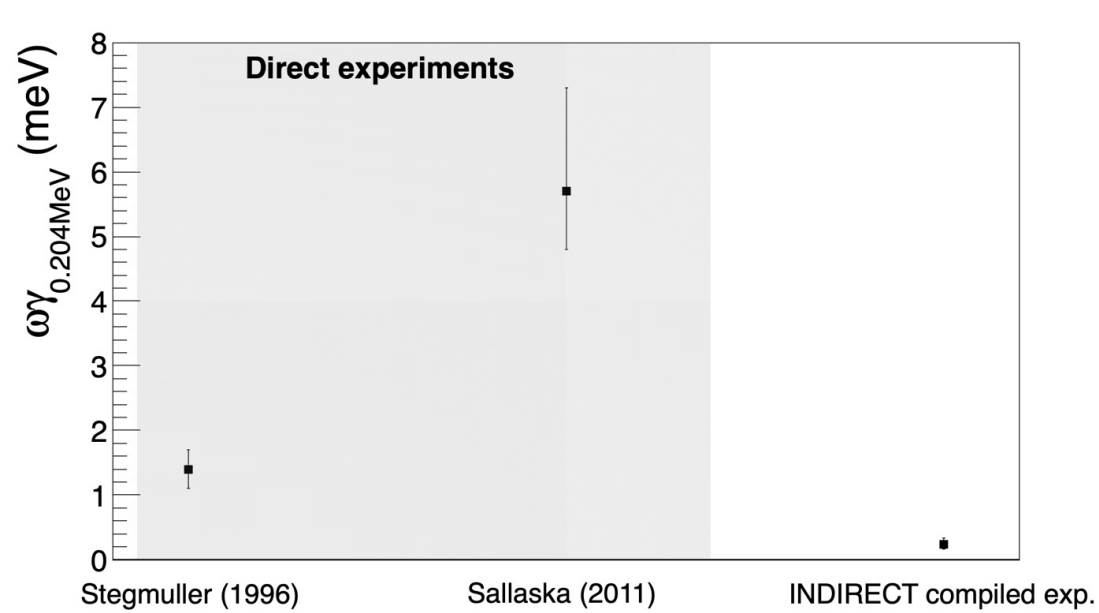
$$\omega\gamma = \frac{2J_{23\text{Mg}} + 1}{(2J_{22\text{Na}} + 1)(2J_p + 1)} \times \frac{\hbar}{\tau} \times \text{BR}_p(1 - \text{BR}_p)$$



Disagreement in $\omega\gamma$

Indirect access to $\omega\gamma$ at $E_R = 0.204$ MeV

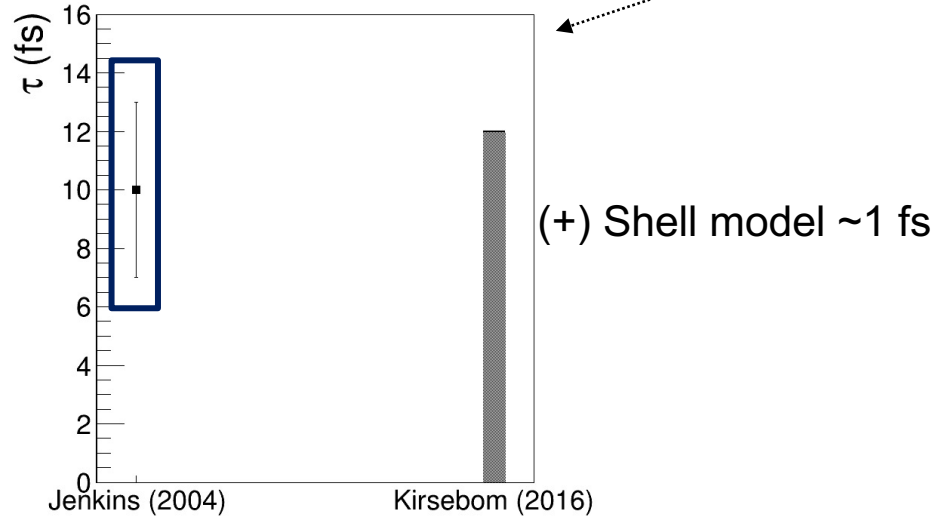
$$\omega\gamma = \frac{2J_{23\text{Mg}} + 1}{(2J_{22\text{Na}} + 1)(2J_p + 1)} \times \frac{\hbar}{\tau} \times \text{BR}_p(1 - \text{BR}_p)$$



Disagreement in $\omega\gamma \rightarrow$ predicted $^{22}\text{Na} \sim \times 10$

Indirect access to $\omega\gamma$ at $E_R = 0.204$ MeV

$$\omega\gamma = \frac{2J_{23\text{Mg}} + 1}{(2J_{22\text{Na}} + 1)(2J_p + 1)} \times \frac{\hbar}{\tau} \times \text{BR}_p(1 - \text{BR}_p)$$



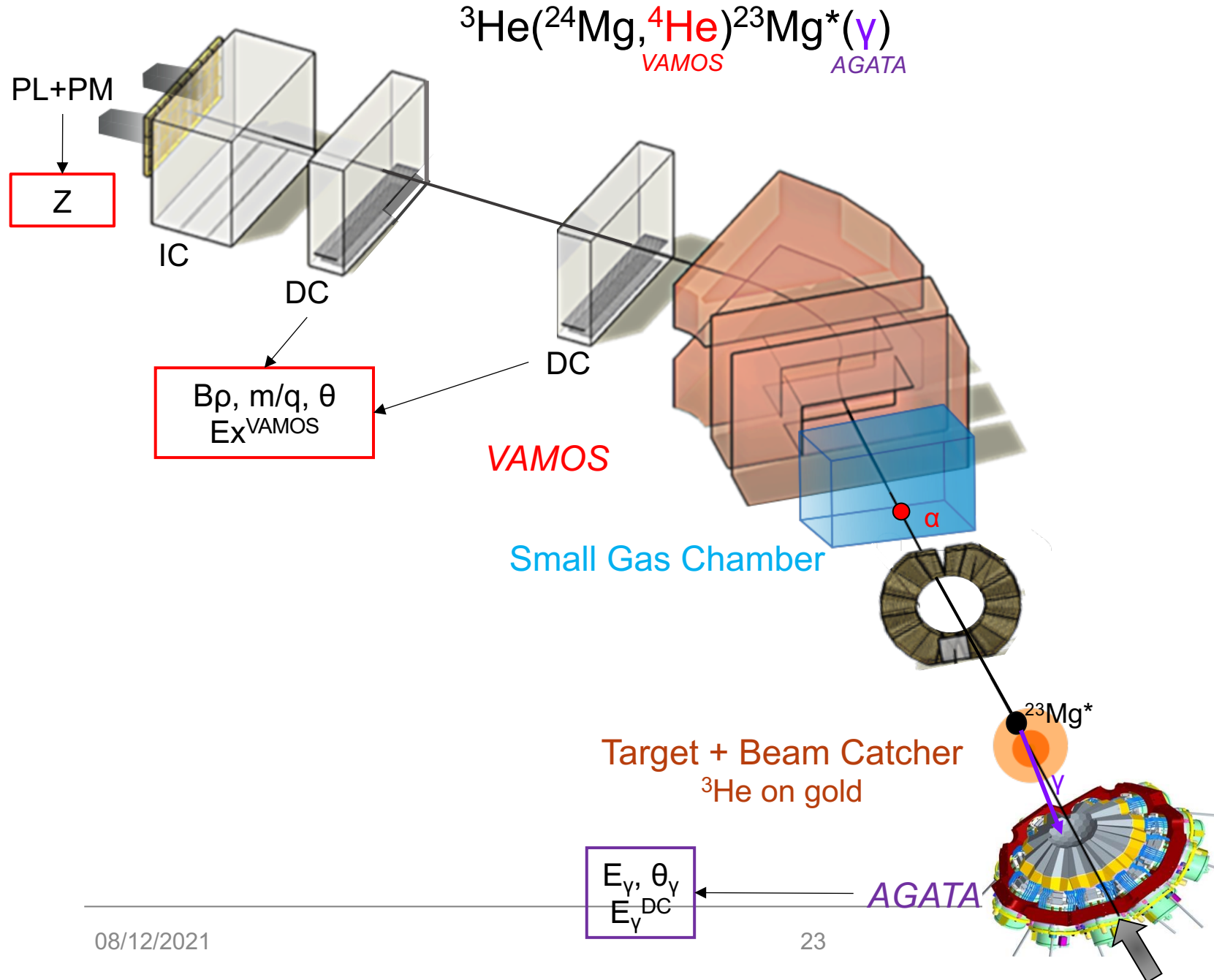
E710 indirect method on $E_x=7.785$ MeV in $^{23}\text{Mg}^*$
(τ , BR_p)

Use of AGATA \rightarrow fs resolution by DSAM on $^{15}\text{O}^*$
Michelagnoli Ph.D. thesis (2013)

Experimental approach

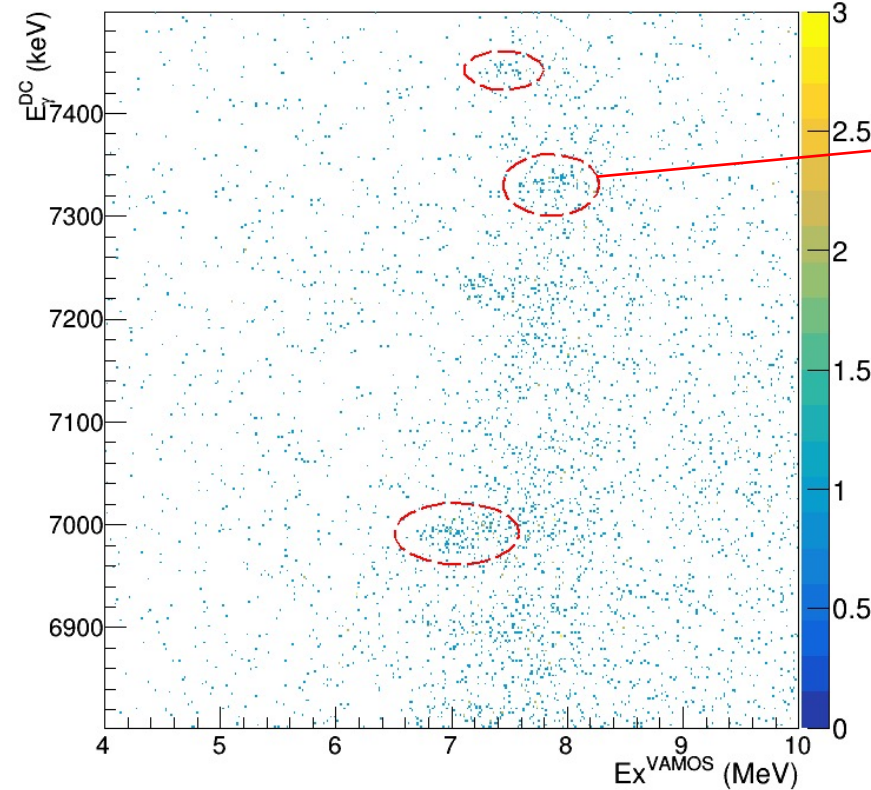
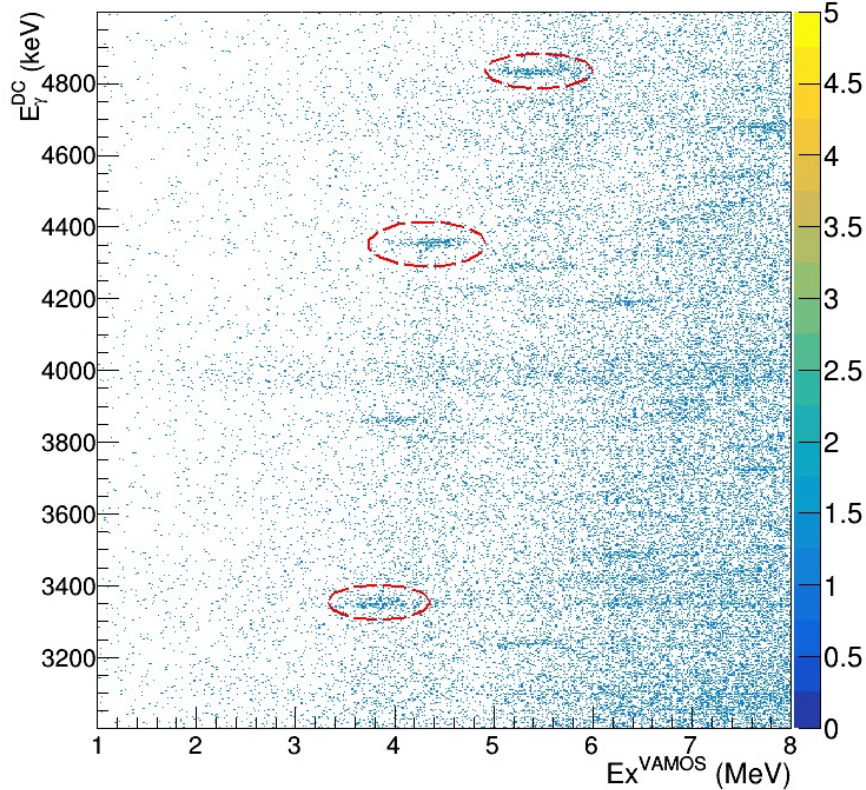
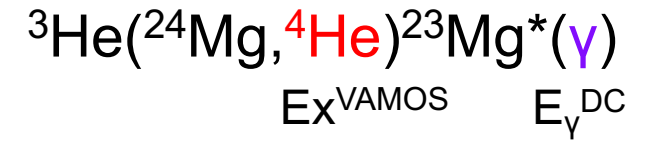
Indirect E710@GANIL
C. Michelagnoli et al.

Set-up



BEAM
²⁴Mg at 4.6 MeV/u

Population of states in $^{23}\text{Mg}^*$

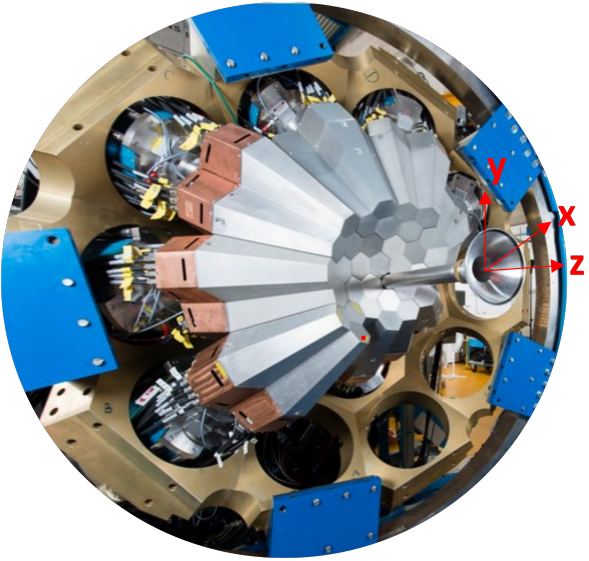


Ex=7.785 MeV state

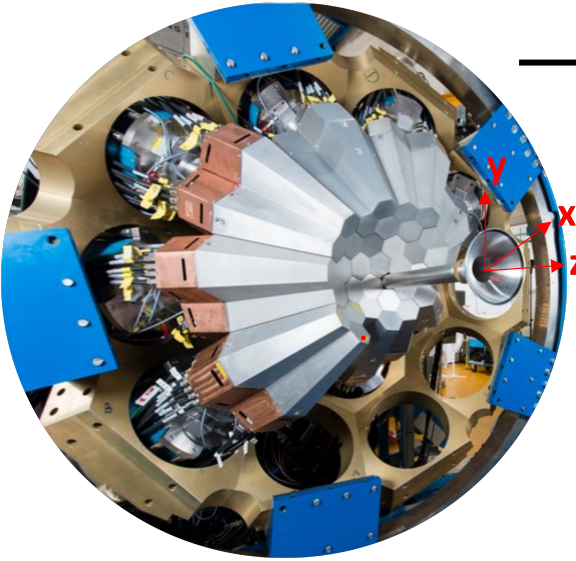
${}^{23}\text{Mg}^*(E_x, E_{\gamma,0})$ MeV	E_x^{VAMOS} MeV $\pm \sigma$
3.794, 3.344	3.79(1) \pm 0.27
4.356, 4.356	4.35(1) \pm 0.19
5.287, 4.836	5.25(2) \pm 0.16
6.984, 6.984	6.99(1) \pm 0.17
7.450, 7.443	7.44(8) \pm 0.31
7.785, 7.333	7.78(1) \pm 0.15

22 states in ${}^{23}\text{Mg}^*$ identified and isolated at $E_x \pm 0.3$ MeV

Accessing γ -ray transition with AGATA



Accessing γ -ray transition with AGATA

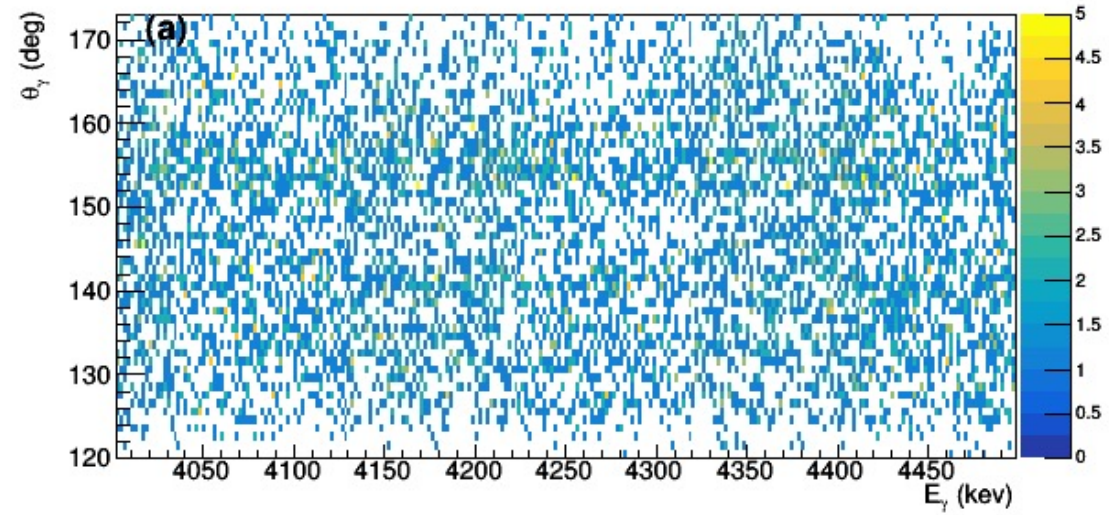


AGATA

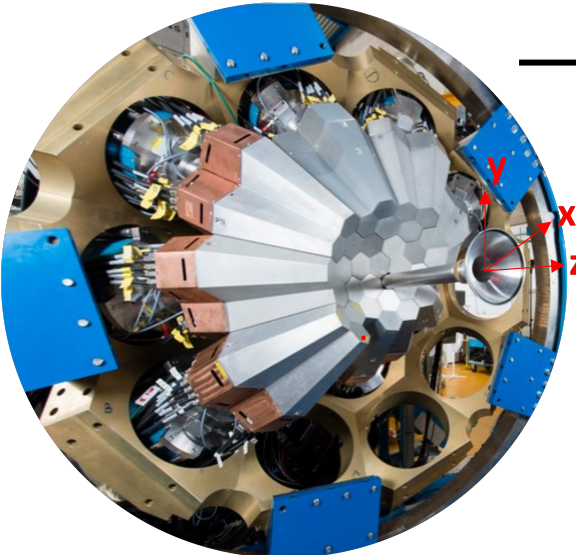
high resolution
continuous
angular coverage

Transition observed in 2-dimensions (E_γ , θ_γ)

no selection on E_x^{VAMOS}



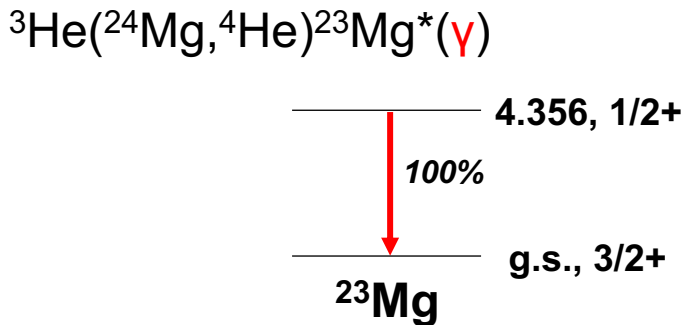
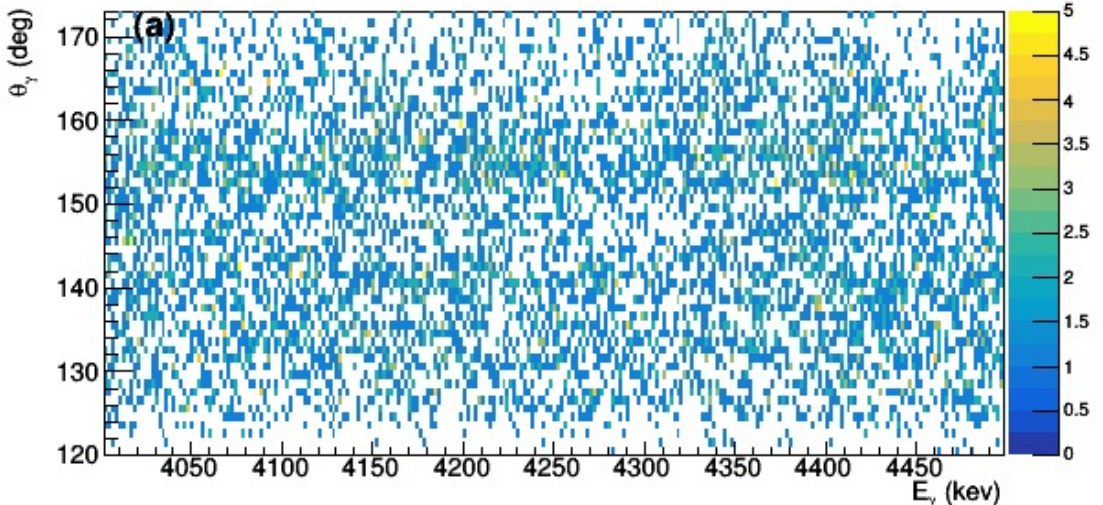
Accessing γ -ray transition with AGATA



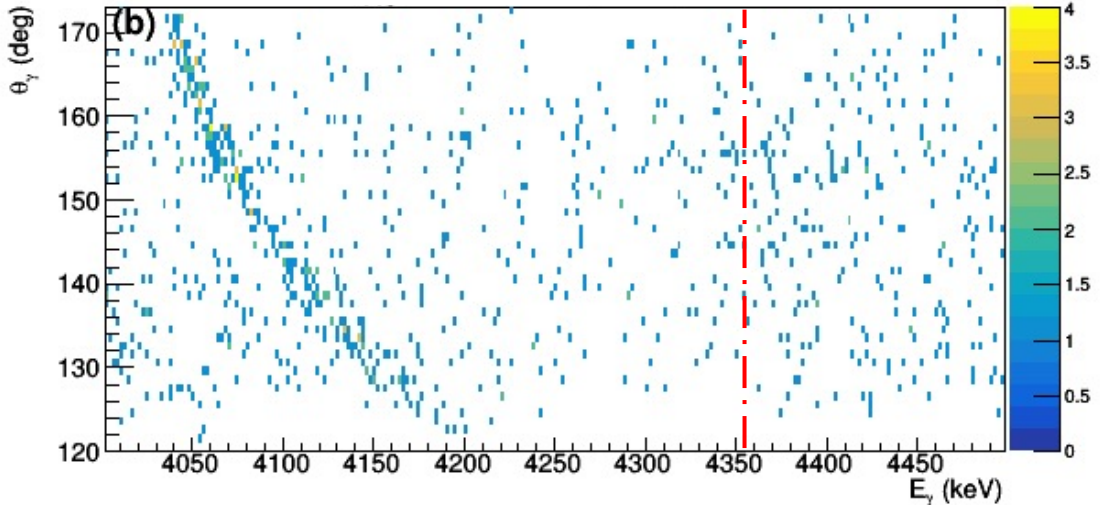
AGATA
 high resolution
 continuous
 angular coverage

Transition observed in 2-dimensions (E_γ , θ_γ)

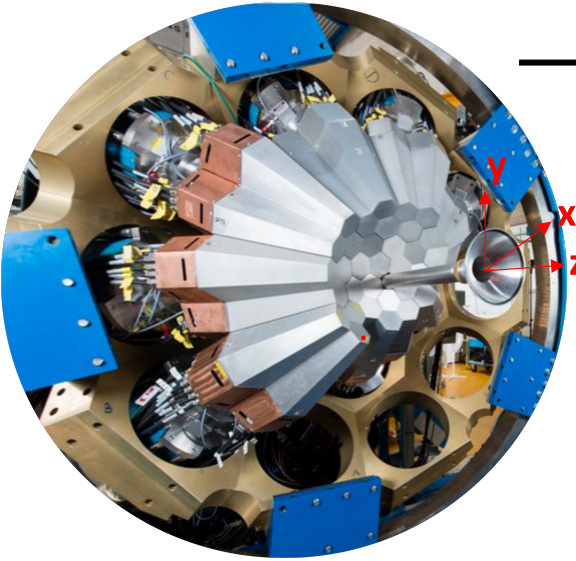
no selection on E_x^{VAMOS}



selection on $E_x^{\text{VAMOS}} = 4.35 \pm 0.2 \text{ MeV}$

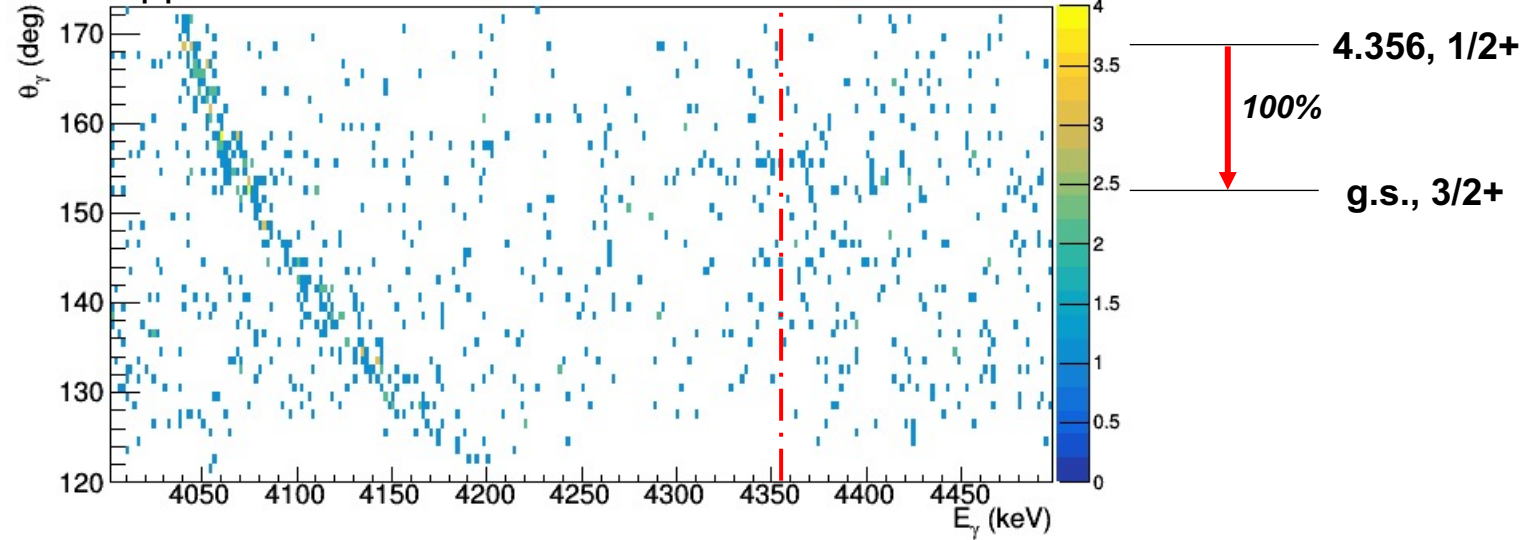


Accessing γ -ray transition with AGATA

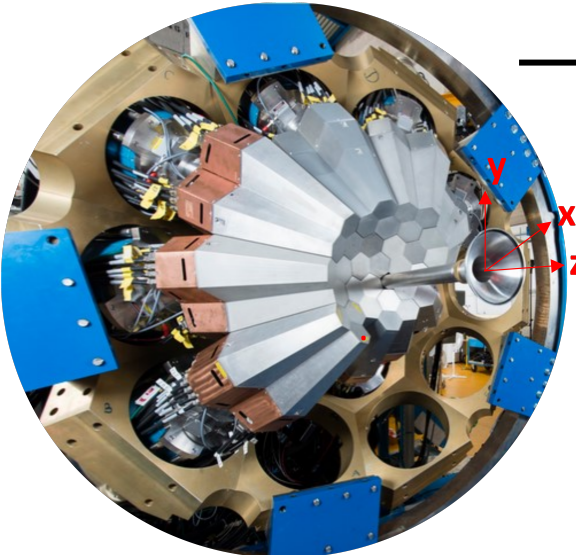


AGATA
high resolution
continuous
angular coverage

No Doppler Correction

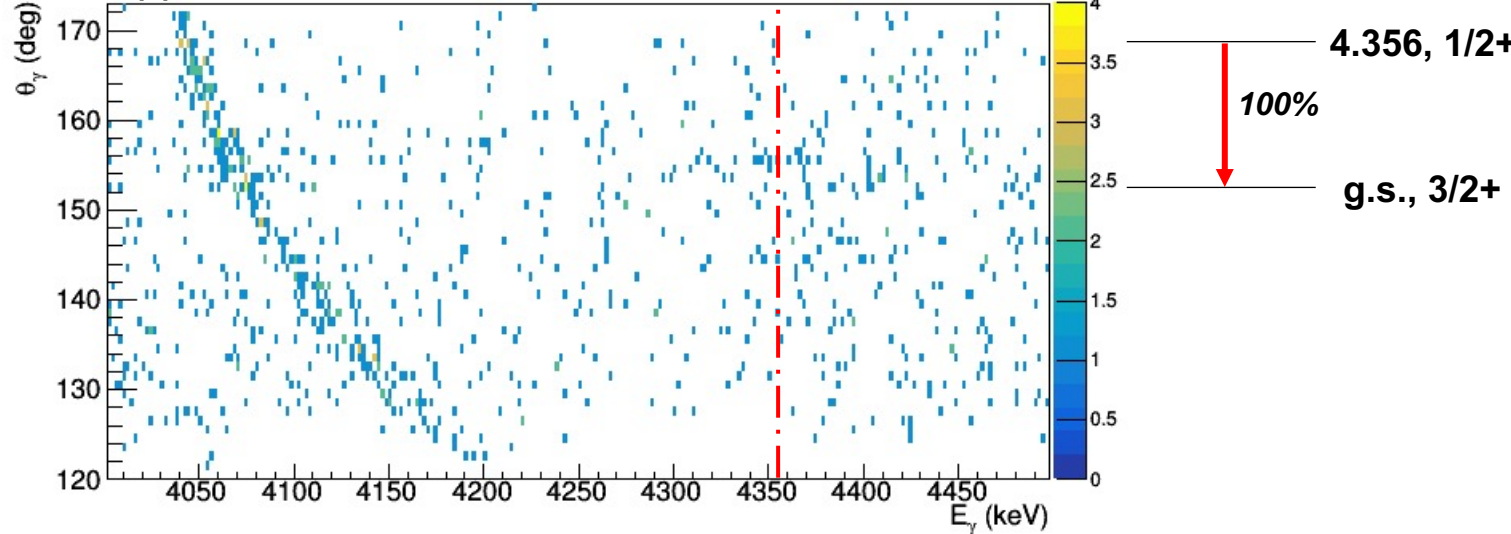


Accessing γ -ray transition with AGATA

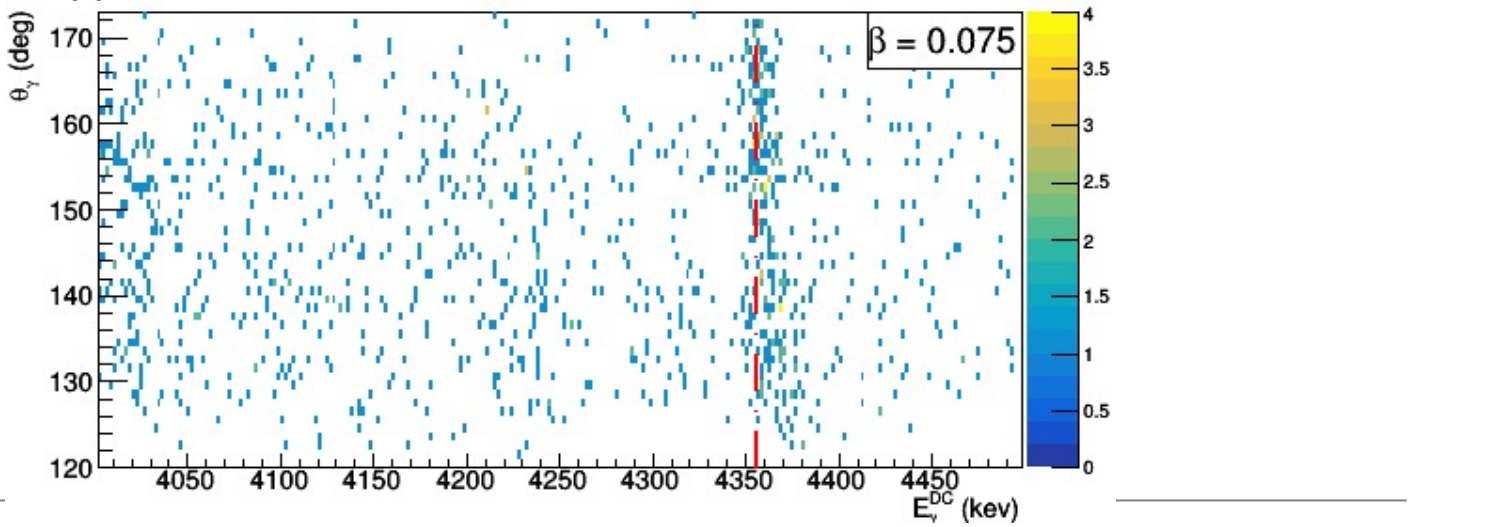


AGATA
high resolution
continuous
angular coverage

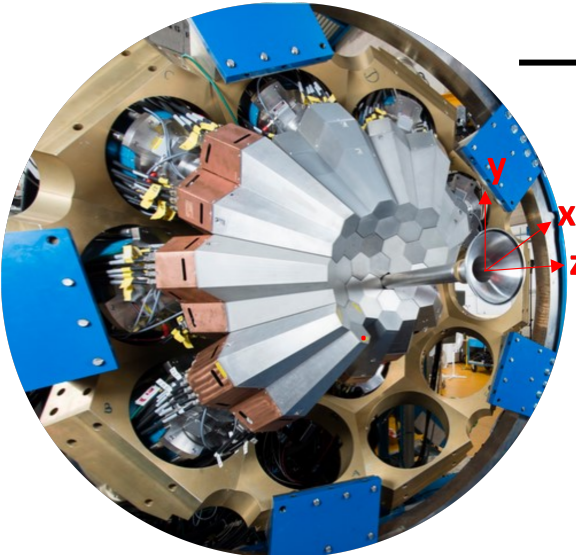
No Doppler Correction



Doppler Correction

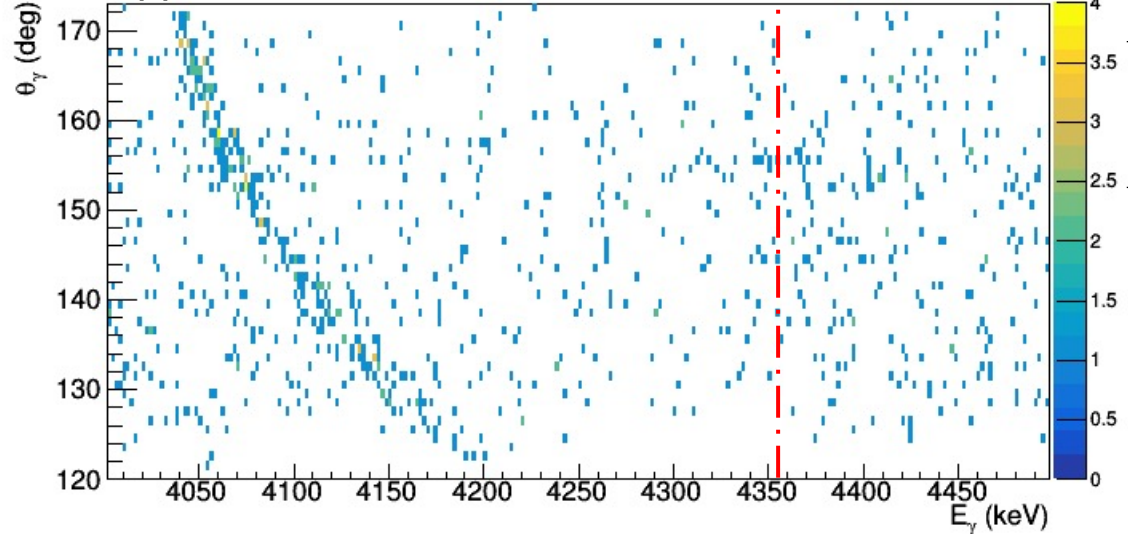


Accessing γ -ray transition with AGATA



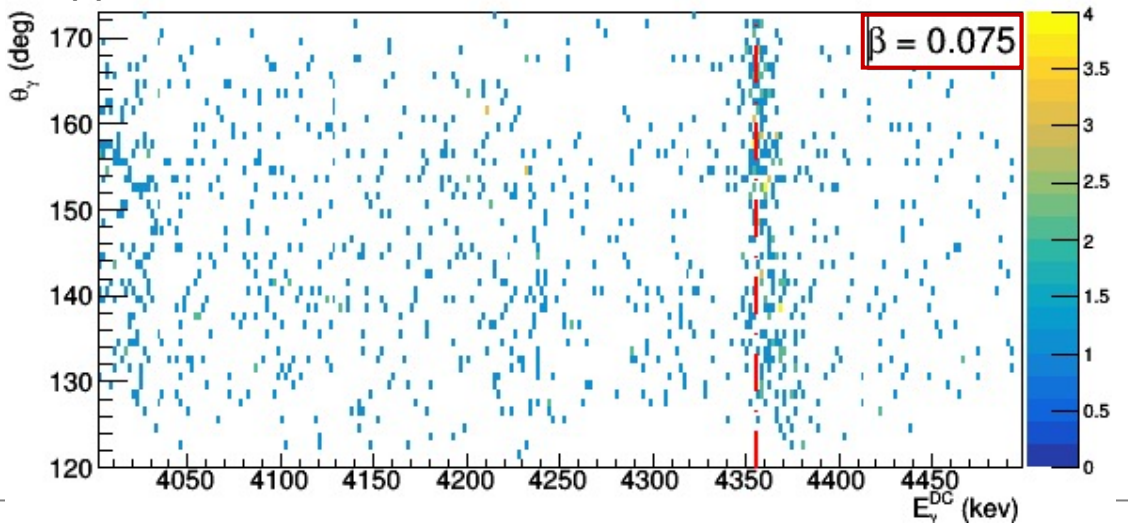
AGATA
high resolution
continuous
angular coverage

No Doppler Correction



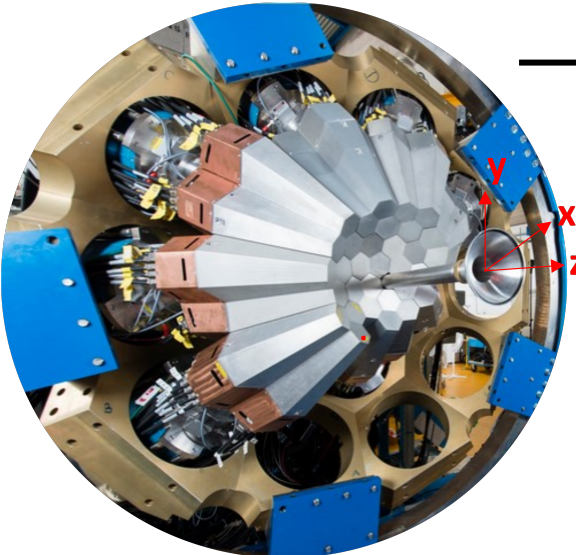
4.356, 1/2+
100%
g.s., 3/2+

Doppler Correction



mean $\beta=0.075(1)$

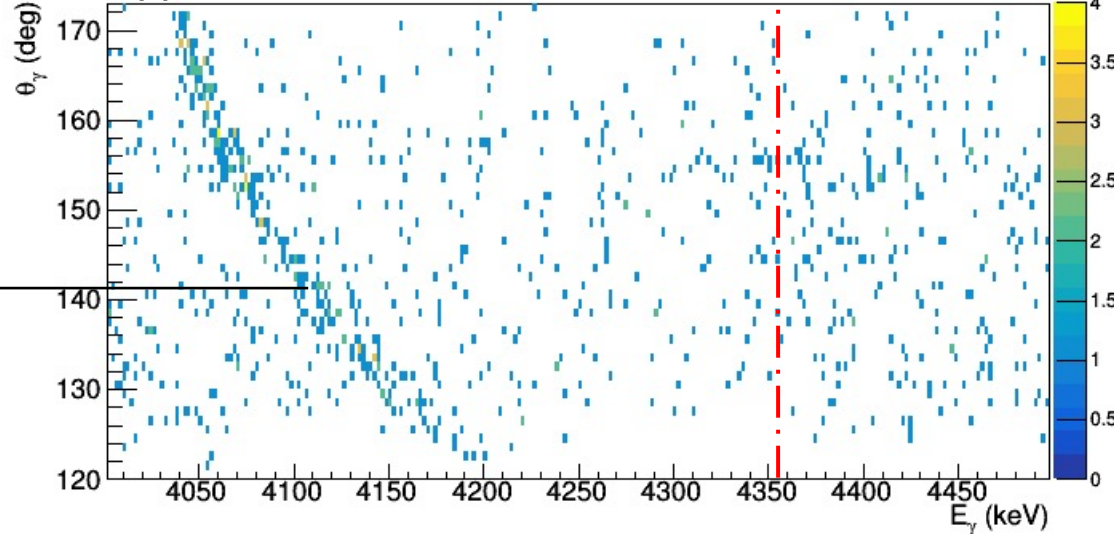
Accessing γ -ray transition with AGATA



AGATA
 high resolution
 continuous
 angular coverage

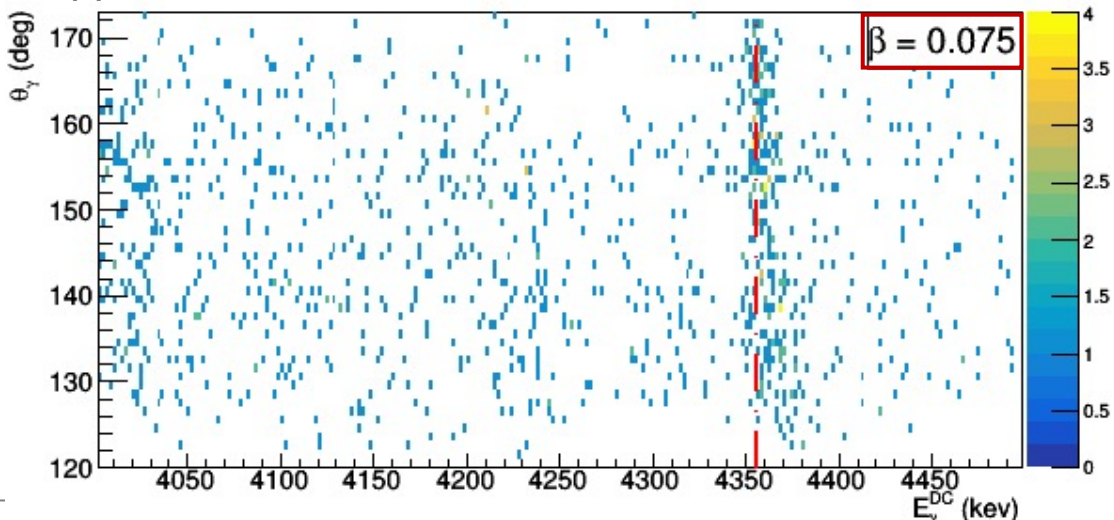
Reconstruct β on event basis

No Doppler Correction



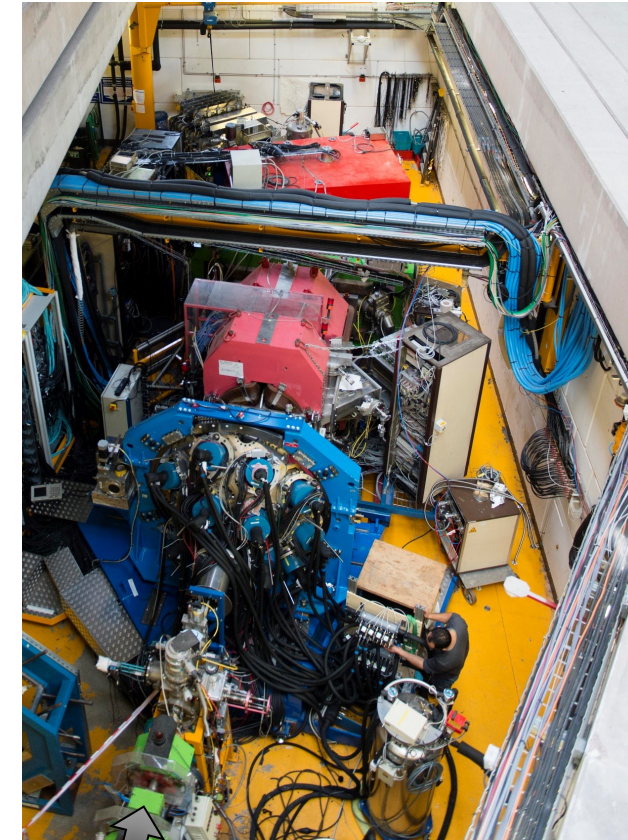
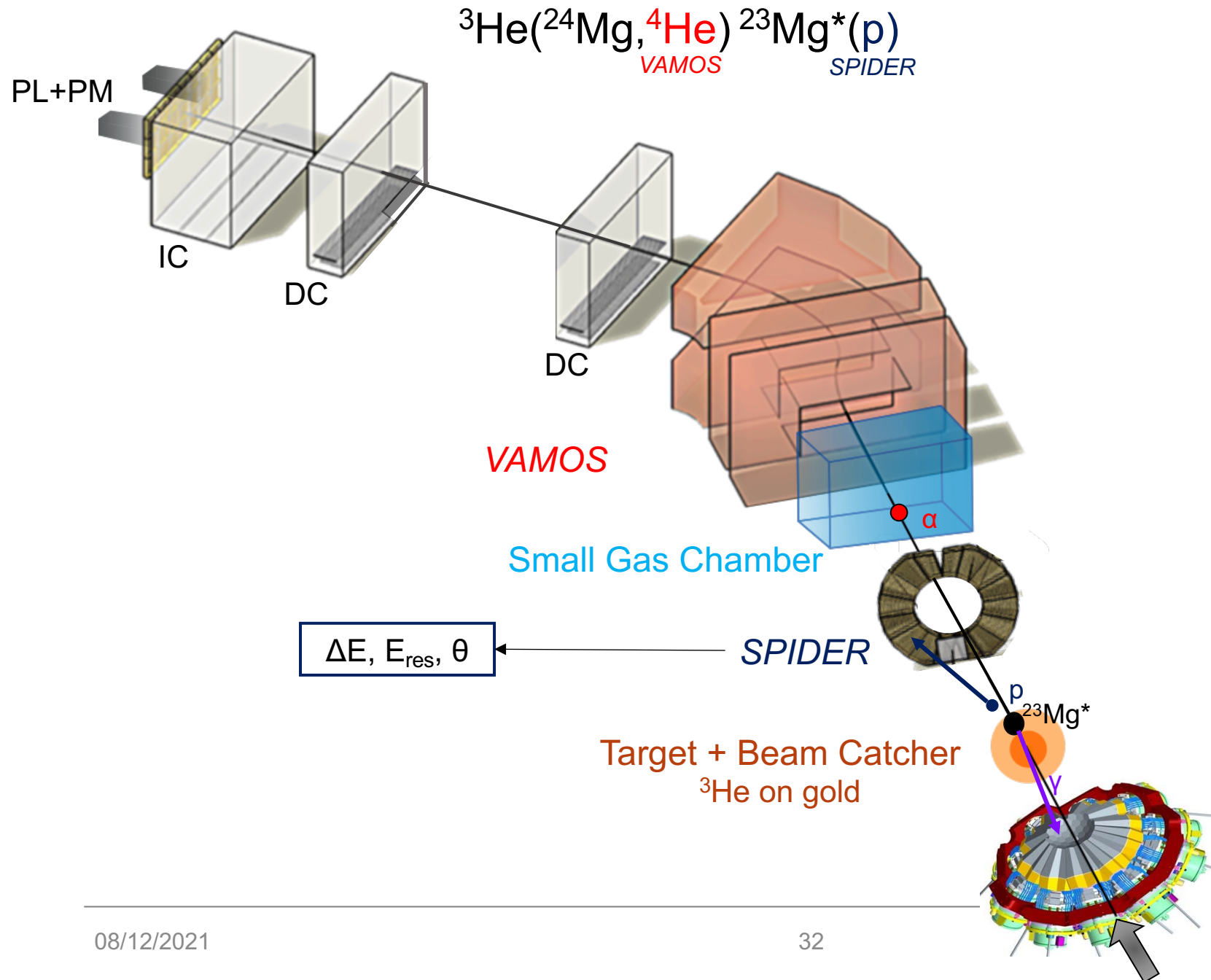
4.356, 1/2+
 100%
 g.s., 3/2+

Doppler Correction



mean $\beta=0.075(1)$

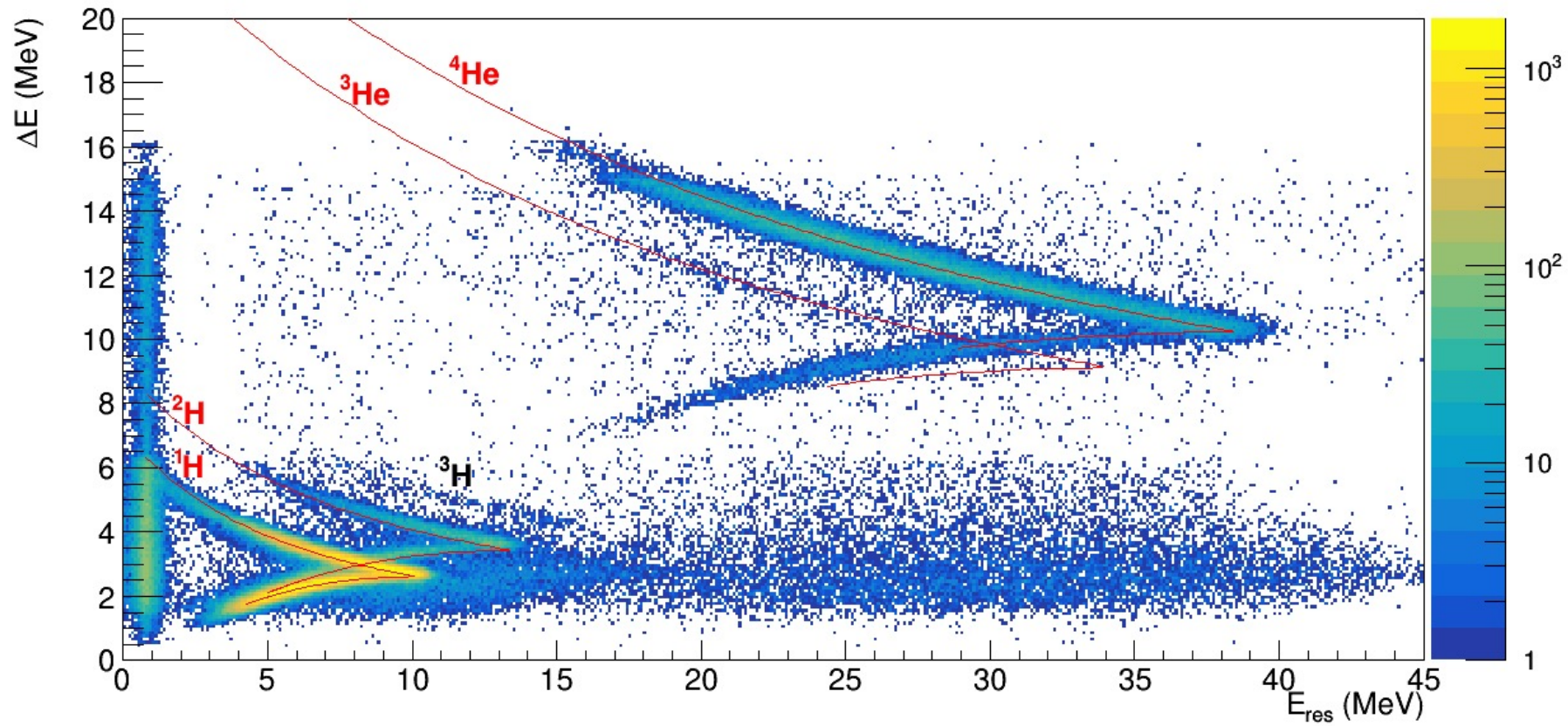
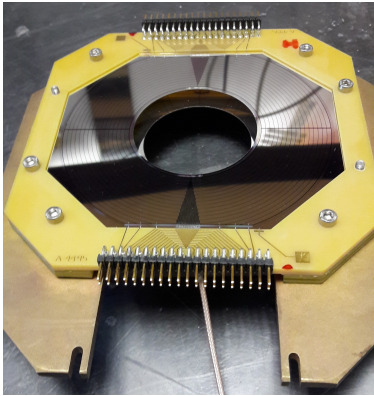
Set-up



BEAM
 ${}^{24}\text{Mg}$ at 4.6 MeV/u

SPIDER

Identification of ejectiles and p decay



Preliminary results

Spectroscopy of the $E_x=7.785$ MeV excited state in $^{23}\text{Mg}^*$

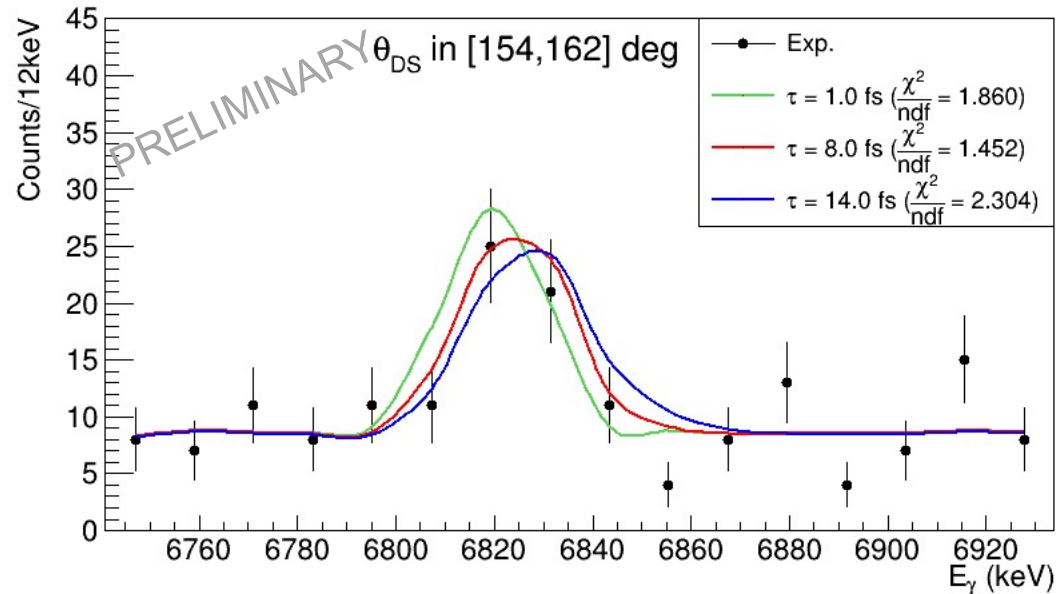
Accessing to lifetimes (1)

Based on lineshape analysis where experiment compared with simulations (EVASIONS code built for E710)

Accessing to lifetimes (1)

Method N°1: DSAM *classical*

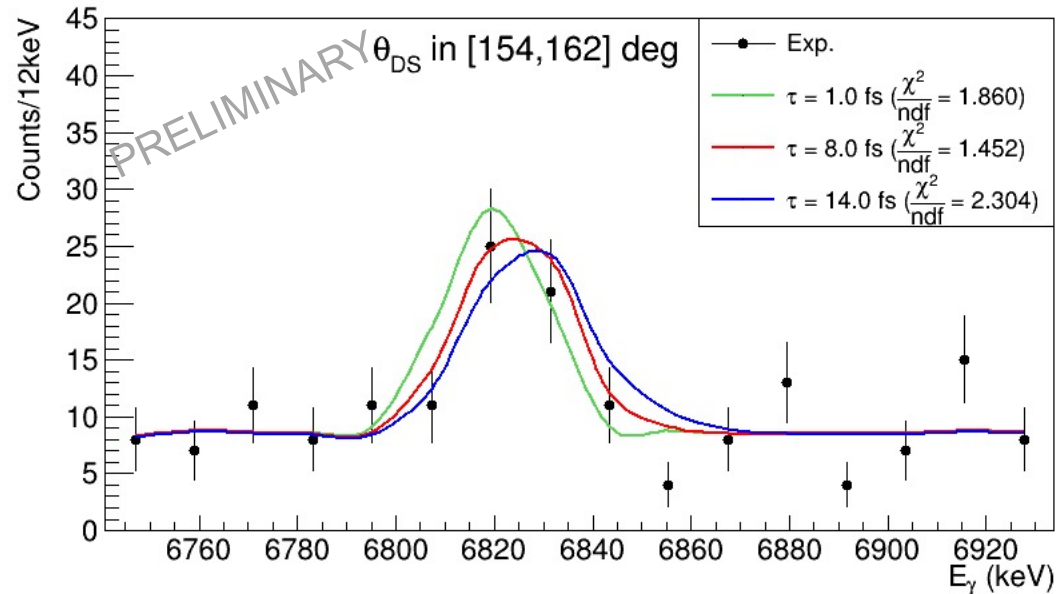
Doppler shifted E_γ projected on angle slices $\longrightarrow E_\gamma = E_{\gamma,0} \frac{\sqrt{1 - \beta^2}}{1 - \beta \cos(\theta_{DS})}$



Accessing to lifetimes (1)

Method N°1: DSAM *classical*

Doppler shifted E_γ projected on angle slices $\longrightarrow E_\gamma = E_{\gamma,0} \frac{\sqrt{1 - \beta^2}}{1 - \beta \cos(\theta_{DS})}$



$\longrightarrow \tau < 17$ fs

Accessing to lifetimes (2)

Method N°2: DCLM *recent*

Doppler-Corrected Lineshape Method (angle-integrated E_γ^{DC})

$$\longrightarrow E_\gamma^{\text{DC}} = E_\gamma \frac{1 - \beta_{\text{DC}} \cos(\theta_{\text{DS}})}{\sqrt{1 - \beta_{\text{DC}}^2}}$$

$$\text{with } \beta_{\text{DC}} = \text{mean}(\beta^{\text{Sim.}}(\tau))$$

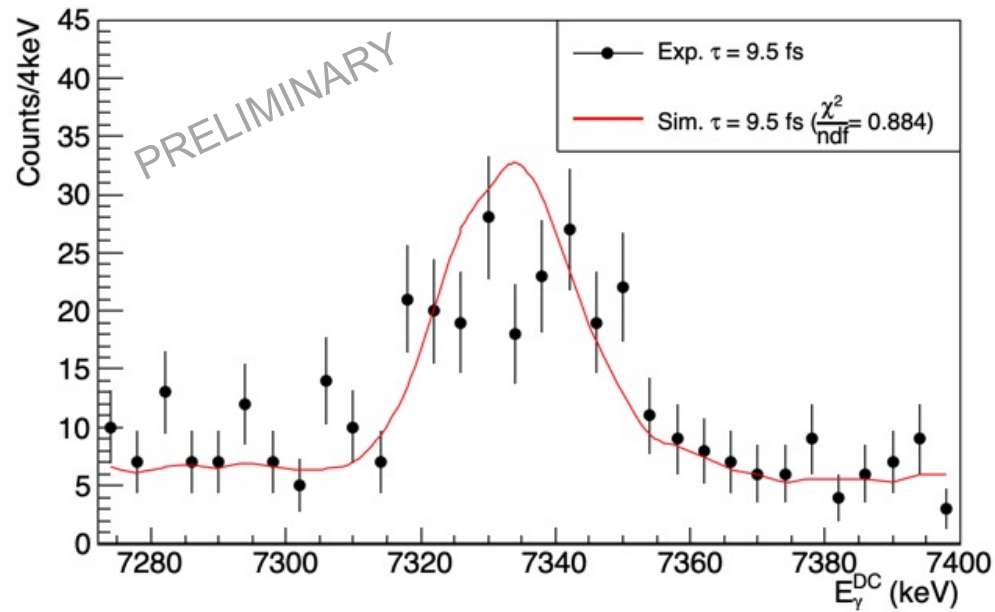
Accessing to lifetimes (2)

Method N°2: DCLM *recent*

Doppler-Corrected Lineshape Method (angle-integrated E_γ^{DC})

$$\longrightarrow E_\gamma^{\text{DC}} = E_\gamma \frac{1 - \beta_{\text{DC}} \cos(\theta_{\text{DS}})}{\sqrt{1 - \beta_{\text{DC}}^2}}$$

$$\text{with } \beta_{\text{DC}} = \text{mean}(\beta^{\text{Sim.}}(\tau))$$



$$\longrightarrow \tau = 9.5^{+3}_{-2} \text{ fs}$$

Accessing to lifetimes (3)

Method N°3: β distribution *new*

Distribution of β reconstructed from (E_γ, θ_{DS})

$$\longrightarrow \beta = \frac{R^2 \cos(\theta_{DS}) + \sqrt{1 + R^2 \cos(\theta_{DS})^2 - R^2}}{R^2 \cos(\theta_{DS})^2 + 1}$$

$$R = \frac{E_\gamma}{E_{\gamma,0}}$$

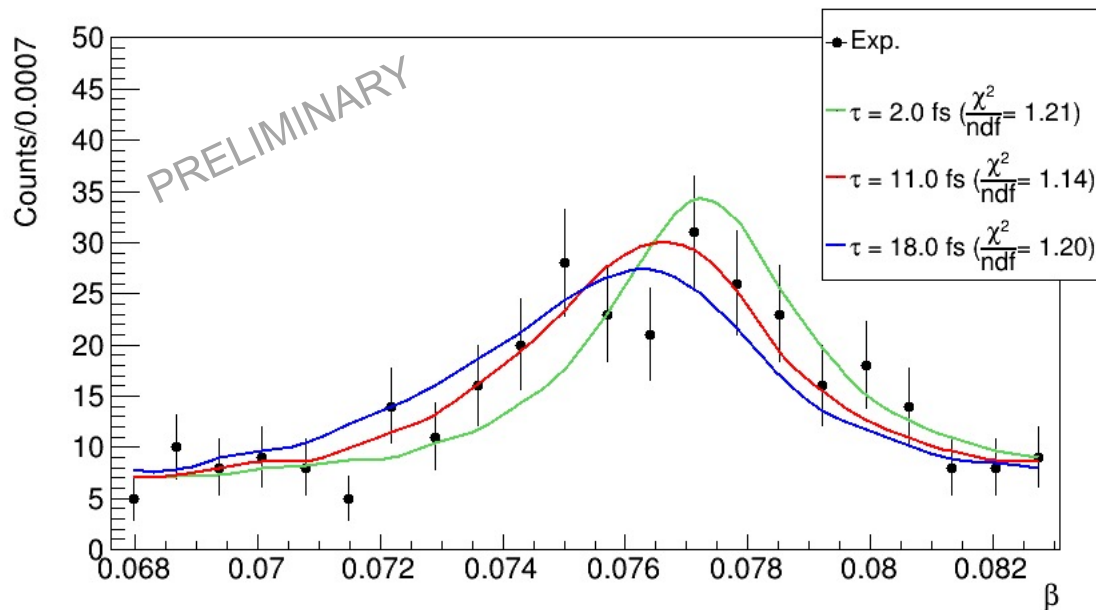
Accessing to lifetimes (3)

Method N°3: β distribution *new*

Distribution of β reconstructed from (E_γ, θ_{DS})

$$\beta = \frac{R^2 \cos(\theta_{DS}) + \sqrt{1 + R^2 \cos(\theta_{DS})^2 - R^2}}{R^2 \cos(\theta_{DS})^2 + 1}$$

$$R = \frac{E_\gamma}{E_{\gamma,0}}$$

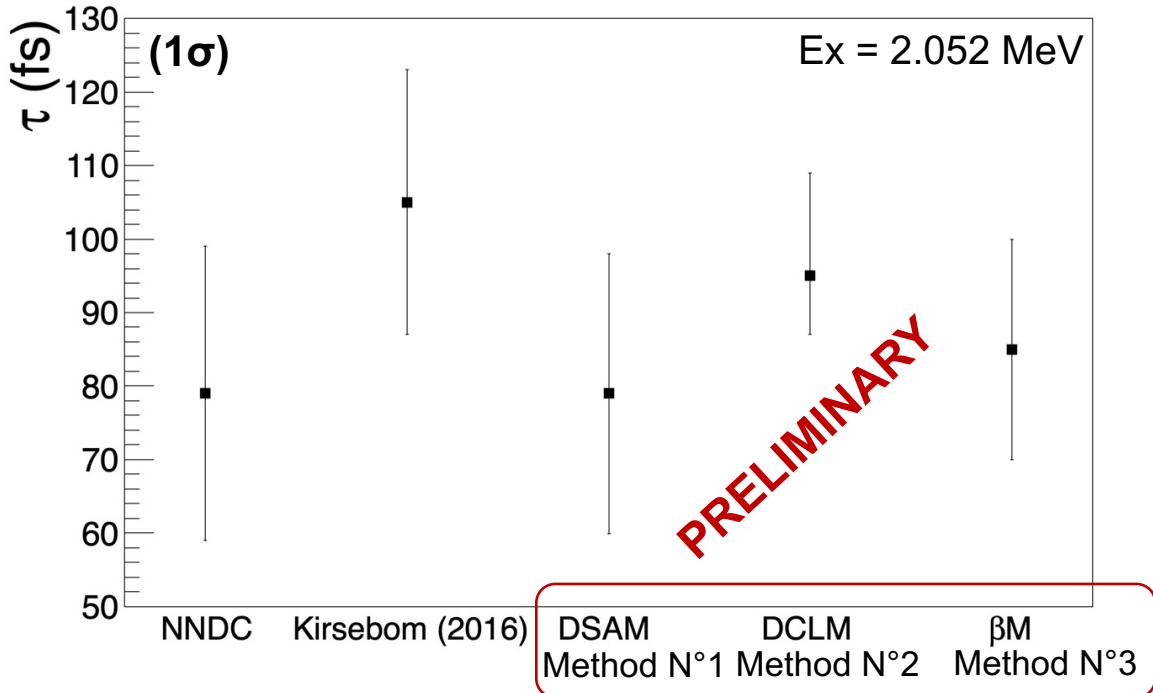


$$\longrightarrow \tau = 11^{+6}_{-4} \text{ fs}$$

Results in lifetimes of $^{23}\text{Mg}^*$

Preliminary tests

Present work



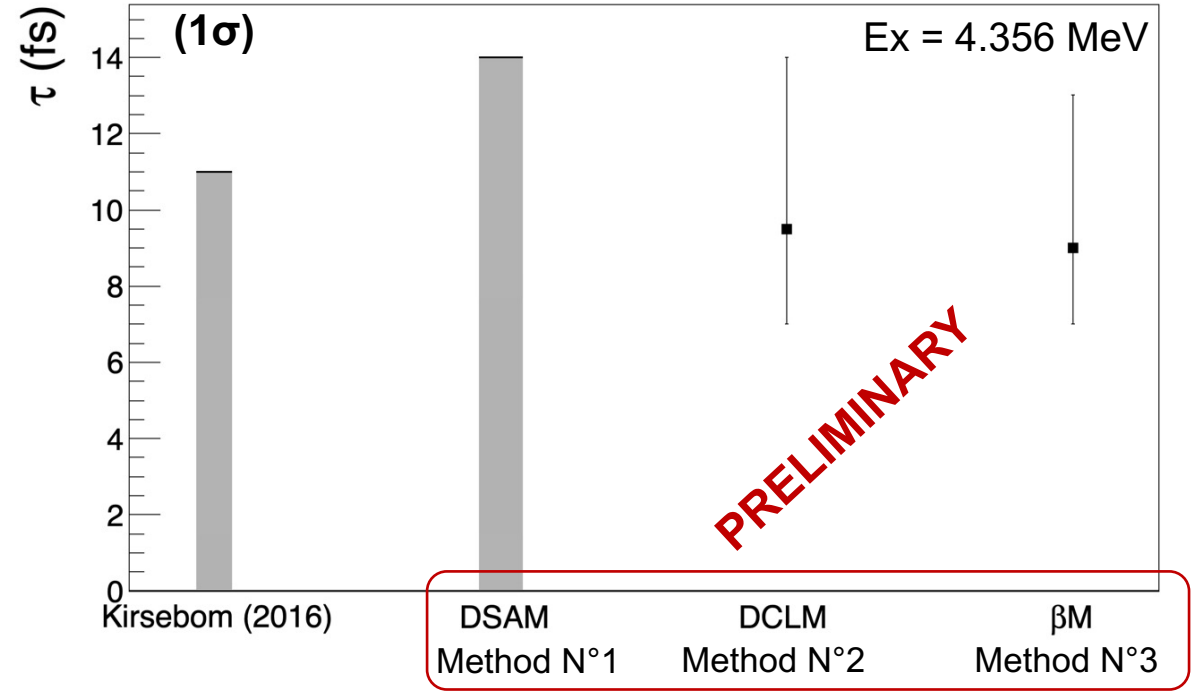
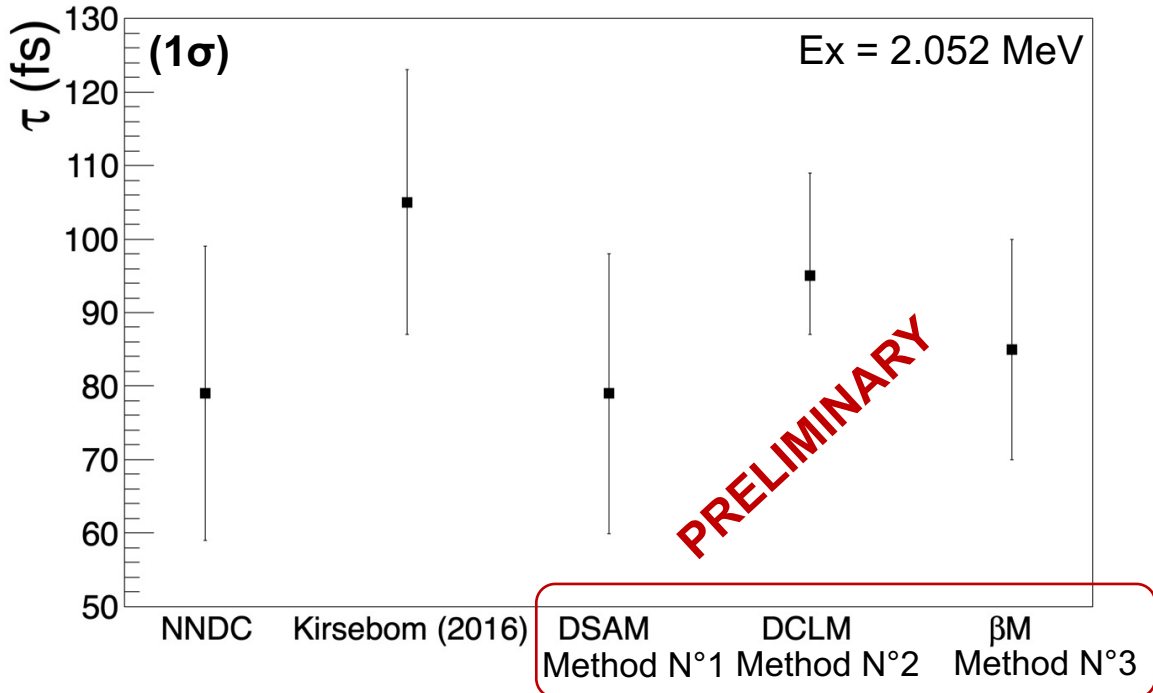
C. Fougères et al.

Results to be submitted, presented at XXIInd GANIL Colloque, AGATA Collaboration meeting (2021)

Results in lifetimes of $^{23}\text{Mg}^*$

Preliminary tests

Present work

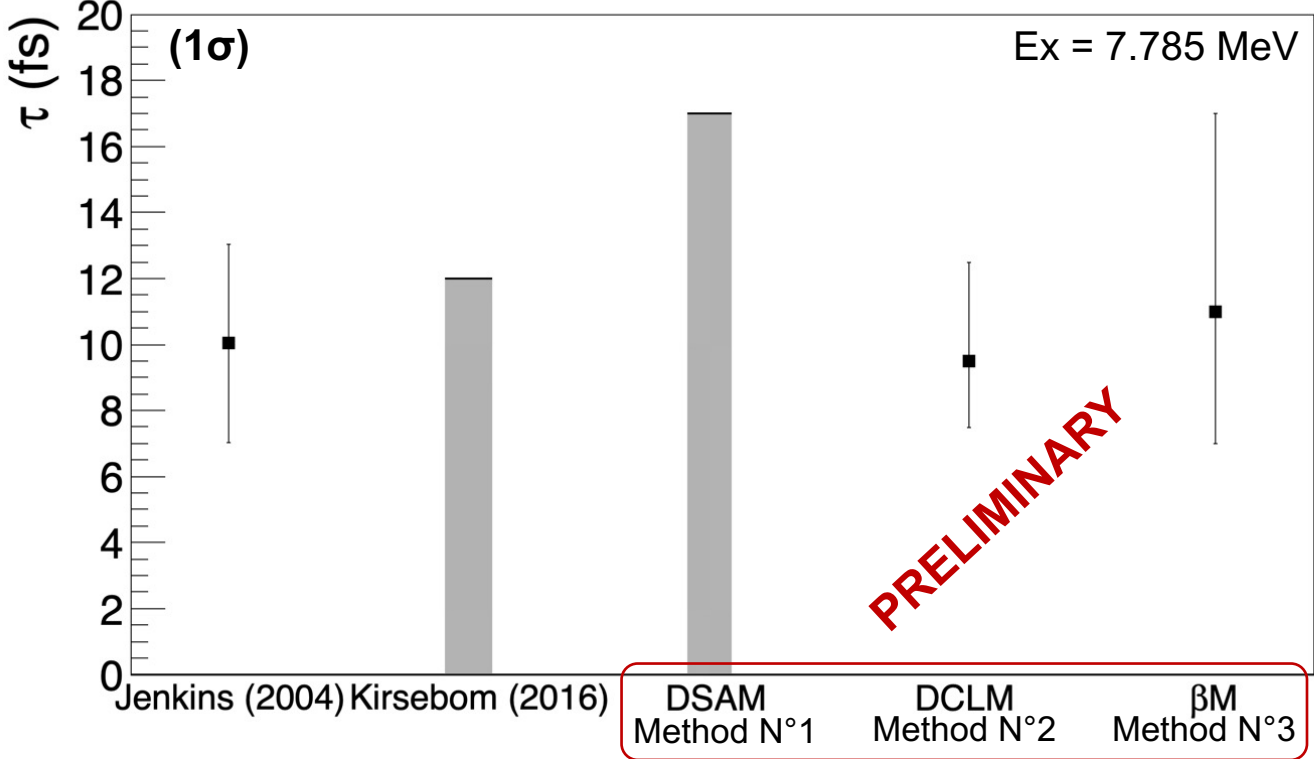


C. Fougères et al.

Results to be submitted, presented at XXIInd GANIL Colloque, AGATA Collaboration meeting (2021)

Results in lifetime of the key state

Present work

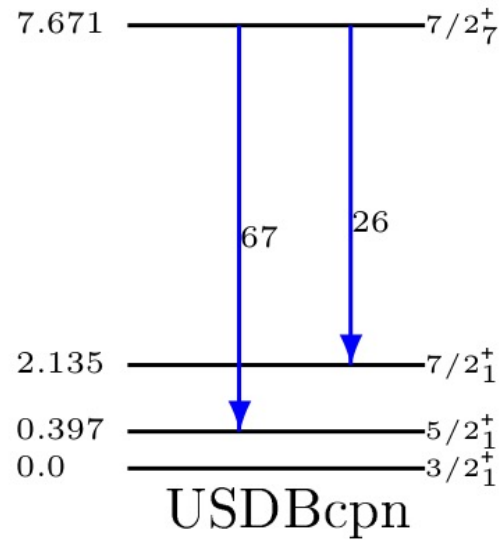
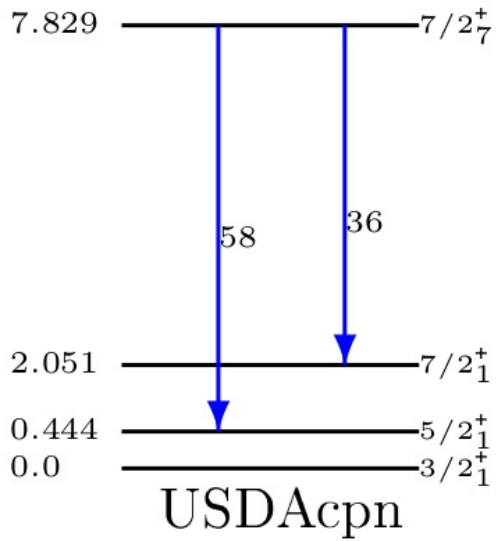
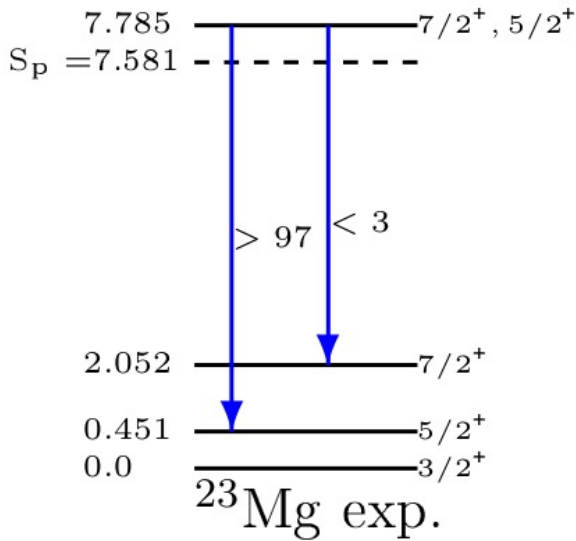


C. Fougères et al.

Results to be submitted, presented at XXIInd GANIL Colloque, AGATA Collaboration meeting (2021)

Considerations on spin

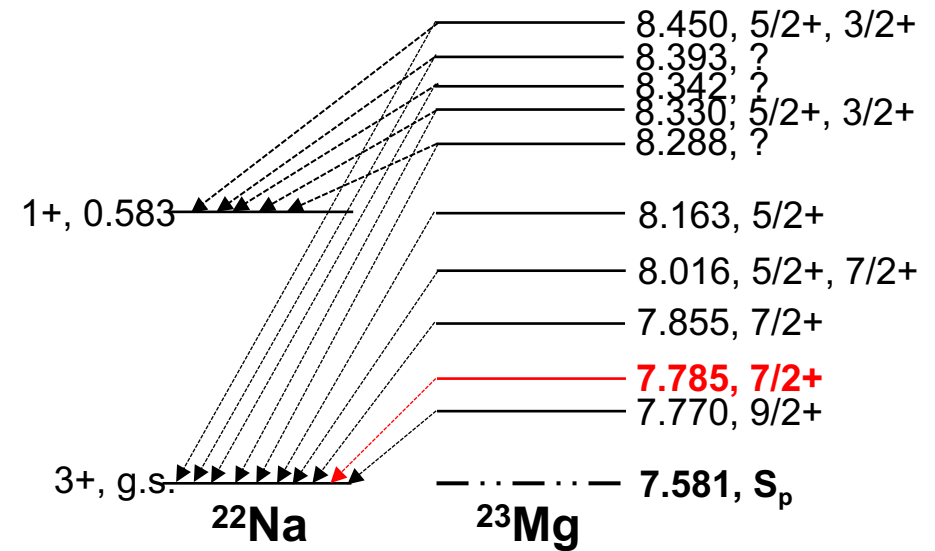
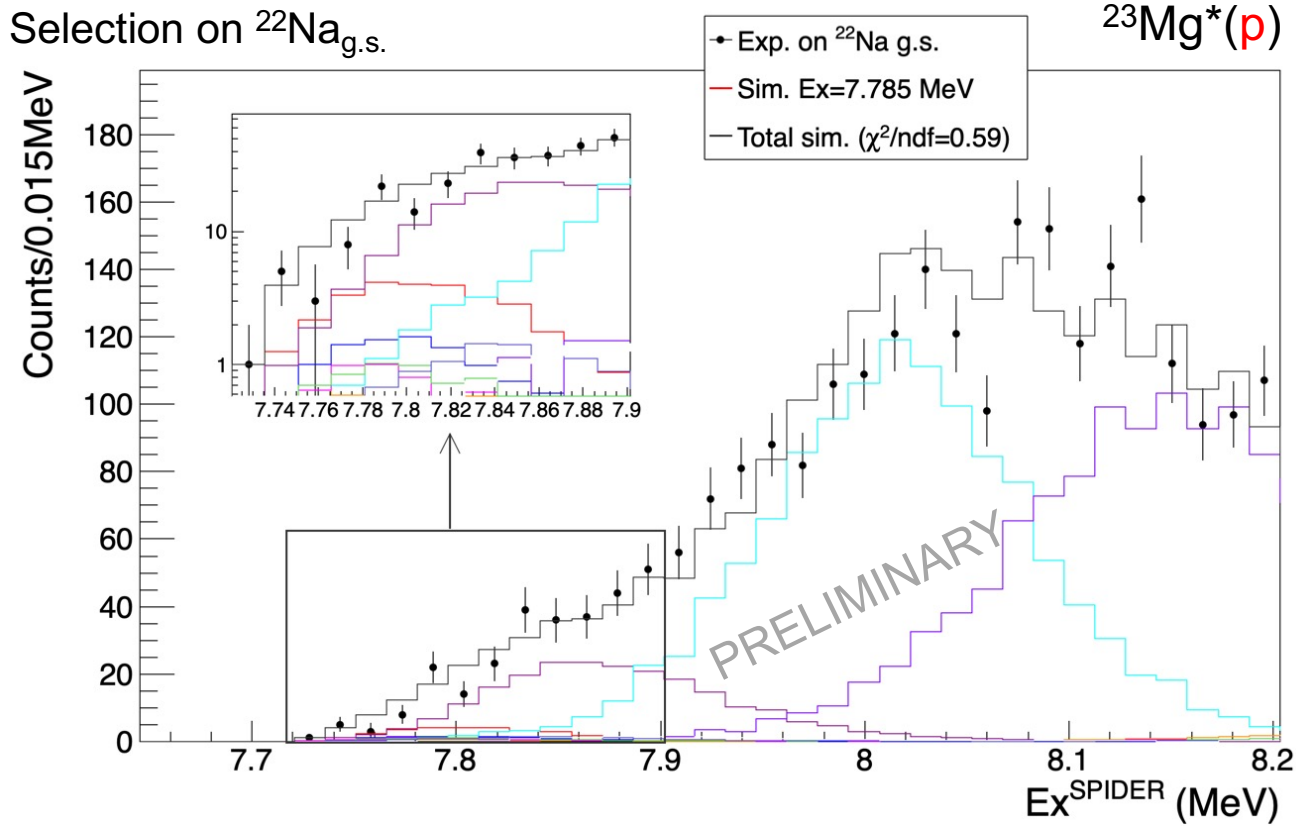
Shell-model calculations (NUSHELLX, DWU)



Identification **7/2+ level**: agreement γ -ray transitions between SM and experiment

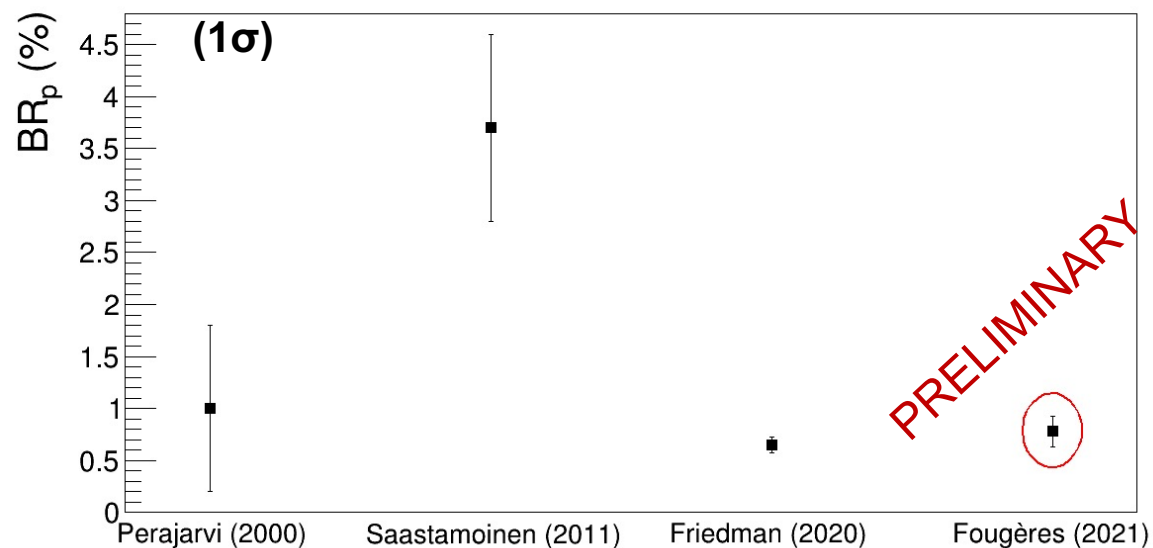
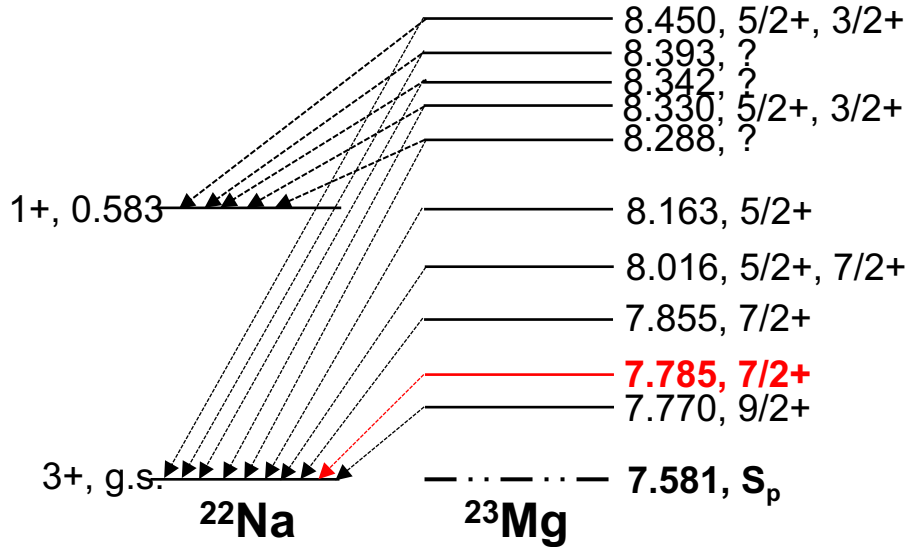
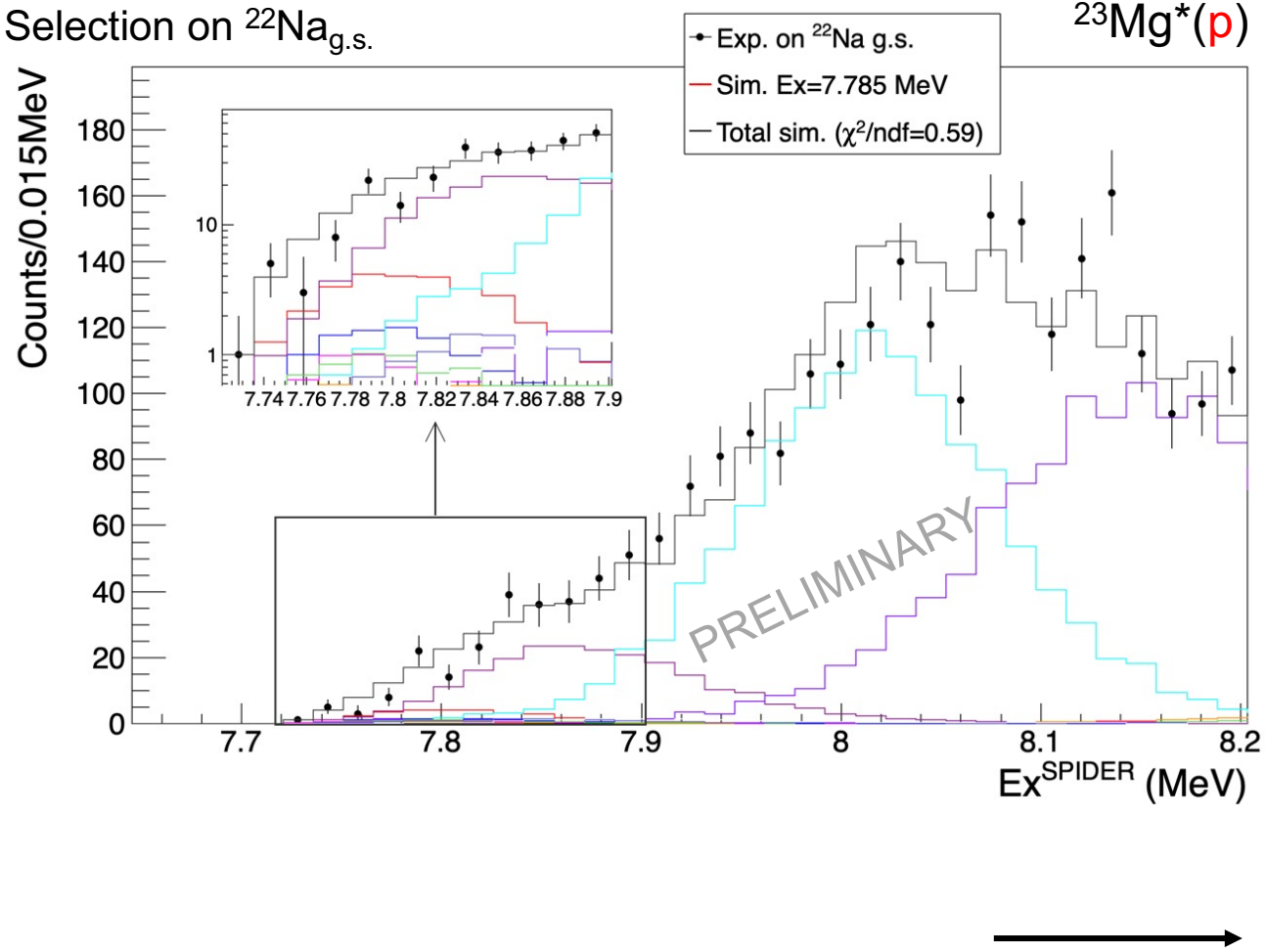
Accessing BR_p

Present work



Accessing BR_p

Present work



Astrophysical impacts

Predictions in ^{22}Na flux

New rate $^{22}\text{Na}(p, \gamma)^{23}\text{Mg}$

Monte-Carlo calculations, with $\omega\gamma = 0.25^{+0.10}_{-0.07}$ meV at $E_R = 0.204$ MeV
Meyer Ph.D. thesis (2020), Longland et al. (2010)

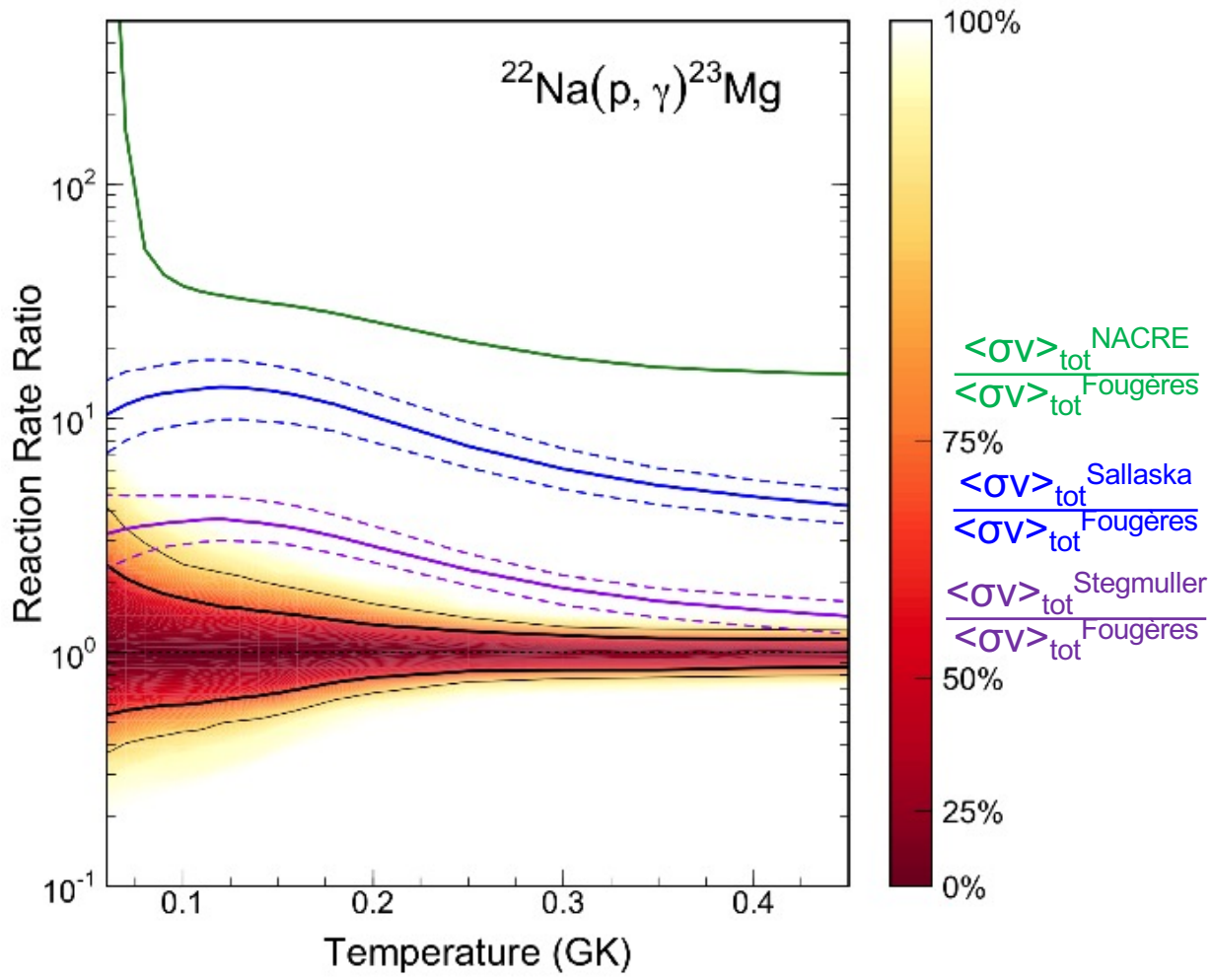


$^{22}\text{Na}(p, \gamma)^{23}\text{Mg}^*$ rate

New rate $^{22}\text{Na}(p, \gamma)^{23}\text{Mg}$

Monte-Carlo calculations, with $\omega\gamma = 0.25^{+0.10}_{-0.07}$ meV at $E_R = 0.204$ MeV
Meyer Ph.D. thesis (2020), Longland et al. (2010)

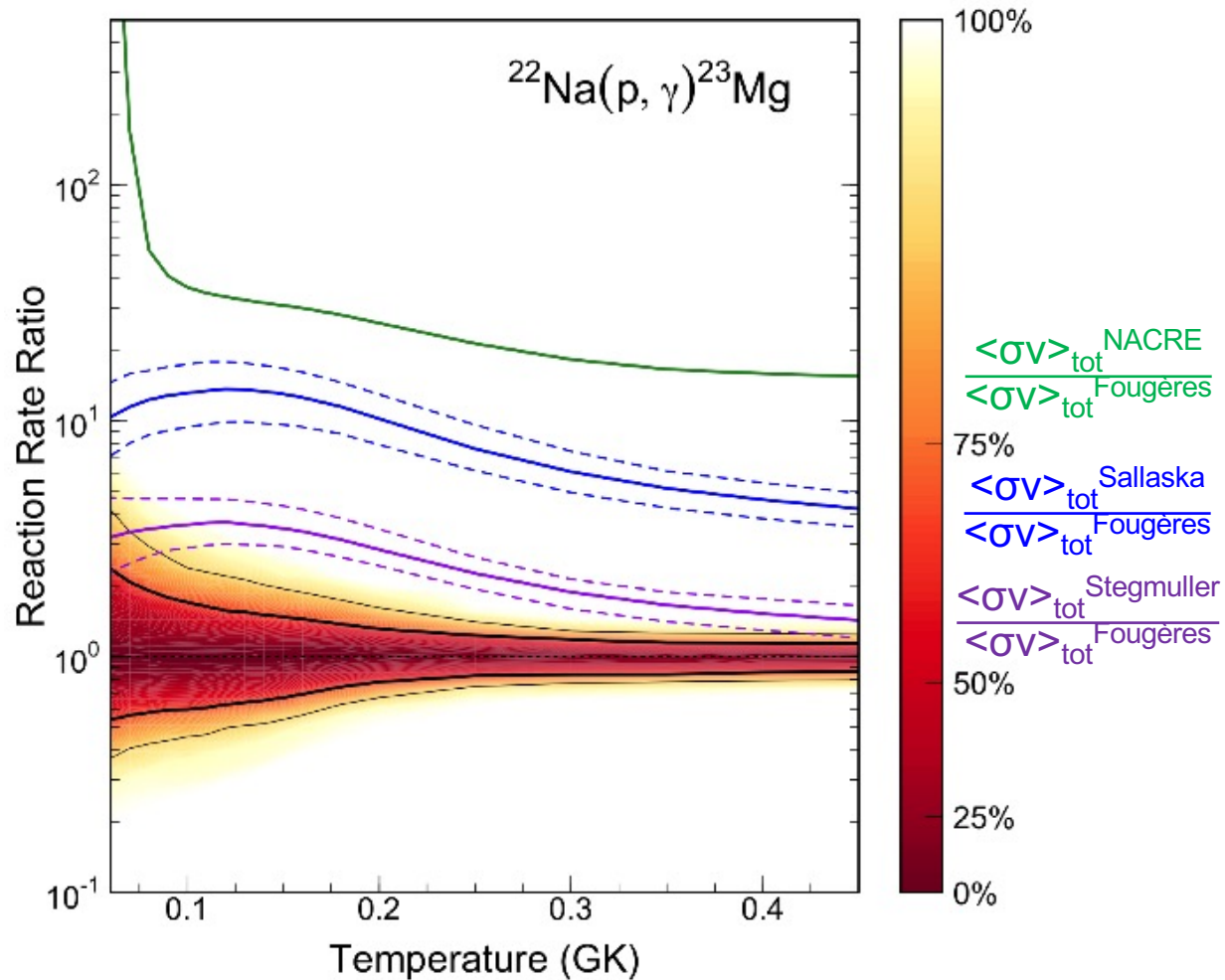
$^{22}\text{Na}(p, \gamma)^{23}\text{Mg}^*$ rate



C. Fougères et al.
Results to be submitted

New rate $^{22}\text{Na}(p, \gamma)^{23}\text{Mg}$

Monte-Carlo calculations, with $\omega\gamma = 0.25^{+0.10}_{-0.07}$ meV at $E_R = 0.204$ MeV
Meyer Ph.D. thesis (2020), Longland et al. (2010)



→ Impact on ejected ^{22}Na from novae ?

*C. Fougères et al.
Results to be submitted*

Predictions in ^{22}Na flux

Simulations of novae

MESA

(Paxton et al, 2013)

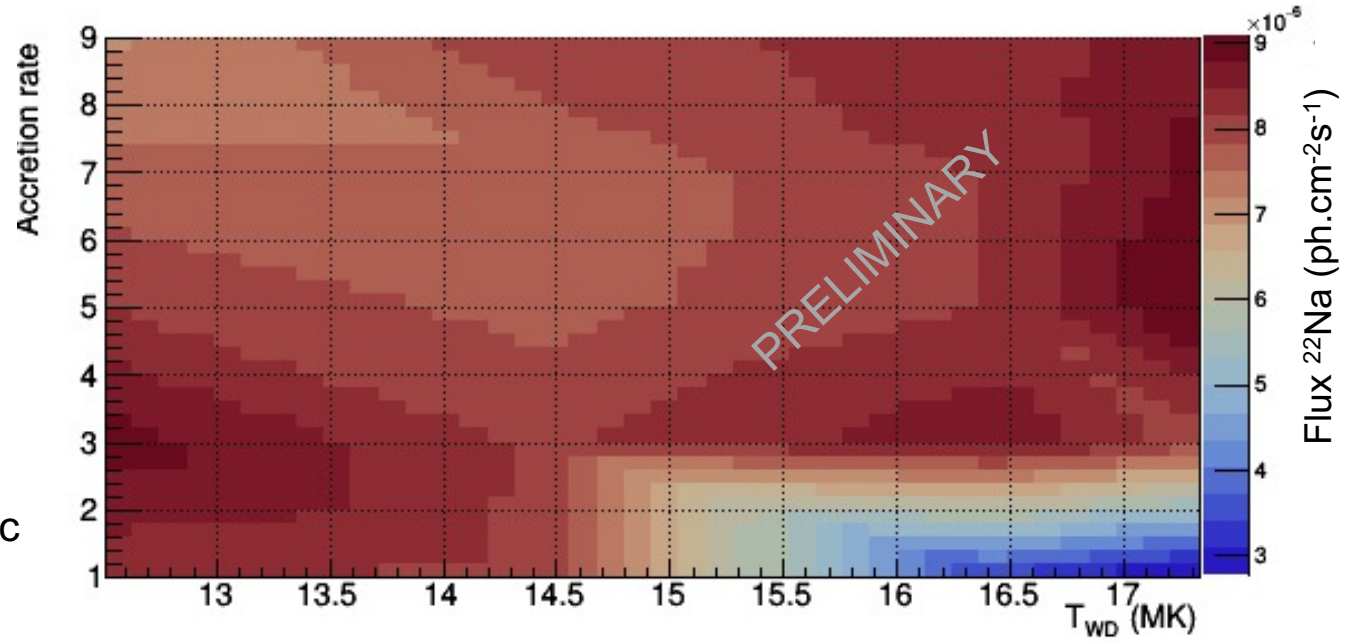
Predictions in ^{22}Na flux

Simulations of novae

MESA

(Paxton et al, 2013)

Nova at 0.5 kpc
 $M_{\text{WD}} = 1.2 M_{\odot}$



*Accretion dynamics,
initial WD temp.*

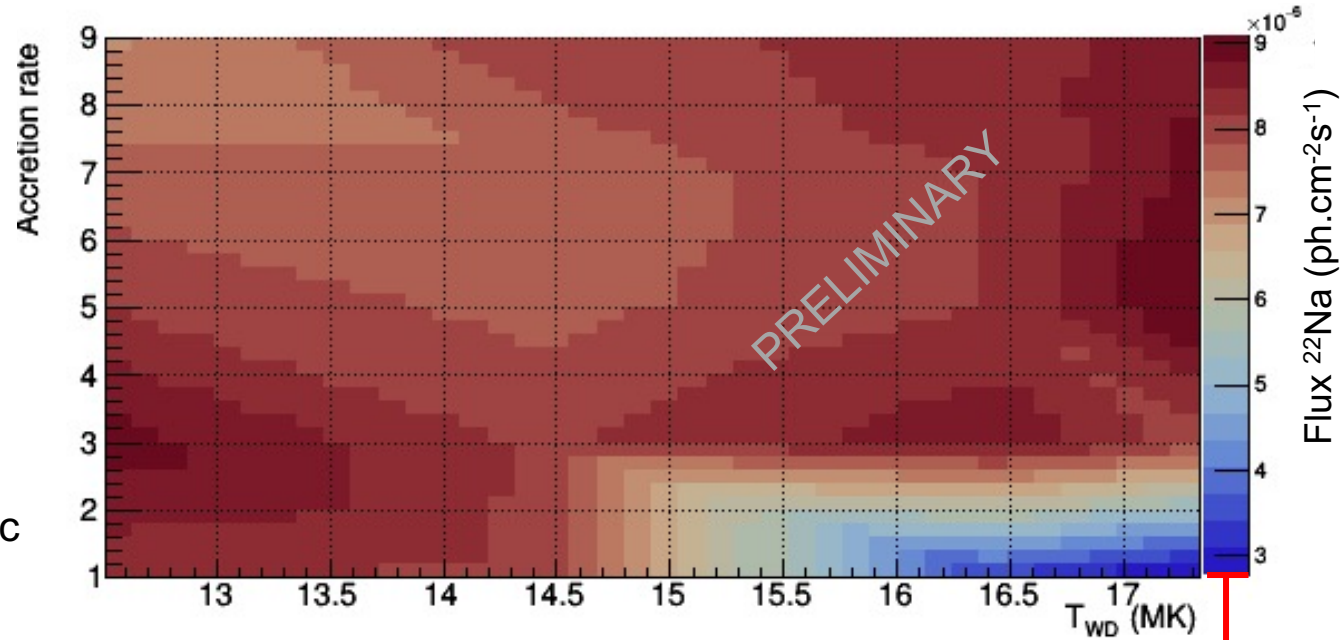
Predictions in ^{22}Na flux

Simulations of novae

MESA

(Paxton et al, 2013)

Nova at 0.5 kpc
 $M_{\text{WD}} = 1.2 M_{\odot}$



*Accretion dynamics,
initial WD temp.*

*^{22}Na abundance in
novae
Detection limit*

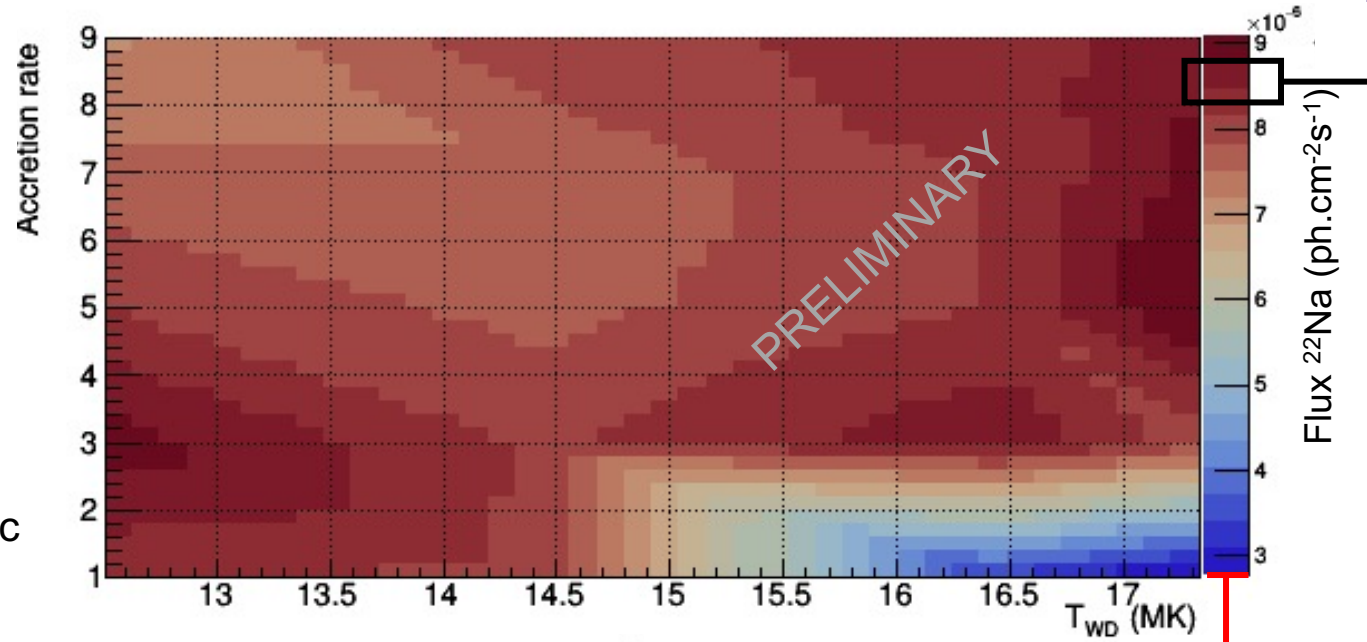
Predictions in ^{22}Na flux

Simulations of novae

MESA

(Paxton et al, 2013)

Nova at 0.5 kpc
 $M_{\text{WD}} = 1.2 M_{\odot}$

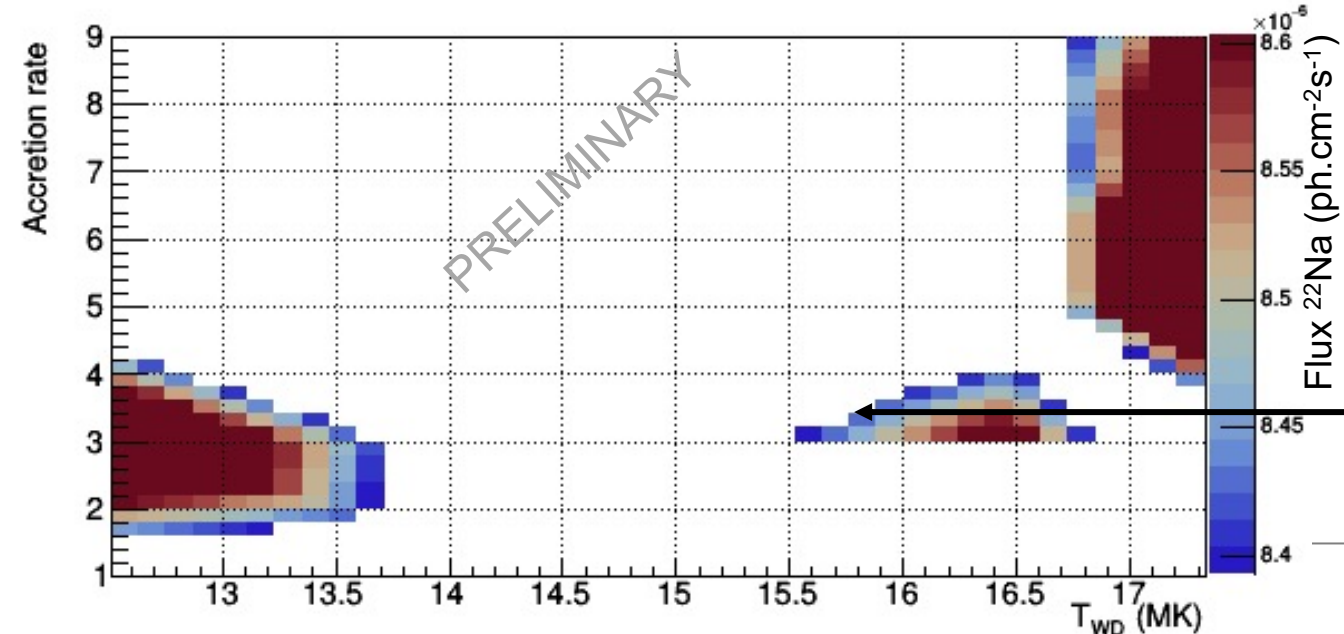


Accretion dynamics,
initial WD temp.

^{22}Na abundance in
novae
Detection limit

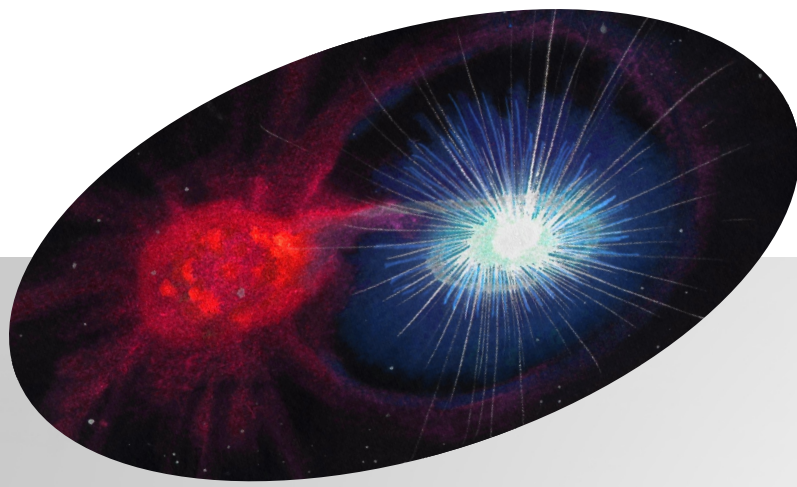
e-ASTROGAM limit

Constrain novae parameters
with observed flux



Outlooks

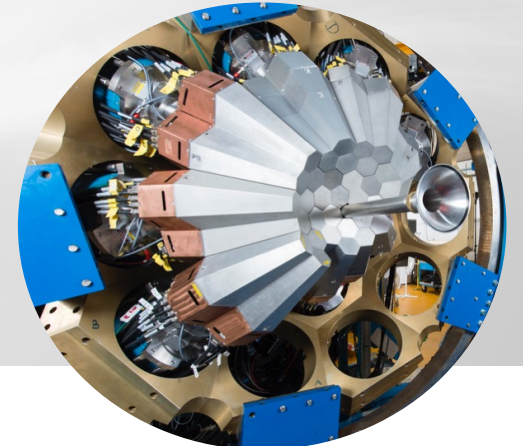
Nova simulations with SHIVA *J.José et al, (1998, 2021)* + other free parameters (composition of thermonuclear medium)



Outlooks

Nova simulations with SHIVA *J. José et al, (1998, 2021)* + other free parameters (composition of thermonuclear medium)

THANKS
to E710 collaboration and to you for the attention



V. Tatischeff et al A. De Angelis. The e-astrogam mission. exploring the extreme universe with gamma rays in the mev-gev range. *Experimental Astronomy*, 44, 2017.

D.C. Black. On the origins of trapped helium, neon and argon isotopic variations in meteorites - i. gas-rich meteorites, lunar soil and breccia. *Geochimica and Cosmochimica Acta*, 36, 1972.

R. Diehl. Cosmic gamma-ray spectroscopy. *Astronomical Review*, 8, 2013.

A. Saastamoinen et al. Experimental study of β -delayed proton decay of ^{23}Al for nucleosynthesis in novae. *Physical Review C*, 83, 2011.

A.L Sallaska et al. Direct Measurements of $^{22}\text{Na}(p,\gamma)^{23}\text{Mg}$ Resonances and Consequences for ^{22}Na Production in Classical Novae. *Physical Review Letters*, 105, 2010.

B. Cederwall et al. Measurement of ultra-fast γ -ray transitions from heavy-ion compound nucleus reactions. *Nucl. Instrum. Methods. Phys. Res. A*, 353, 1995.

B. Paxton et al. Modules for Experiments in Stellar Astrophysics (MESA). *The Astrophysical Journal Supplement Series*, 4, 2013.

D. Watson et al. Identification of strontium in the merger of two neutron stars. *Nature*, 574, 2019.

D.G Jenkins et al. Reevaluation of the $^{22}\text{Na}(p,\gamma)$ Reaction Rate : Implications for the detection of ^{22}Na Gamma Rays from Novae. *Physical Review Letters*, 92, 2004.

F. Stegmuller et al. $^{22}\text{Na}(p,\gamma)^{23}\text{Mg}$ resonant reaction at low energies. *Nuclear Physics A*, 601, 1996.

K. Perajarvi et al. Measurement of the IAS resonance strength in ^{23}Mg . *Physical Review B*, 492, 2000.

M. Friedman et al. Low-energy ^{23}Al β -delayed proton decay and ^{22}Na destruction in novae. *Physical Review C*, 101, 2020.

M.S. Kwag et al. Spin assignments for ^{23}Mg levels and the astrophysical $^{22}\text{Na}(p,\gamma)^{23}\text{Mg}$ reaction. *European Physical Journal A*, 56, 2020.

O.S Kirsebom et al. Measurements of lifetimes in ^{23}Mg . *Physical Review C*, 93, 2016.

S.J. Jin et al. Resonant scattering of $^{22}\text{Na} + p$ studied by the thick-target inverse-kinematic method. *Physical Review C*, 88, 2013.

V. Tripathi et al. Split Isobaric Analog state in ^{55}Ni : Case of Strong Isospin Mixing. *Physical Review Letters*, 111, 2013.

R.B. Firestone. <https://www.nndc.bnl.gov>, 2019.

J. José and M. Hernanz. Nucleosynthesis in Classical Novae: CO versus ONe White Dwarfs. *Astrophysical Journal*, 494, 1998.

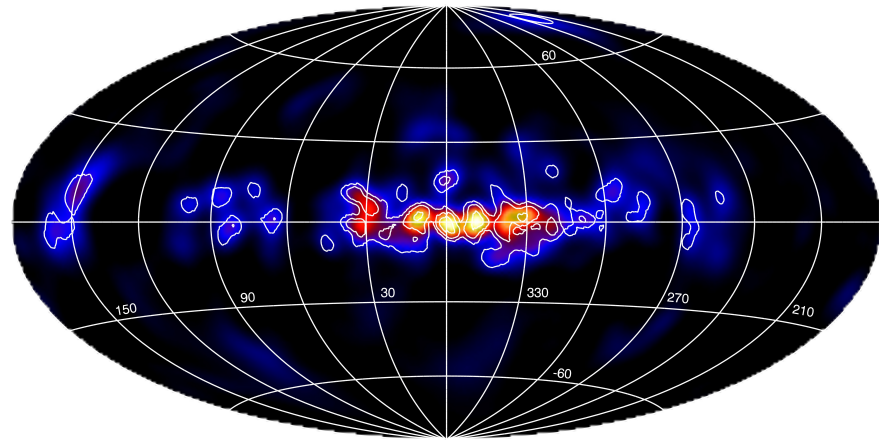
A. Meyer. *Etudes expérimentale des réactions $^{13}\text{N}(\alpha, p)^{16}\text{O}$ et $^{30}\text{P}(p, \gamma)^{31}\text{S}$, et impact sur les abondances isotopiques extrêmes en ^{13}C , ^{15}N et ^{30}Si dans les grains pré-solaires.* 2020.

C. Michelagnoli. *The lifetime of the 6.79 MeV state in ^{15}O as a challenge for nuclear astrophysics and γ -ray spectroscopy: a new DSAM measurement with the AGATA Demonstrator array.* 2013.

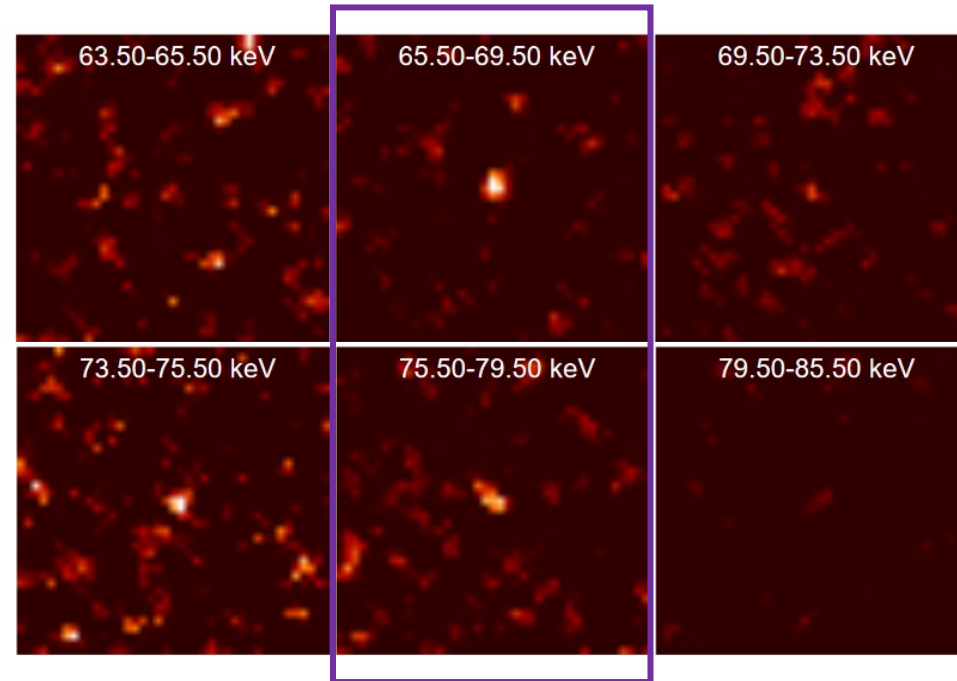
Appendices

Radioelements observations

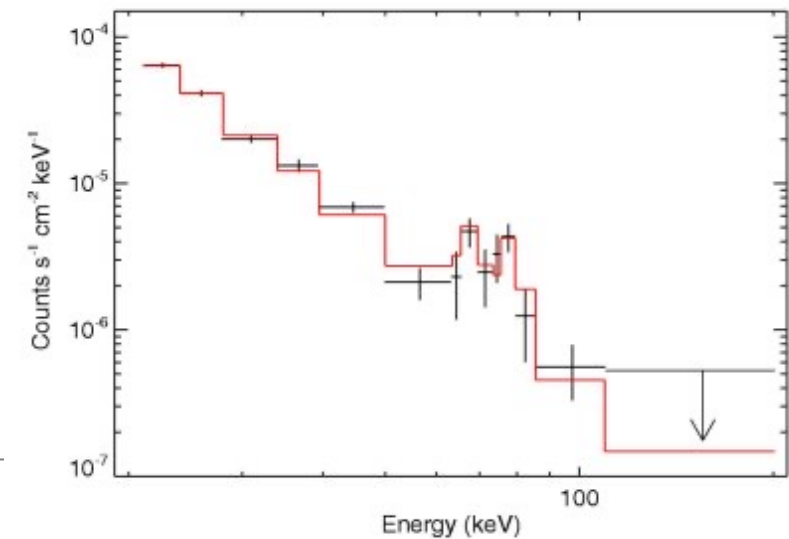
$$E_\gamma = \{67.9, 78.4\} \text{ keV from } {}^{44}\text{Ti}$$



Min  Max
Sky map at $E_\gamma = 1.809$ ${}^{26}\text{Al}$ SPI ©ESA

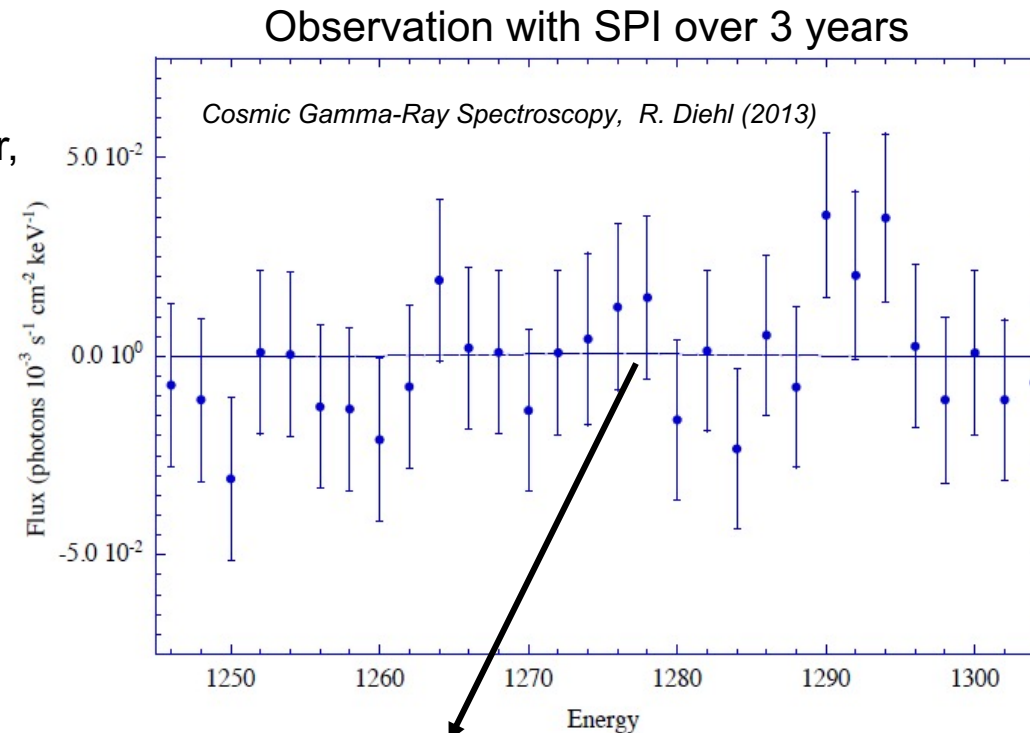


SN CasA SPI ©ESA, Renaud et al. (2006)



Current results in ^{22}Na cosmic observations

Flux here: cumulative emission toward Galactic Center, fitted by an assumed novae spatial distribution.



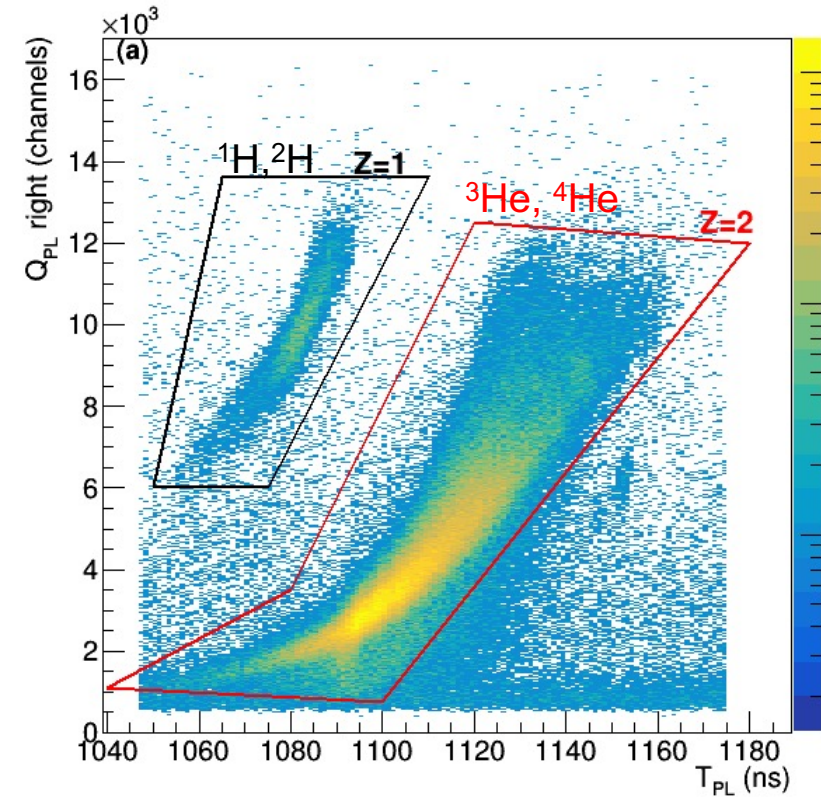
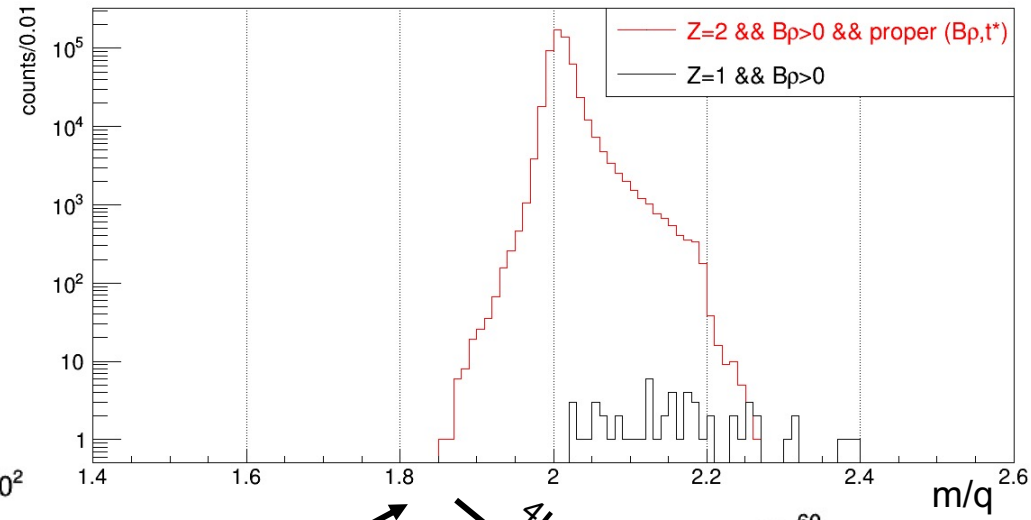
Line at 1.275 MeV ($1.3 \cdot 10^{-5} \text{ ph.cm}^{-2}.\text{s}^{-1}$ (1σ))

1/3 One novae at $30.\text{yr}^{-1}$ \rightarrow $< 2.5\text{-}5.7 \cdot 10^{-7} M_{\odot}$ per outburst

Instrument background level high at 1.275 MeV energy (from activation by CR of Al material near SPI)

VAMOS

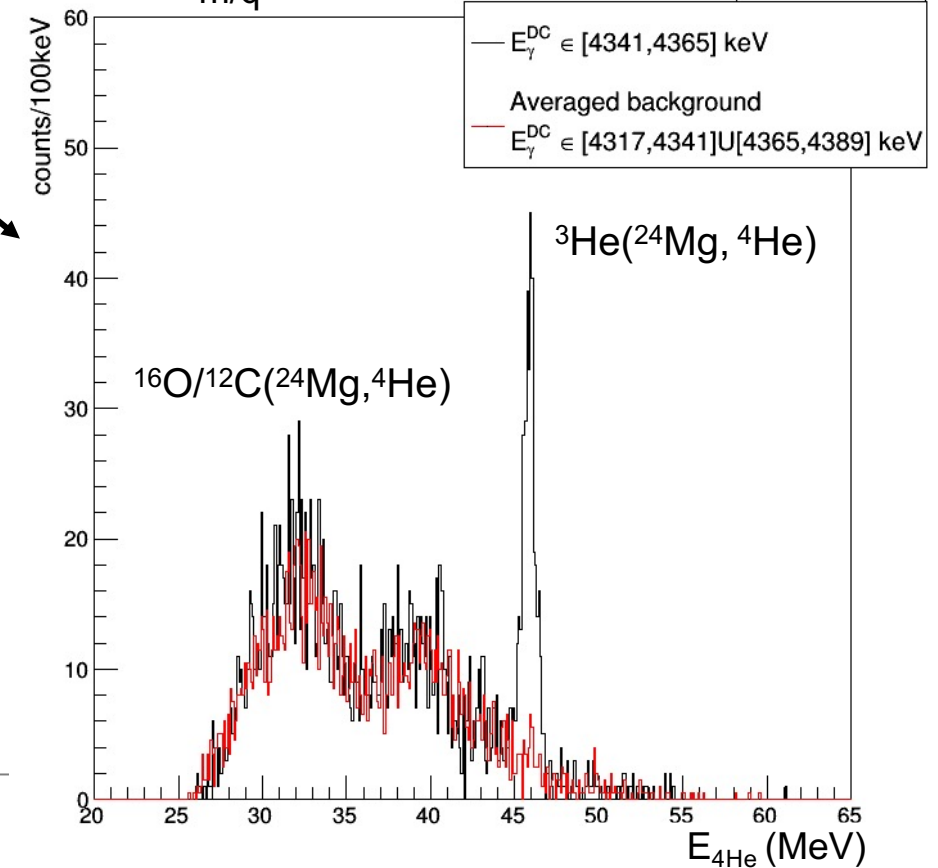
Identification of ejectiles (Z, m/q, E)



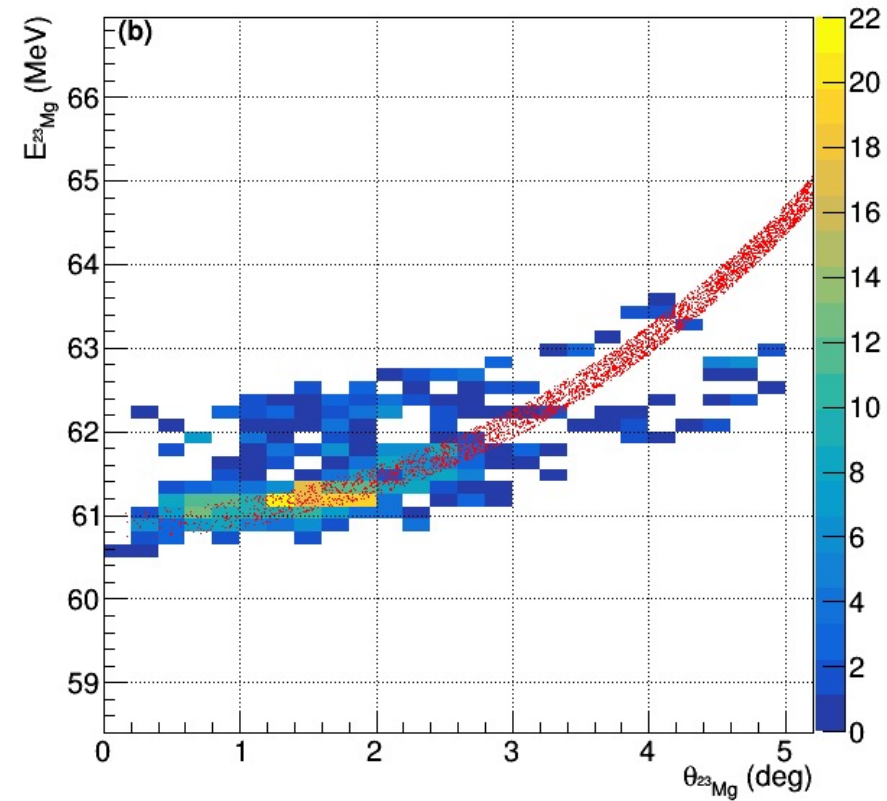
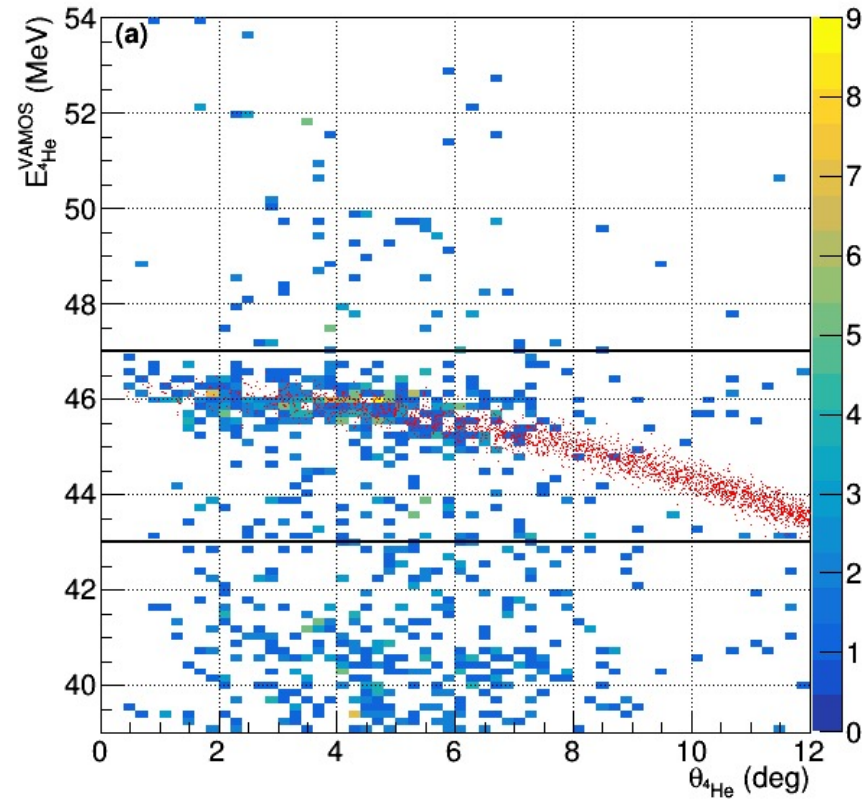
(+) $B\rho$

4He events
(+) γ transition

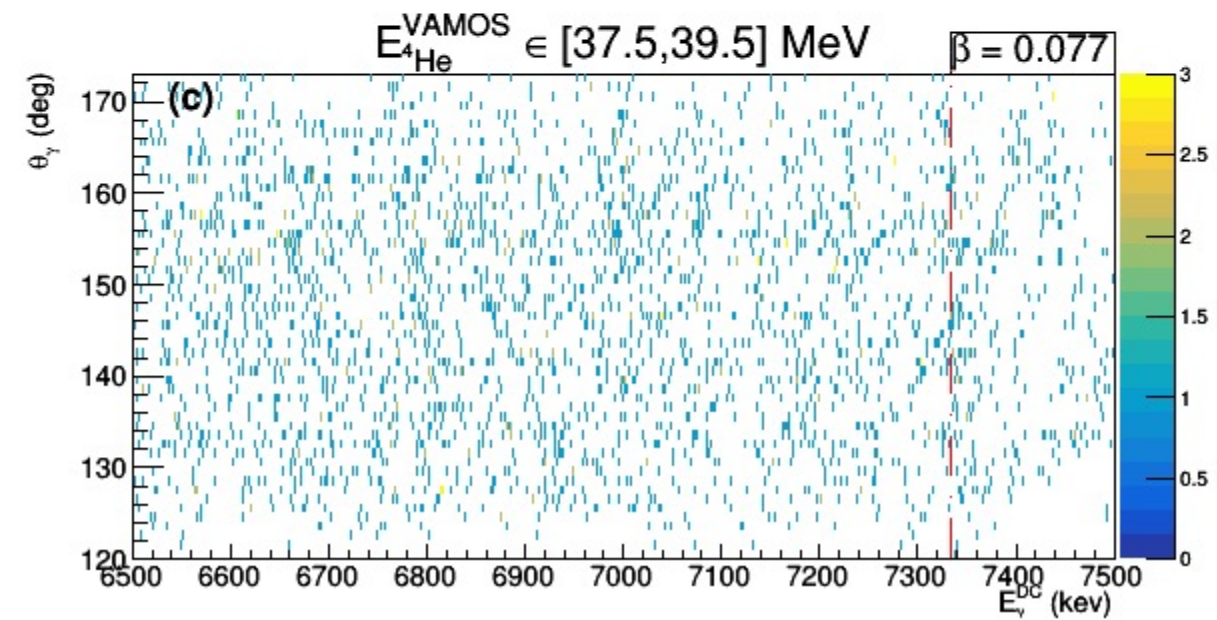
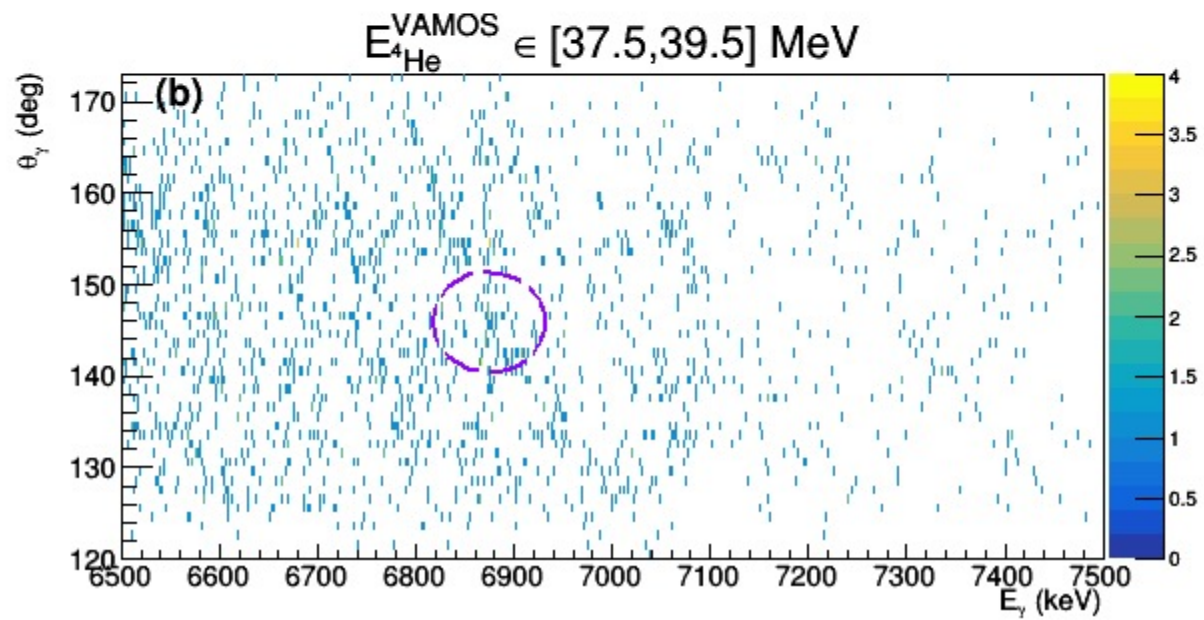
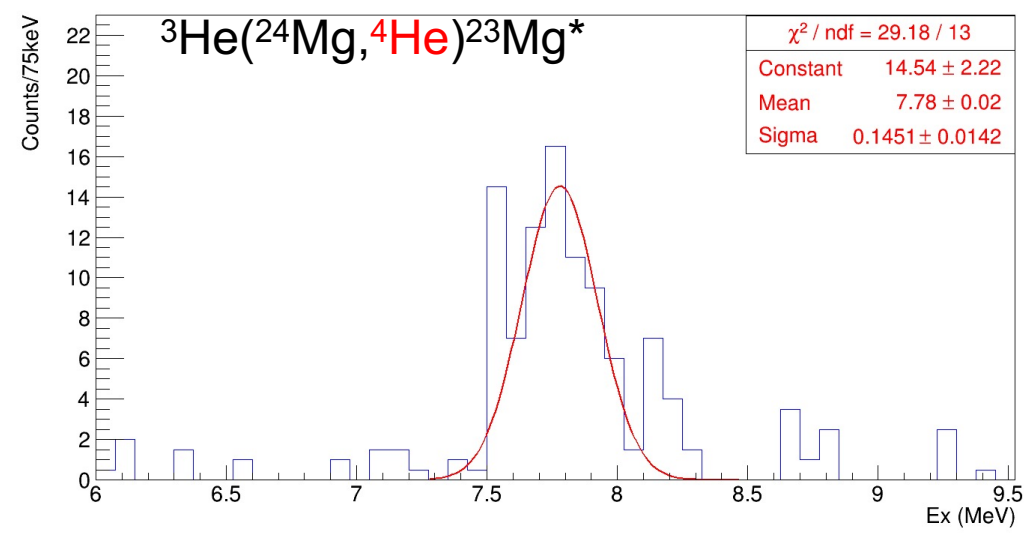
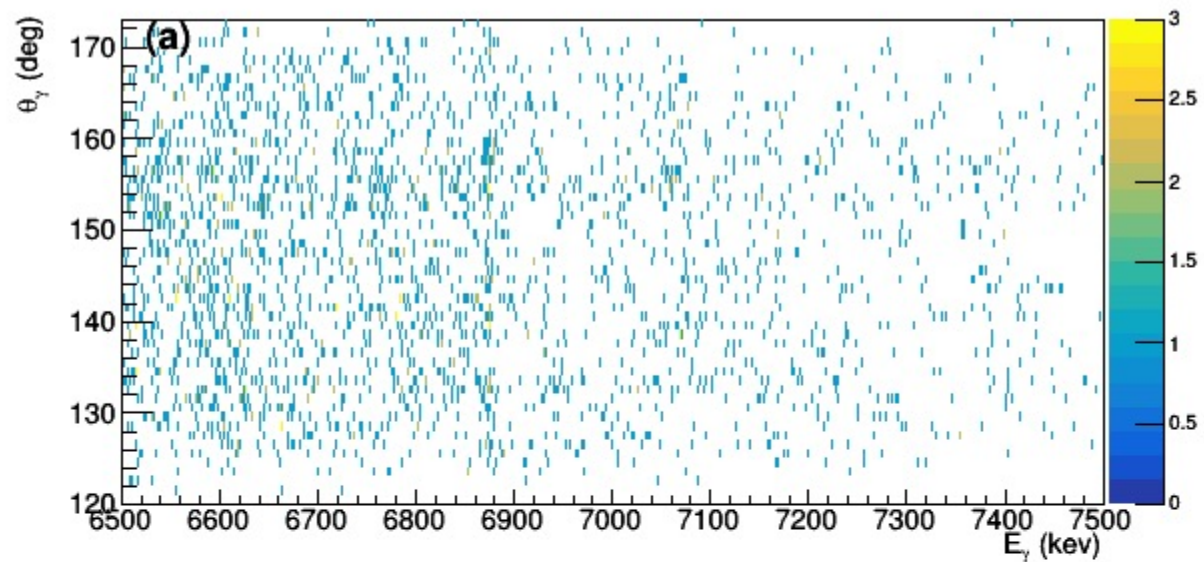
Reconstruct $^{23}\text{Mg}^* \text{ Ex ?}$



Kinematics

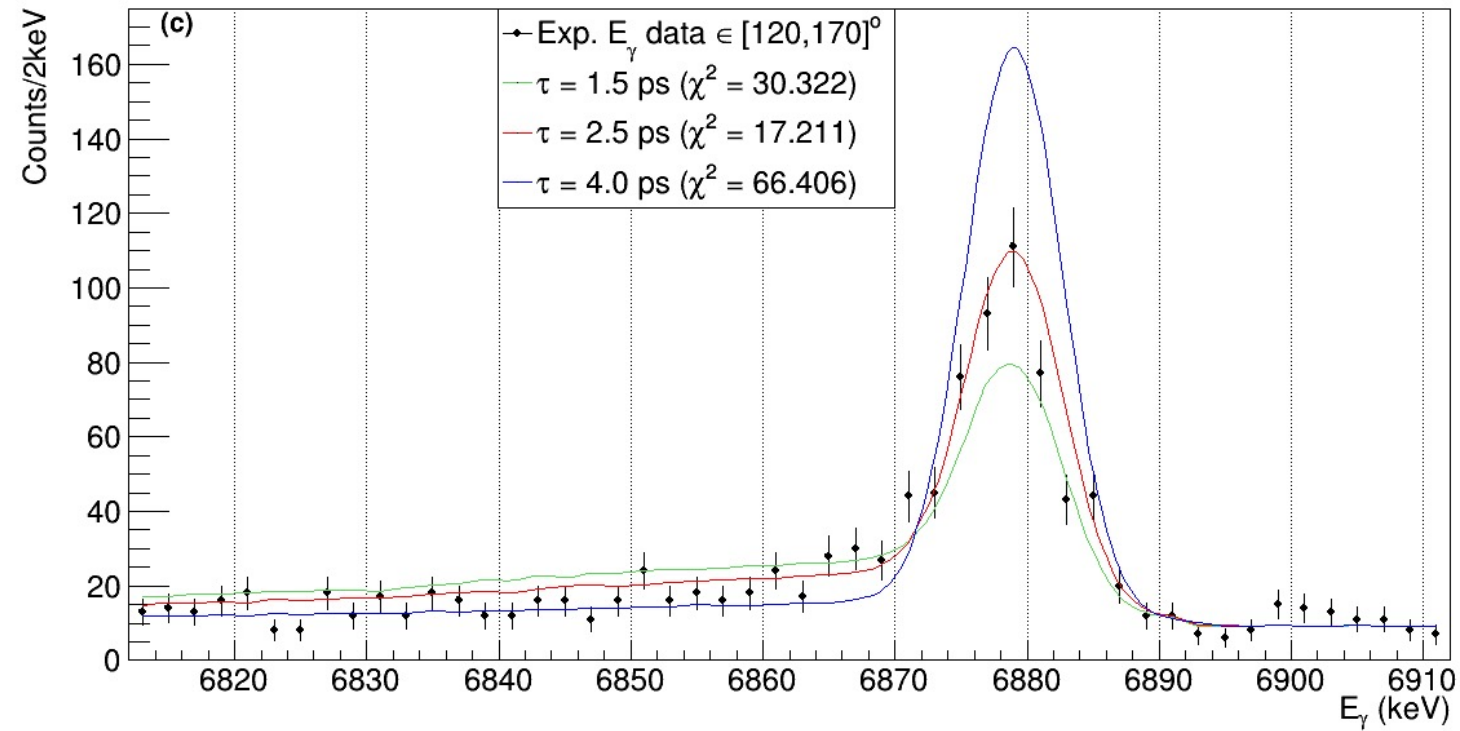


$^{23}\text{Mg}^*$ Ex = 7.785 MeV

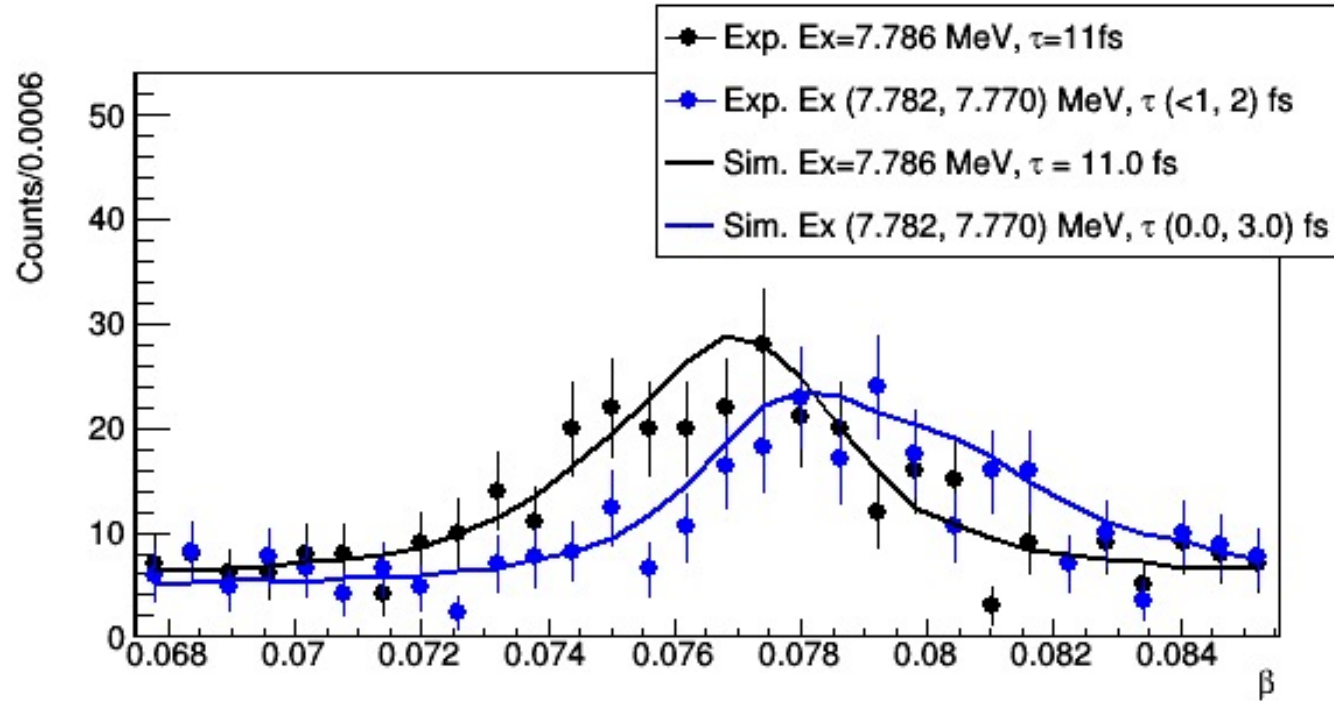


EVASIONS validation: τ of $^{28}\text{Si}^*$ $E_x = 6.879$ MeV

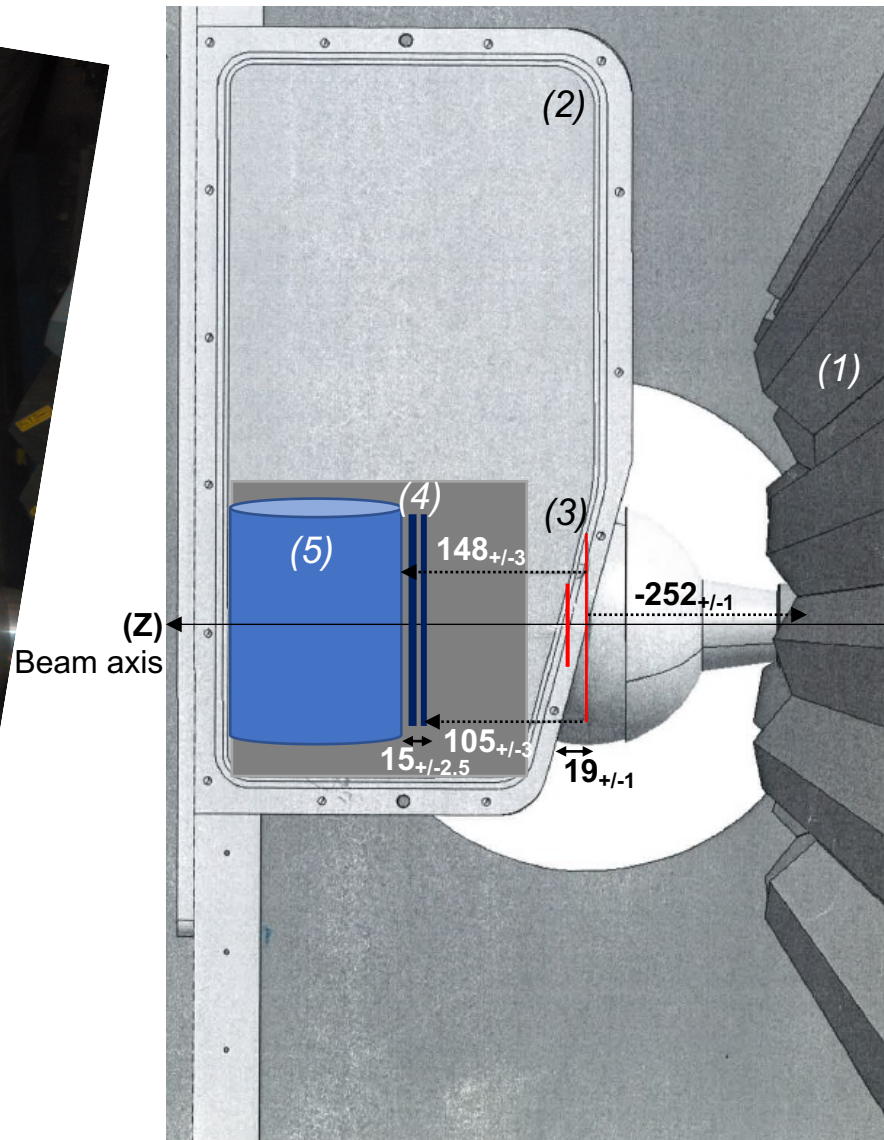
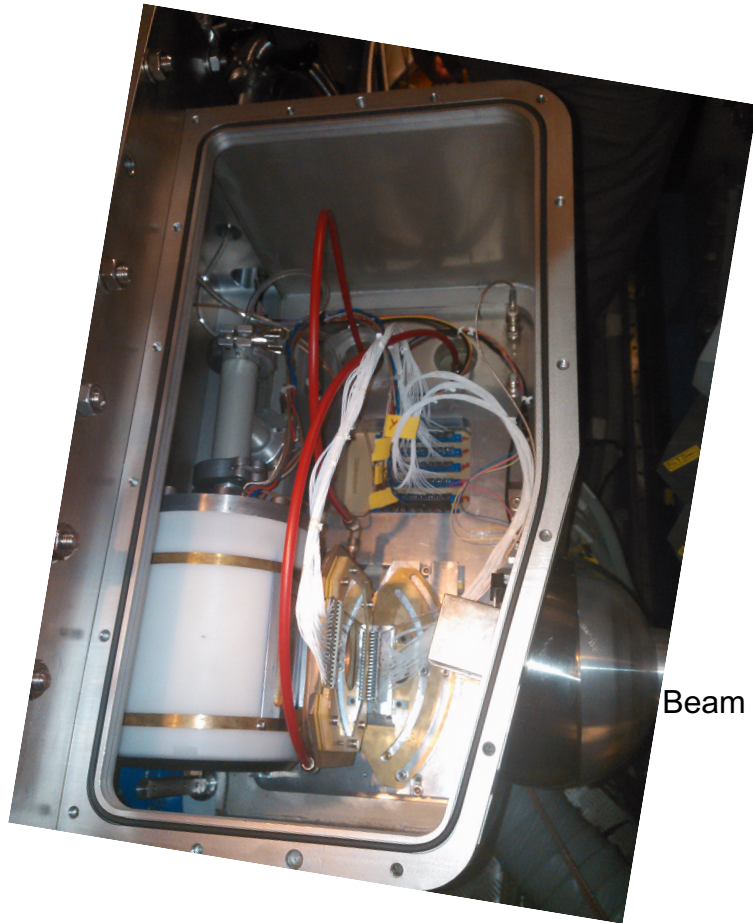
Method (1) DSAM (classic)



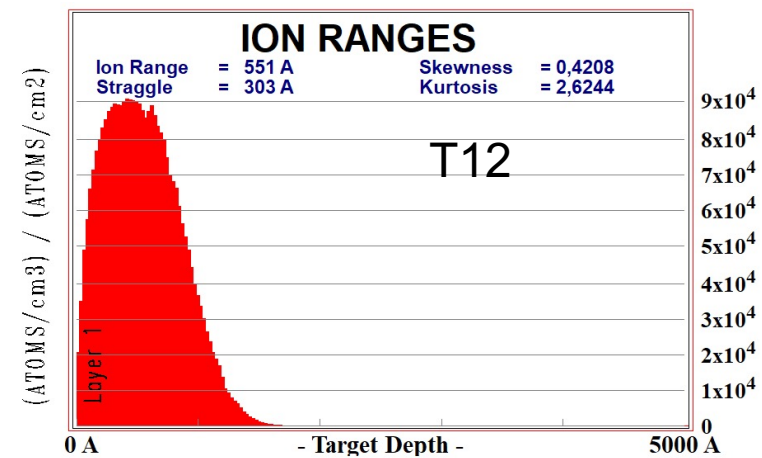
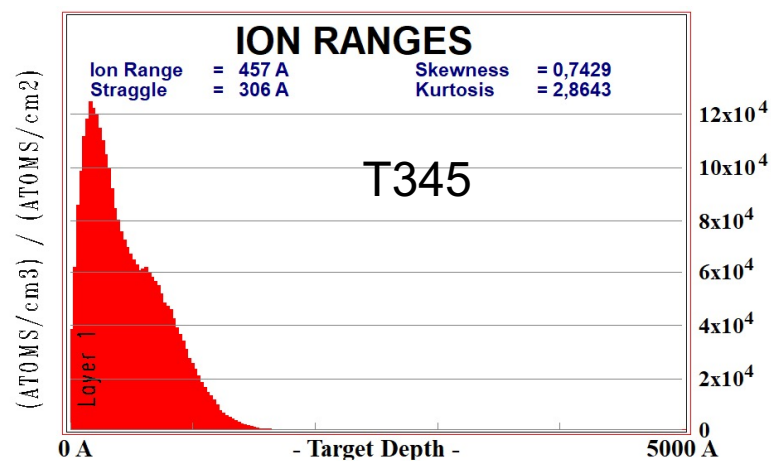
Low lifetimes in $^{23}\text{Mg}^*$



Target chamber

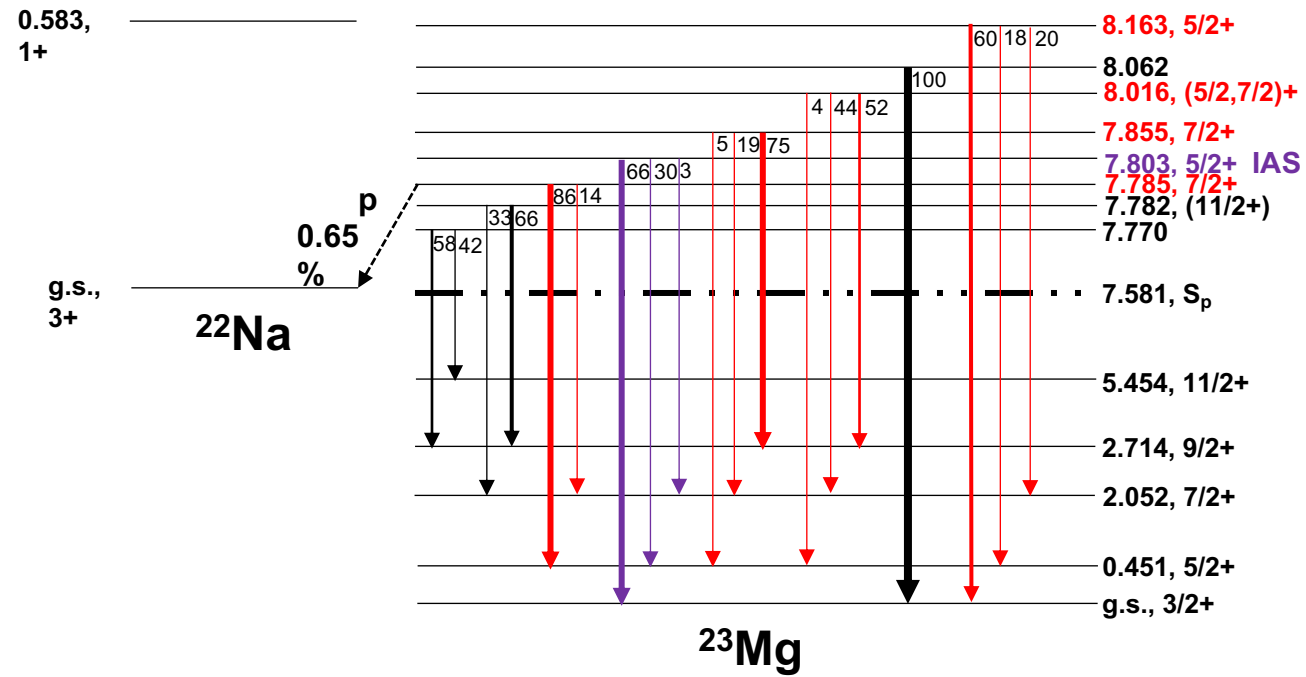


- (1) AGATA
- (2) Charade Chamber
- (3) Target holder + gold beam catcher (20 μ m)
- (4) SPIDER rings dE-Eres (298, 580 μ m)
- (5) Small Gas Chamber



Target n ^o	measured ³ He density (10 ¹⁷ at.cm ⁻²)	$\frac{\text{measured}}{\text{implanted}}$ (%)
1	2.1±0.21	37±4
2	1.9±0.19	34±3
3	1.5±0.15	19±2
4	2.5±0.25	31±3
5	2.2±0.22	27±3
8	1.0±0.10	18±2
10	/	/

Decays from states of interest

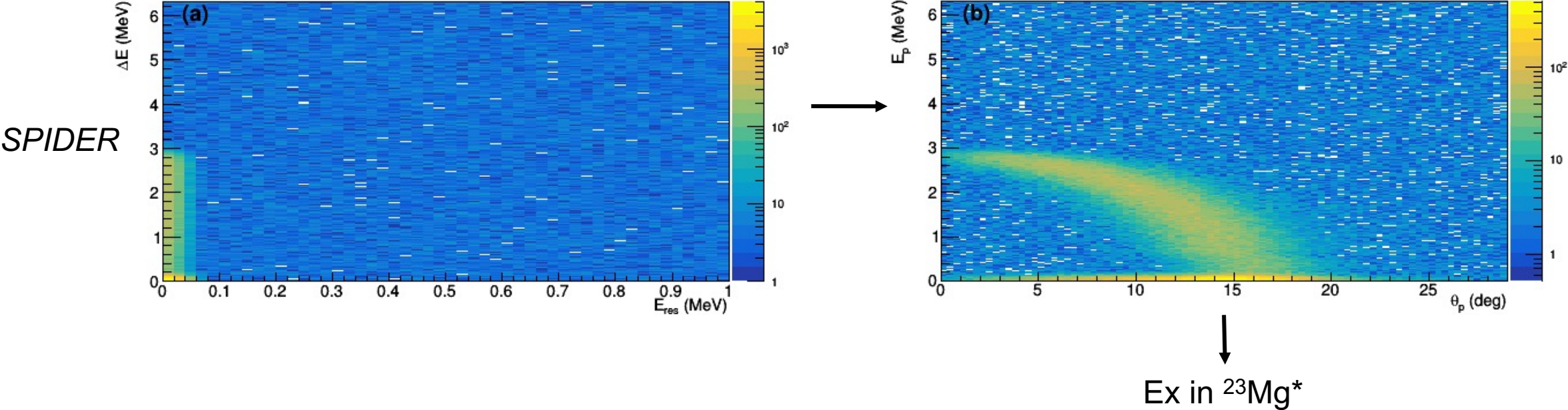


Simulations of the experiment: p decay

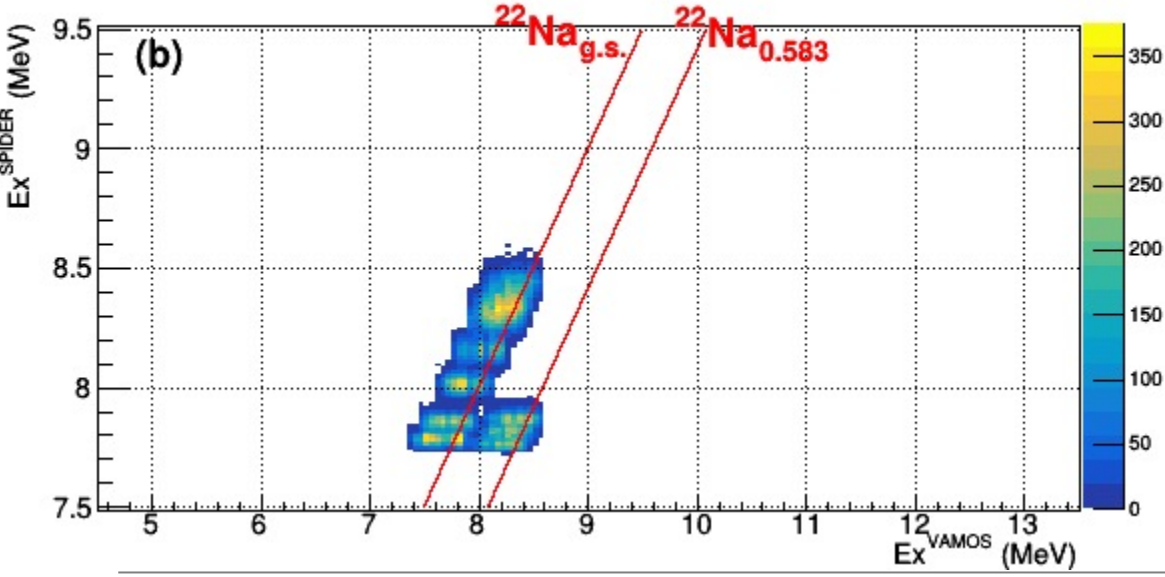
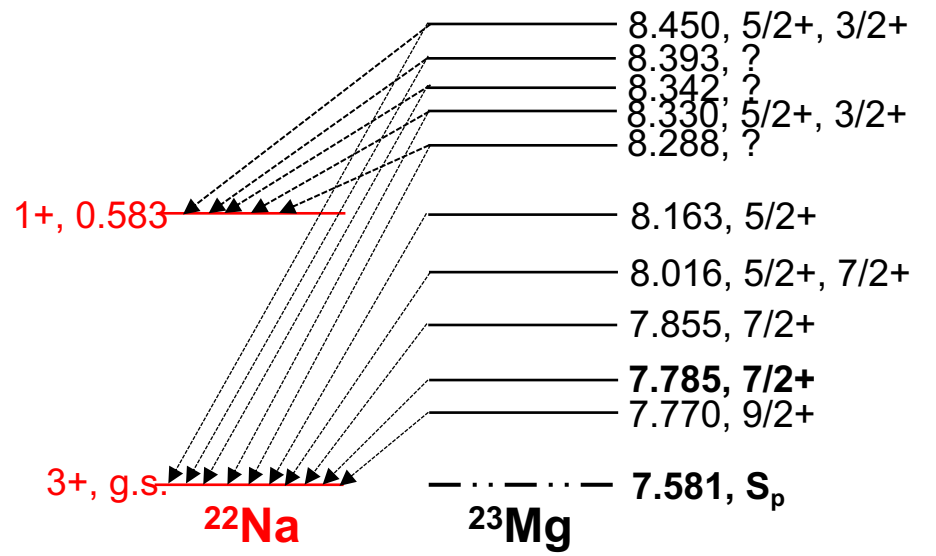
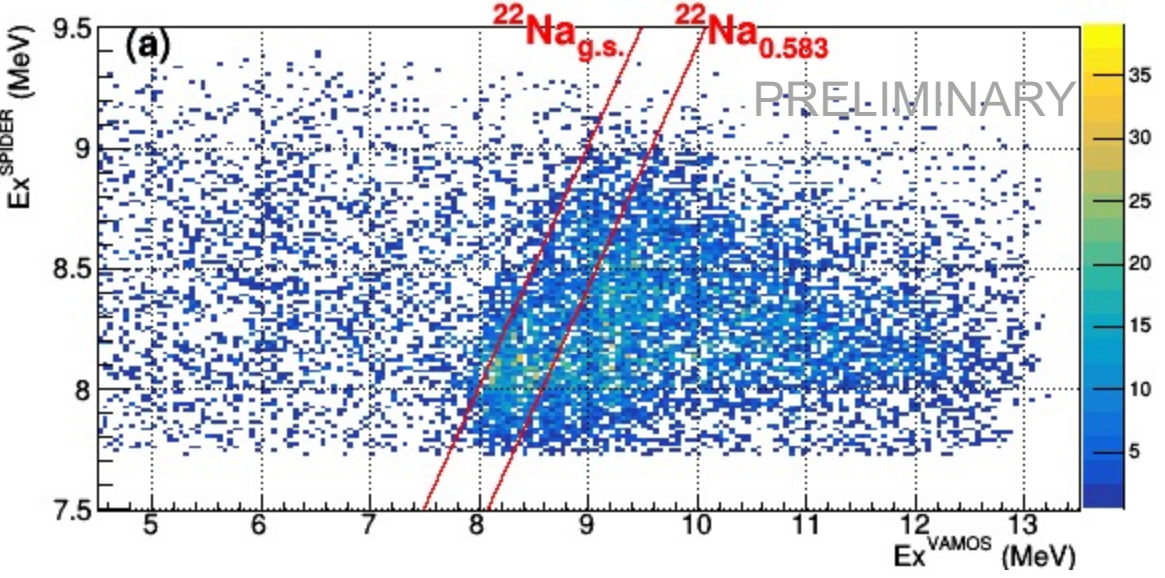
MC simulations with the **EVASIONS** code

$^{23}\text{Mg}^*$ Ex = 7.785 MeV

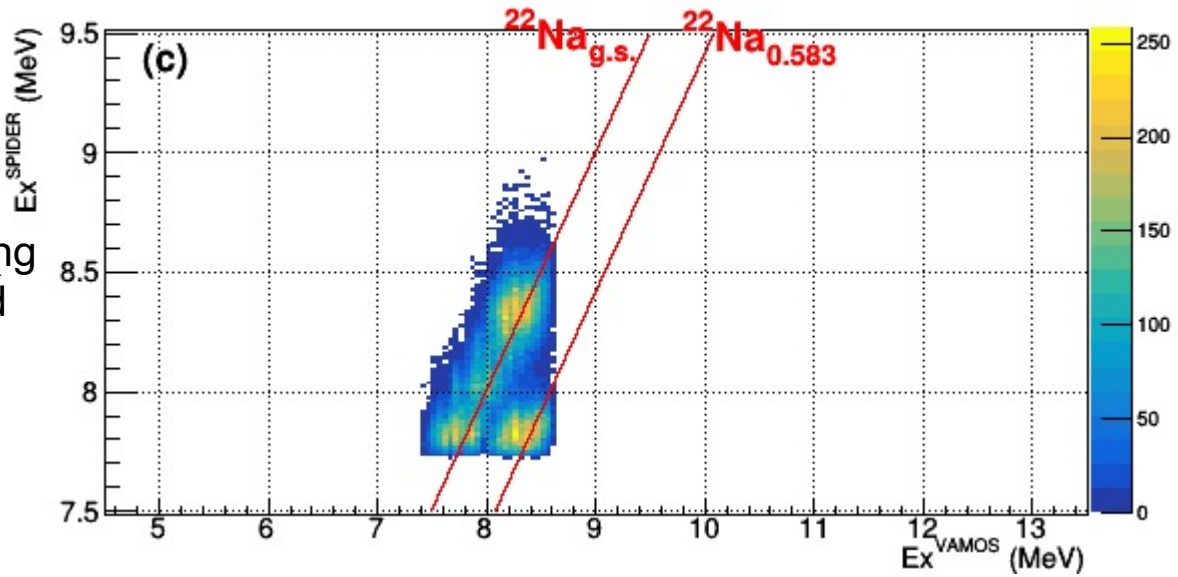
$^{23}\text{Mg}^*(p)$



Proton resolution

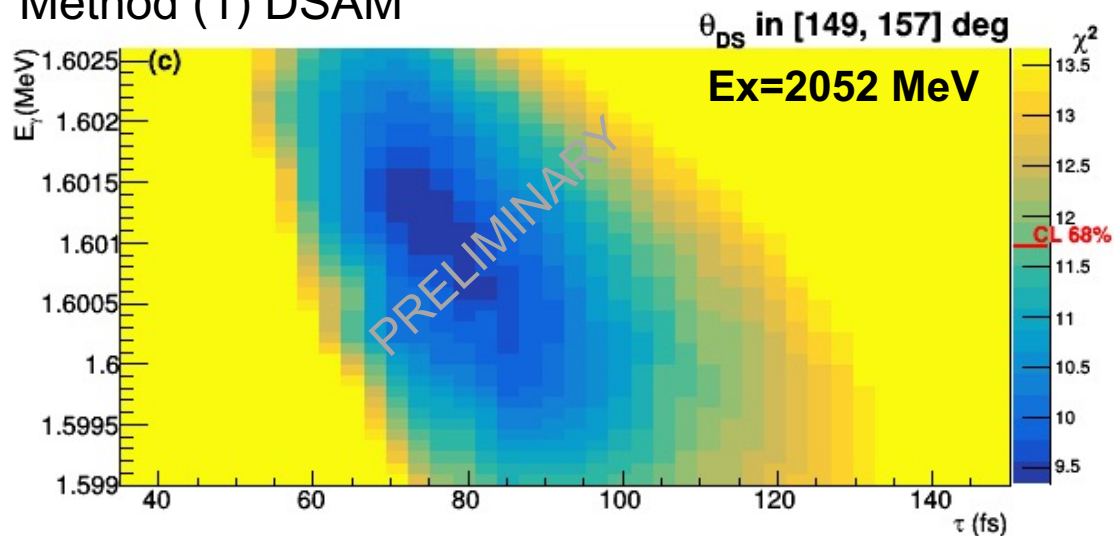


scattering
in gold →

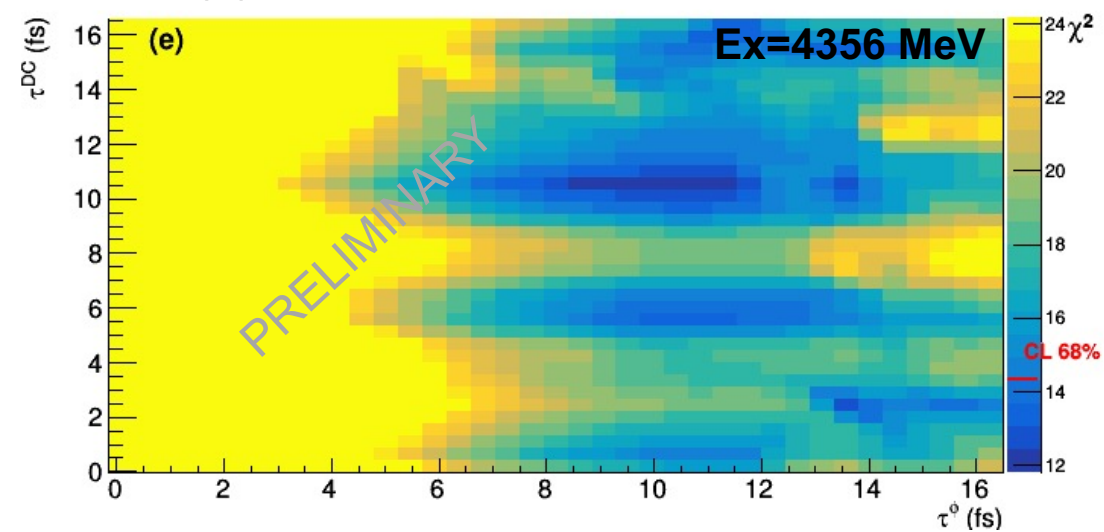


Lifetimes in $^{23}\text{Mg}^*$

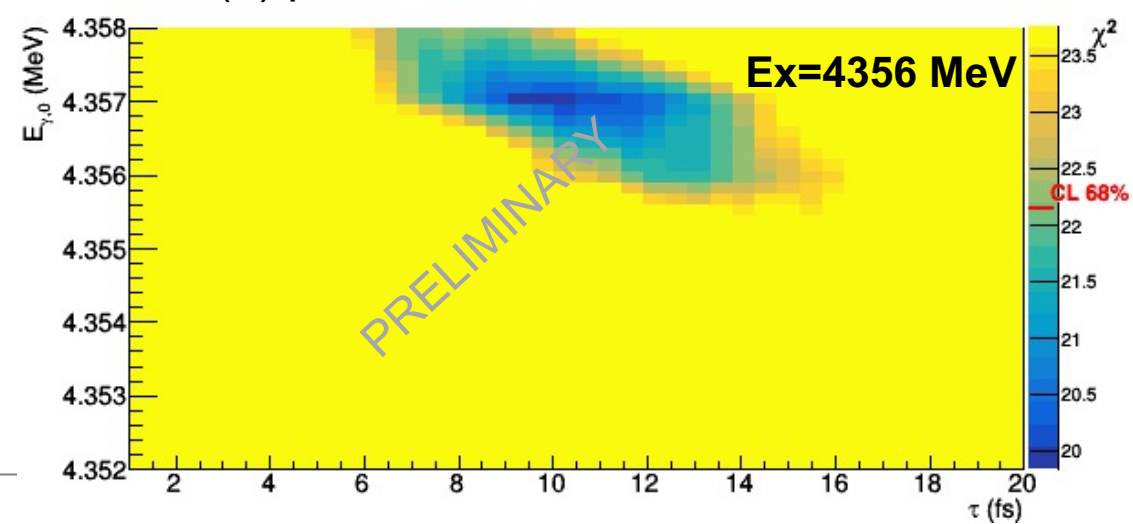
Method (1) DSAM



Method (2) DCLM

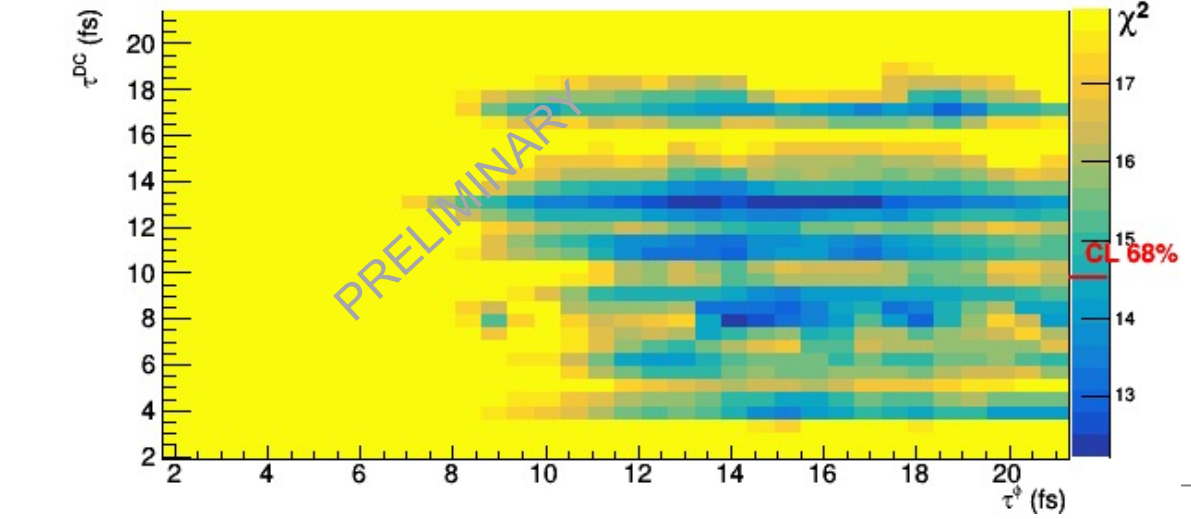
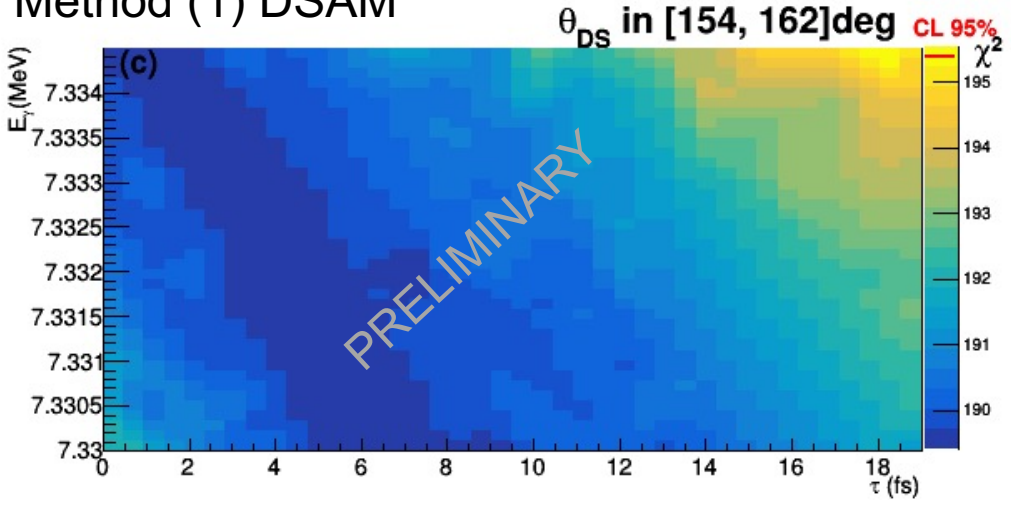


Method (3) βM



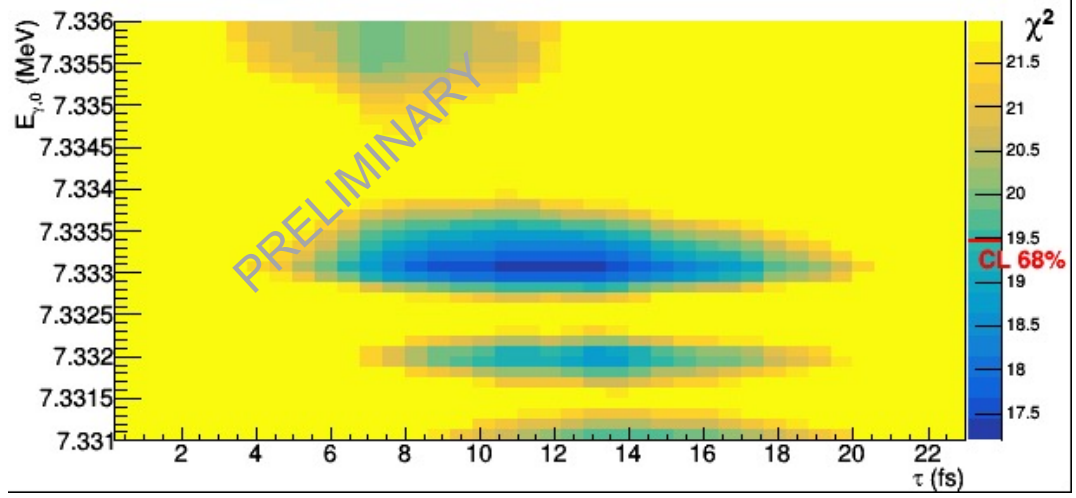
Lifetimes of astrophysical state

Method (1) DSAM



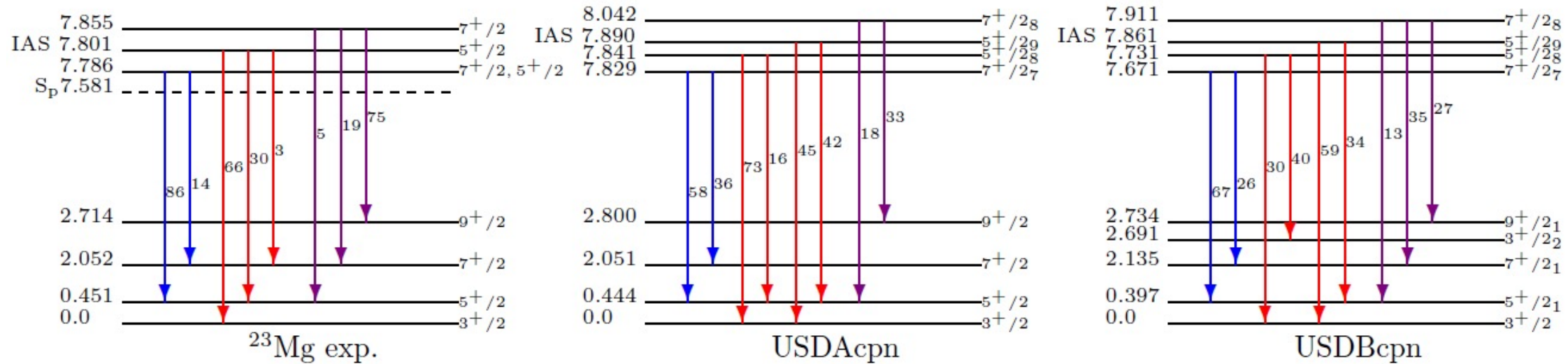
Method (2) DCLM

Method (3) βM



Theoretical considerations

Shell Model calculations with NUSHELLX, DWBU



Identifications: (1) **7/2+ level** with γ -ray decay path \sim measurements

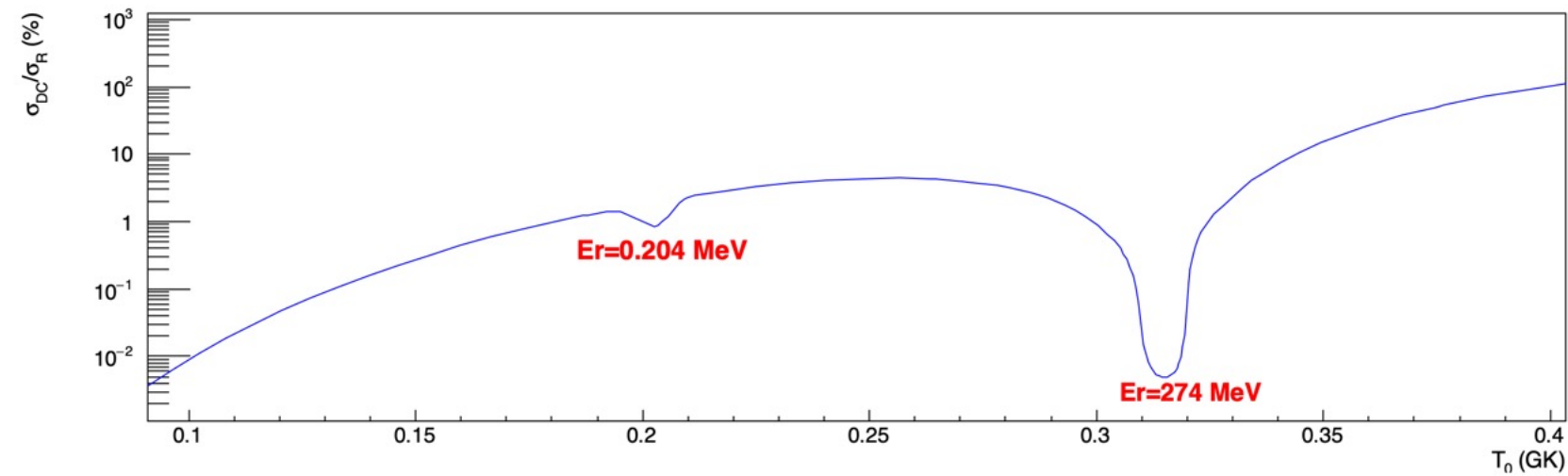
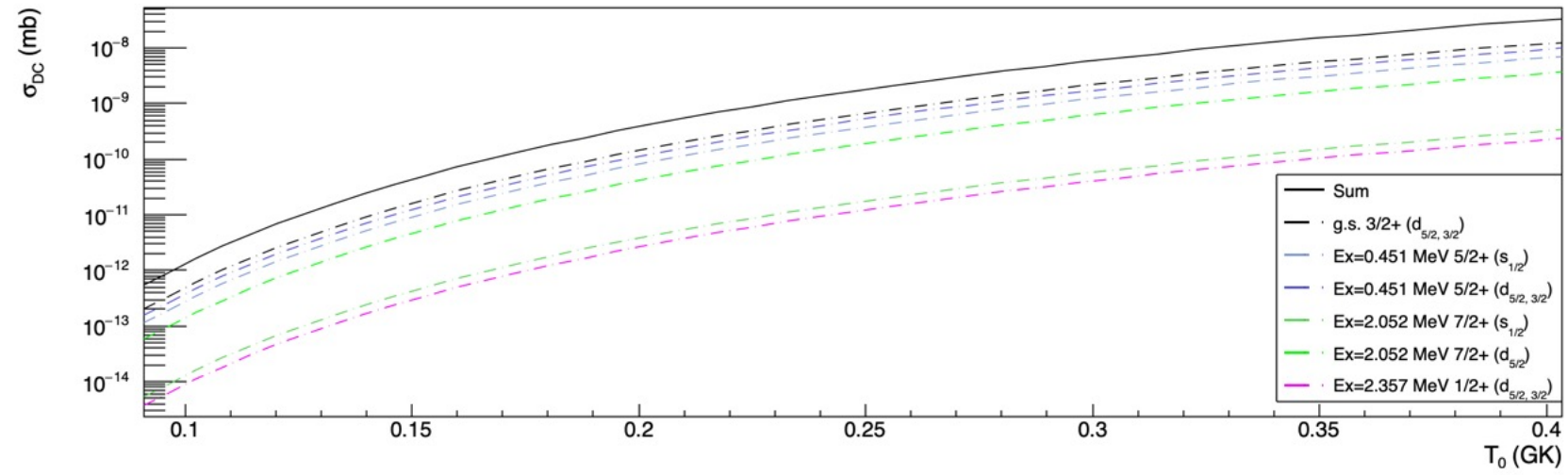
$$\text{SM } \Gamma_p = 6.4^{+10.1}_{-4.9} \text{ meV} \Leftrightarrow \Gamma_p = 2.0^{+6.9}_{-1.5} \text{ meV} \text{ (compiled measurements)}$$

(2) **5/2+ level close to IAS**

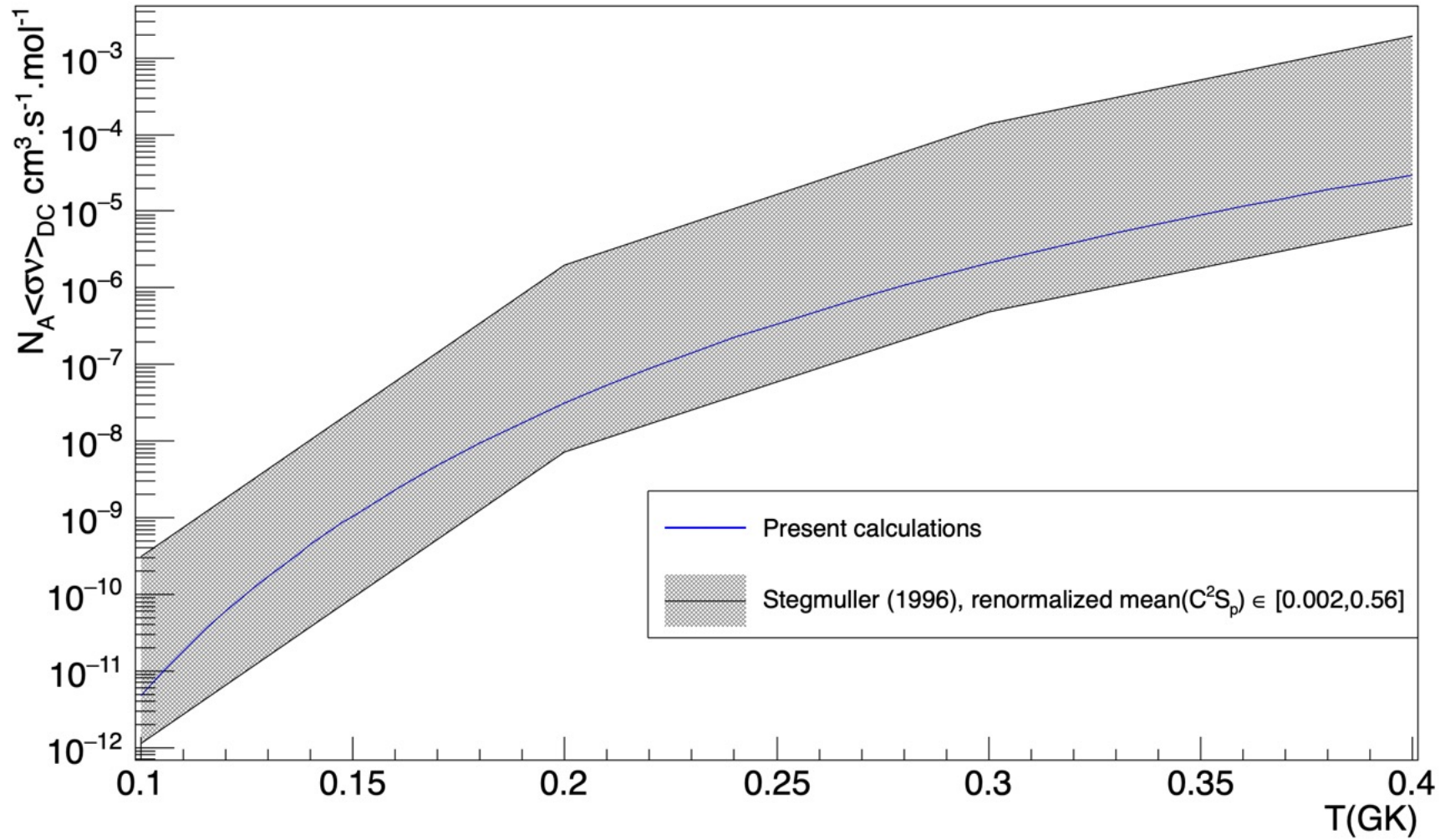
(3) **7/2+ level** \sim higher resonance at $E_R = 0.274 \text{ MeV}$

$$\text{SM } \omega_\gamma = 50^{+7}_{-6} \text{ meV} \Leftrightarrow \omega_\gamma = 39(8) \text{ meV} \text{ (Sallaska et al., 2011)}$$

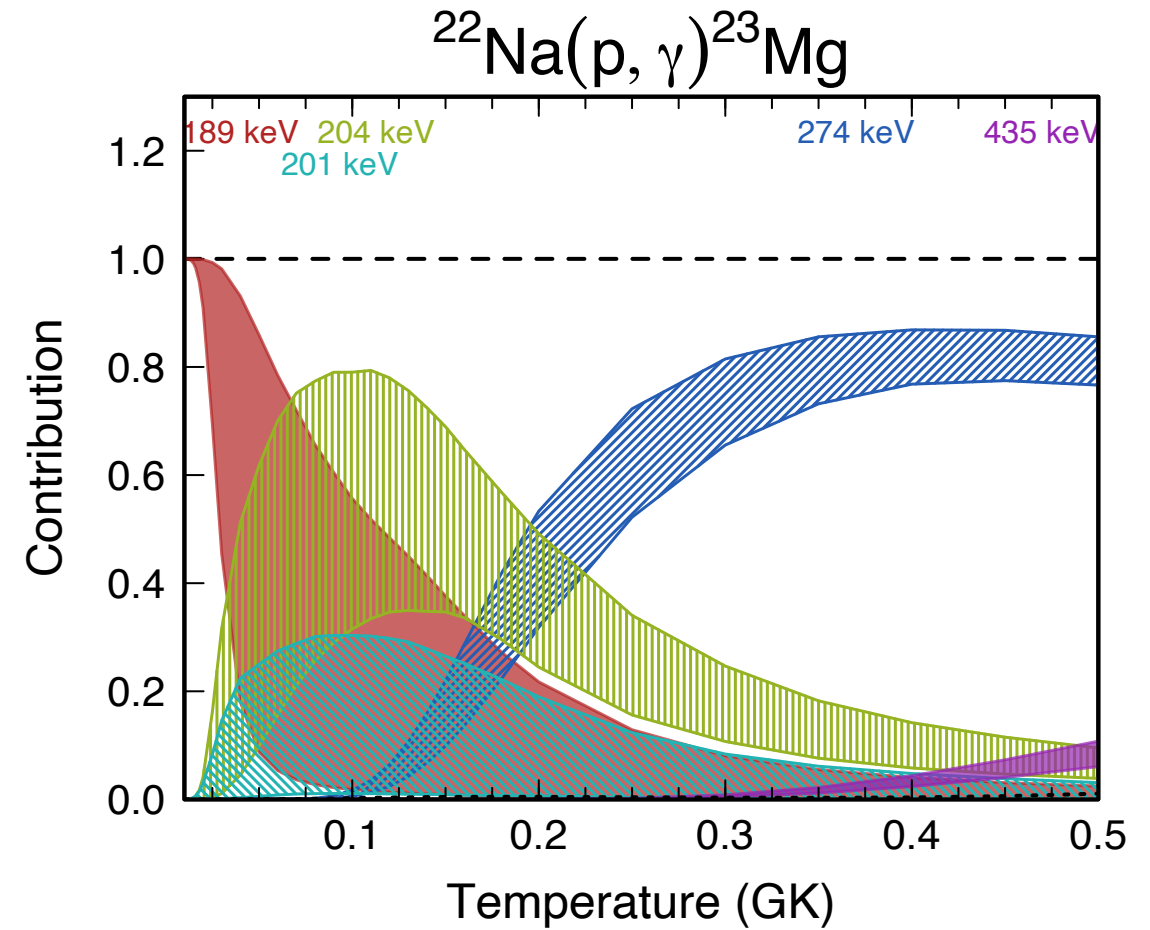
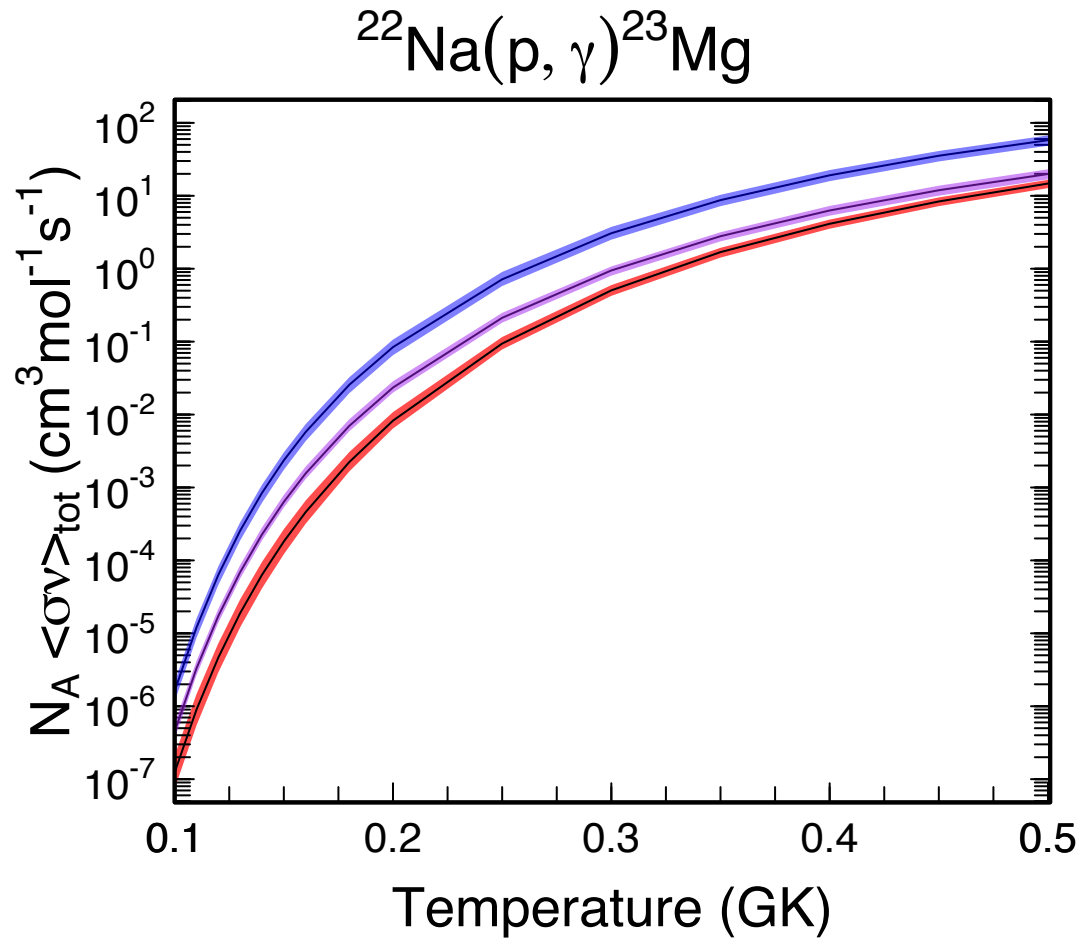
Direct capture contribution



Direct capture rate

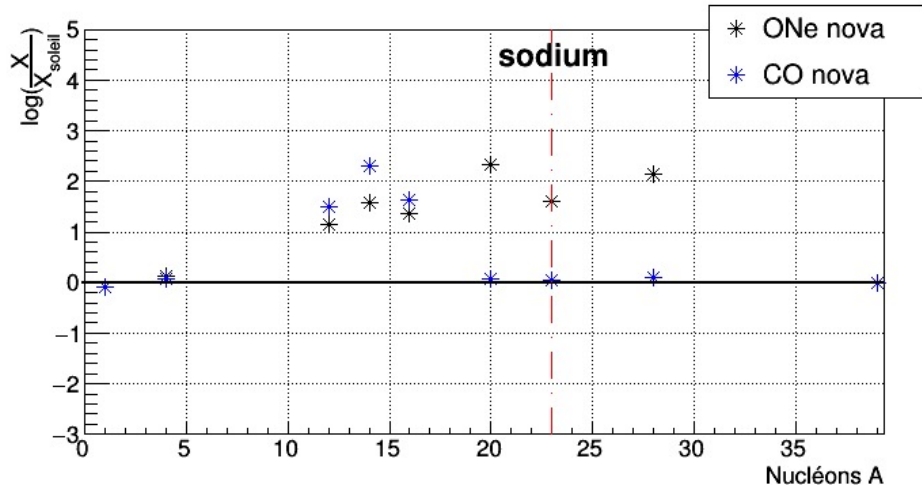


Total reaction rate and resonant contribution

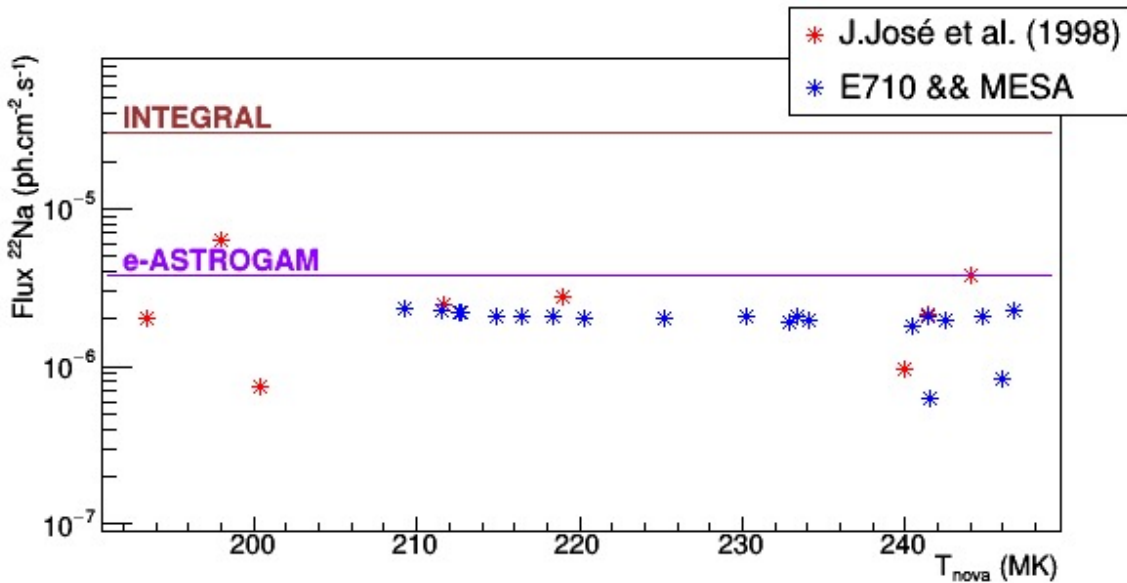
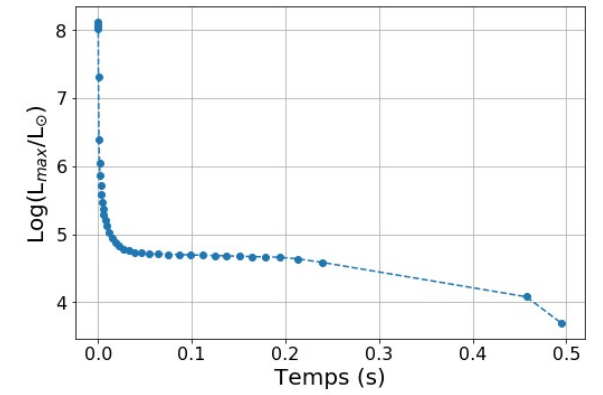
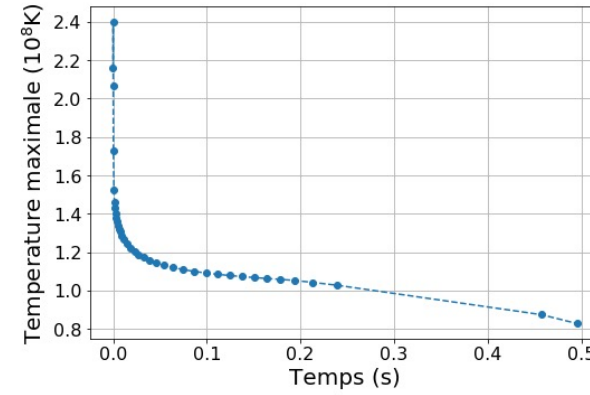


Simulations of novæ

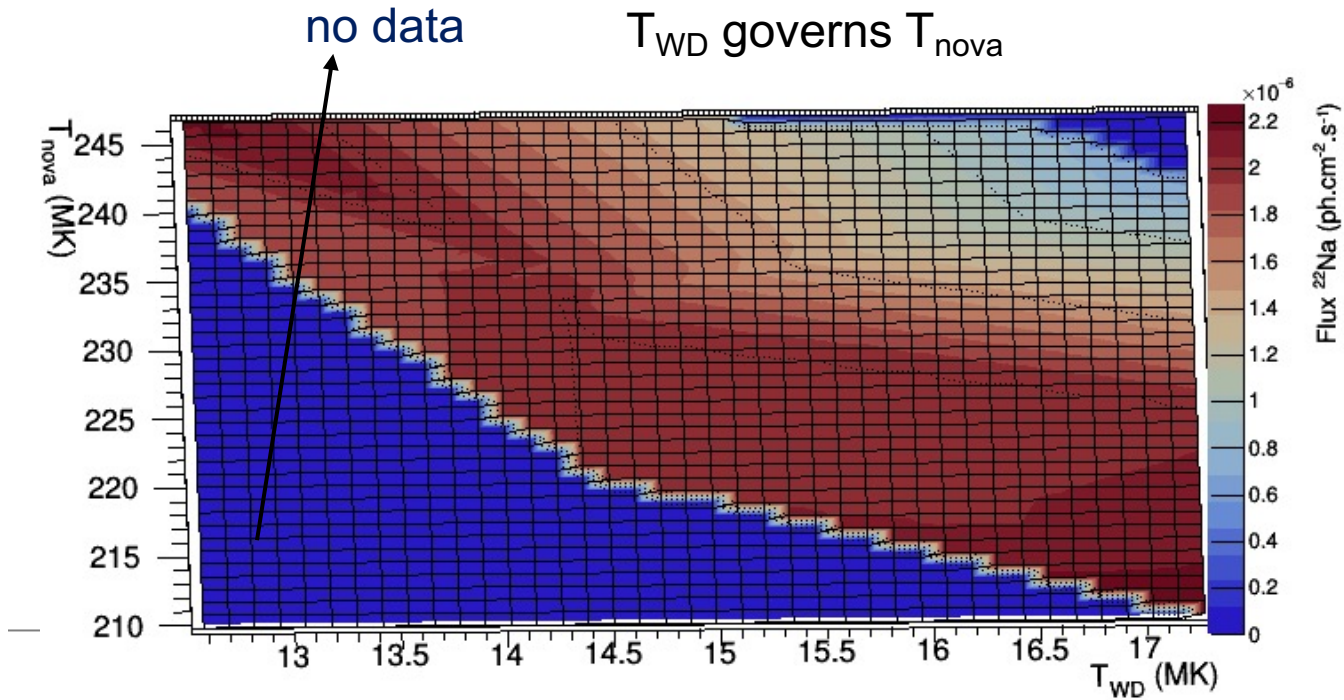
Nova composition w.r.t. WD (CO vs ONe)



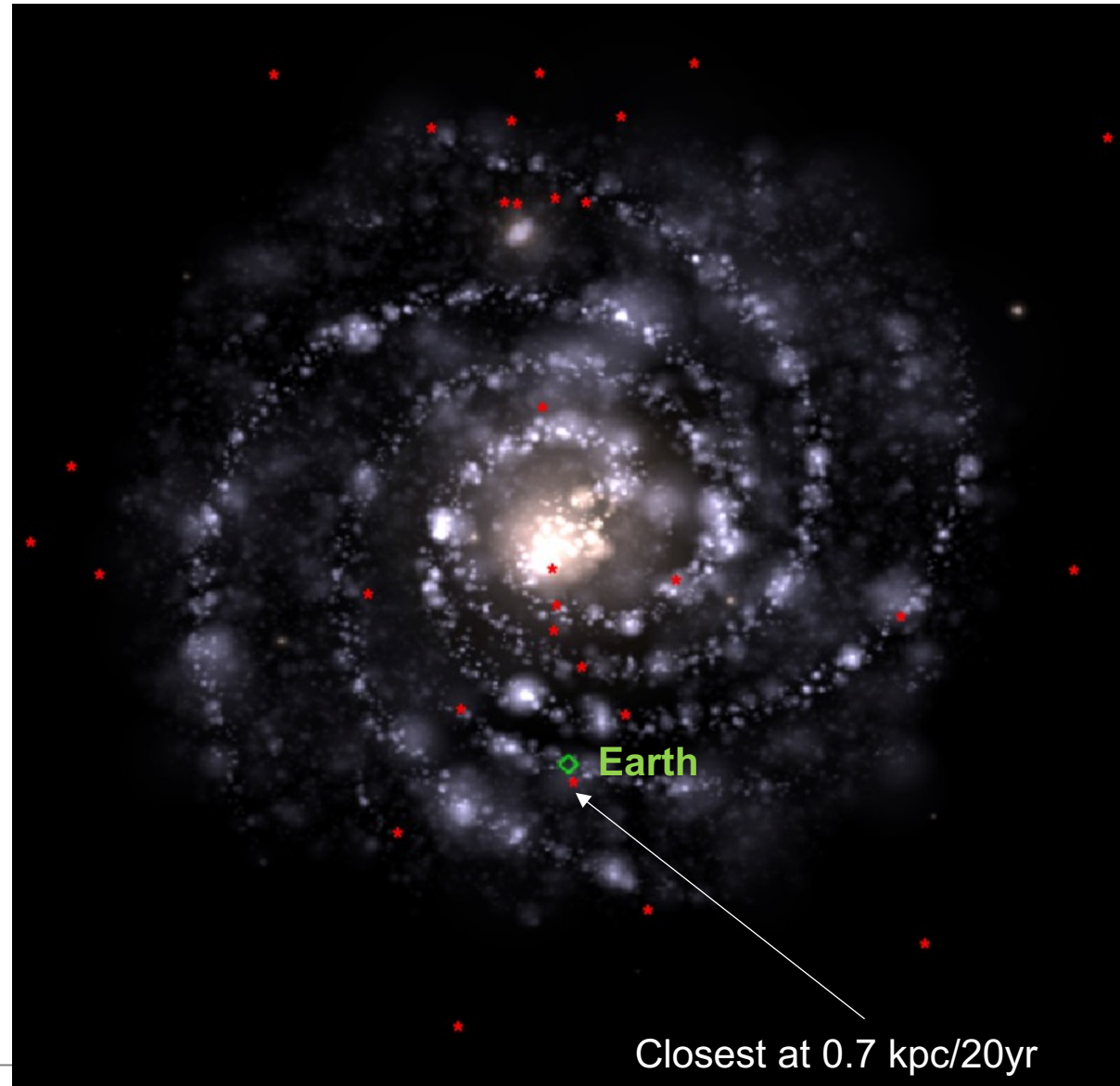
Profiles



Agreement with simulation SHIVA *J. José et al., (1998, 2021)*



Novæ events in our universe



Courtesy of De Oliveira Santos